

The Khovanov Homology of Rational Tangles

Benjamin Thompson

A thesis submitted for the degree of
Bachelor of Philosophy with Honours in Pure Mathematics of
The Australian National University

October, 2016

*Dedicated to my family.
Even though they'll never read it.*

“To feel fulfilled, you must first have a goal that needs fulfilling.”

Hidetaka Miyazaki, *Edge (280)*

“Sleep is good. And books are better.”

(Tyrion) George R. R. Martin, *A Clash of Kings*

“Let’s love ourselves then we can’t fail to make a better situation.”

Lauryn Hill, *Everything is Everything*

Declaration

Except where otherwise stated, this thesis is my own work prepared under the supervision of Scott Morrison.

Benjamin Thompson
October, 2016

Acknowledgements

What a ride. Above all, I would like to thank my supervisor, Scott Morrison. This thesis would not have been written without your unflagging support, sublime feedback and sage advice. My thesis would have likely consisted only of uninspired exposition had you not provided a plethora of interesting potential topics at the start, and its overall polish would have likely diminished had you not kept me on track right to the end. You went above and beyond what I expected from a supervisor, and as a result I've had the busiest, but also best, year of my life so far.

I must also extend a huge thanks to Tony Licata for working with me throughout the year too; hopefully we can figure out what's really going on with the bigradings!

So many people to thank, so little time. I thank Joan Licata for agreeing to run a Knot Theory course all those years ago. I thank Pierre Portal for being a fantastic mentor. We've ridden the highs together... as well as the inevitable lows. I thank Stephen Hyde for allowing me to do some extremely interesting research with him.

Last, but certainly not least, I wish to thank my family for the remarkable amount of support they've provided over the years. I couldn't have done it without you.

Abstract

The aim of this thesis is to describe the Khovanov homology of rational tangles. To this extent we describe rational tangles, followed by Khovanov homology, then combine the two at the end.

In Chapter 1 we review the main points of the theory of rational tangles. In particular, we show that rational tangles are classified by a function known as the tangle fraction, which associates to each rational tangle a rational number. This classification theorem implies that each rational tangle can be constructed by adding and multiplying together multiple copies of certain types of tangle.

In Chapter 2 we review the Khovanov homology theory we will use to study rational tangles. After discussing link invariants, the Kauffman bracket, and categorification in general, we develop a generalization of Khovanov homology to tangles due to Bar-Natan [Bar04]. We then specialize this to a ‘dotted’ theory, which is equivalent to Khovanov’s original theory [Kho99] on links and is significantly easier to work with.

In Chapter 3, we combine the previous topics to develop a theory of the Khovanov homology of rational tangles. We determine the Khovanov complexes of integer tangles, before presenting a helpful isomorphism and discussing its implications. We then combine these to prove Theorem 3.3.1, the main result of this thesis.

Finally, in Chapter 4 we briefly discuss some of the application of Theorem 3.3.1. Unexpectedly, we find that the bigradings of the subobjects in the Khovanov complexes can be described by matrix actions, and that one can recover from this action the reduced Burau representation of B_3 , the three-strand braid group. The full ramifications of this observation are yet to be determined!

Contents

Declaration	v
Acknowledgements	vii
Abstract	ix
1 Rational tangles	1
1.1 Rational tangles	1
1.2 The tangle fraction	7
1.3 Rational links	10
2 Khovanov homology	13
2.1 Link invariants	13
2.2 The Kauffman bracket	18
2.3 Categorifying the Jones polynomial	22
2.4 Bar-Natan's approach	28
2.5 Bar-Natan's dotted theory	37
2.6 Invariance of the Khovanov bracket under the Reidemeister moves	41
3 The Khovanov homology of rational tangles	47
3.1 The Khovanov complex of integer tangles	48
3.2 A new isomorphism	57
3.3 The Khovanov complex of rational tangles	63
4 Theoretical implications of Theorem 3.3.1	71
4.1 Rational knots	71
4.2 The Burau representation from the Khovanov complexes of rational tangles	72

Rational tangles

Tangles are topological objects that generalize knots and links. Rational tangles are in some sense the simplest tangles consisting of two components. They satisfy a fairly strong condition, and satisfy several nice properties. The purpose of this chapter is to describe the main parts of the theory of rational tangles.

In Section 1.1 we define rational tangles (Definition 1.1.5), and discuss some their basic properties. The material in this section, like the rest of the chapter, is adapted from [KL03b].

In Section 1.2 we define the tangle fraction (Definition 1.2.4). This is a function that takes rational tangles to rational numbers. The reason why rational tangles are called rational is because this function actually classifies rational tangles up to isotopy: two rational tangles are isotopic iff their tangle fraction is the same rational number.

In Section 1.3 we briefly examine rational links. These are links obtained by closing the ends of rational tangles, and many of the simplest examples of knots can be obtained in this manner. (Of the first 25 knots, 24 are rational.) The classification of rational tangles with the tangle fraction can be used to classify rational links. This theorem provides many elegant descriptions of properties such as chirality and invertibility for rational links in terms of their tangle fractions.

1.1 Rational tangles

In this section we define rational tangles and describe their structure. Although they can be defined quite generally (Definition 1.1.1), rational tangles satisfy a surprising set of isotopies (Proposition 1.1.9) which allow us to write each in a *standard form* (Definition 1.1.12). The standard form definition of a rational tangle is easier to understand than more abstract definitions.

The notation we develop in this section will be used extensively in Chapter 3 when we describe the Khovanov homology of rational tangles.

Before we jump into the theory of rational tangles, let us first describe tangles in general.

Definition 1.1.1 A *tangle* is an smooth embedding of a compact 1-manifold X , possibly with boundary, into the three-ball B^3 such that the boundary of X is sent to the boundary of B^3 transversely. By a smooth embedding we mean an injective smooth map whose differential is nowhere zero.

We will identify tangles with their image in B^3 . Tangles may also be oriented – an oriented tangle is a tangle where every connected component has the choice of one of the two possible directions on it. We will consider tangles up to isotopy.

Definition 1.1.2 Two tangles T_1, T_2 are said to be *isotopic*, denoted $T_1 \sim T_2$, if one can be transformed into the other via a smooth isotopy fixing the endpoints. That is, via a smooth map $F : X \times [0, 1] \rightarrow B^3$ such that:

- $F(X, t)$ is a tangle for each t ,
- $F(X, 0) = T_1, F(X, 1) = T_2$,
- $F(\partial X, t)$ is constant with respect to t .

The corresponding notion of isotopy for oriented tangles is clear.

We will depict tangles via *tangle diagrams*. That is, we take a regular projection (see below) of the tangle onto a plane whose intersection with B^3 is a great circle, and at each crossing point in the projection (a point whose preimage consists of two points) mark the overcrossings and undercrossings of the tangle in the obvious way. That is, after projection, we mark which branches of the tangle are “higher” and “lower” than the others. Examples of tangle diagrams can be found below in Figure 1.1.2.

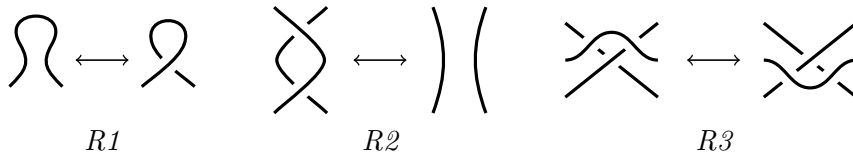
By a regular projection we mean:

1. the boundary points of the tangle are sent to distinct points on the great circle and non-boundary points are sent inside the circle;
2. lines tangent to the tangle, whenever defined, are projected onto lines in the plane;
3. no more than two points of the link are projected to the same point of the plane;
4. the set of crossing points is finite, and at each crossing point the projections of the tangents to the points in the preimage do not coincide.

Oriented tangle diagrams are defined in the same way, only now one marks the orientations of the connected components with arrows.

Isotopic tangles and their diagrams are related by a well-known Theorem due to Reidemeister. ([Rei48])

Theorem 1.1.3 *Two tangles S, T are isotopic iff they have the same endpoints and any tangle diagram of S can be transformed into a tangle diagram of T via planar isotopies fixing the boundary of the projection disk and a finite sequence of local moves taking place in the interior of the disk of the following three types:*



This allows us to think about tangles almost entirely in terms of tangle diagrams. We now introduce the central object of this chapter.

Definition 1.1.4 A *rational tangle* is a smooth embedding of two copies of the unit interval I_1, I_2 into B^3 (in which the boundary of $I_1 \sqcup I_2$ is sent to the boundary of B^3 transversely), such that there exists a homeomorphism of pairs

$$h : (B^3, I_1 \sqcup I_2) \rightarrow (D^2 \times I, \{x, y\} \times I).$$

This definition is fairly abstract, and not as easy to understand as our next definition of a rational tangle (Definition 1.1.5), but we have nonetheless included it for completeness.

The definition is equivalent to saying that rational tangles are isotopic to tangles obtained by applying a finite number of consecutive twists to neighbouring endpoints of two untangled arcs, illustrated in Figure 1.1.1 below.

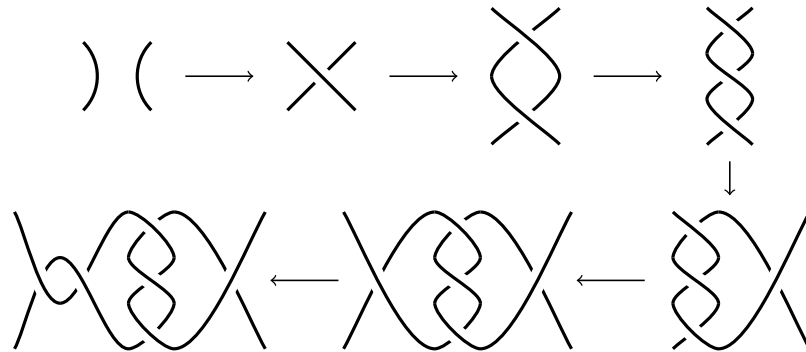


Figure 1.1.1: Constructing a rational tangle. Beginning with two untangled arcs, various twists of neighbouring endpoints are applied. Each arrow represents a twist; the first three arrows are twists of the top or bottom endpoints, the others are twists of the left and right endpoints.

It will be convenient to have a concise notation to describe the structure of rational tangles, which we now develop.

The simplest rational tangles are those which admit a crossingless diagram; we call these the $[0]$ and $[\infty]$ tangles. The next simplest are the *integer tangles* $[n]$ and the *vertical tangles* $[\bar{n}]$, made of n horizontal or vertical twists respectively. Their tangle diagrams are in Figure 1.1.2 below.

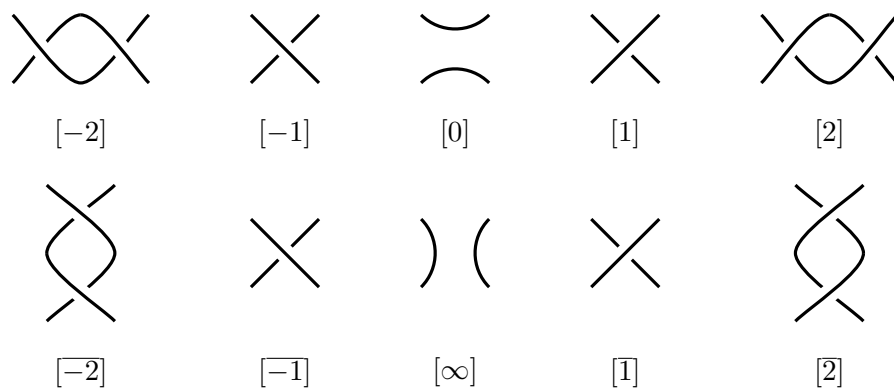


Figure 1.1.2: Some simple integer $[n]$ and vertical $[\bar{n}]$ tangles.

Note the sign conventions: if n is positive, so are the gradients of the overcrossings in the tangle diagrams above. These are the same conventions that Conway used in [Con70], but different to those used by Kauffman and Lambropoulou in [KL03b].

Rational tangles are a subclass of tangles with four boundary points, called *4 boundary point tangles* or just *4 point tangles*. On 4 point tangles one can define binary operations referred to as *addition* $(+)$ and *multiplication* $(*)$. The definition of $T + S$ and $T * S$ for arbitrary 4 point tangles is given in Figure 1.1.3 below. The operations are well-defined up to isotopy.

Note that addition and multiplication of 4 point tangles are associative but not commutative. The sum or product of rational tangles is not necessarily rational.

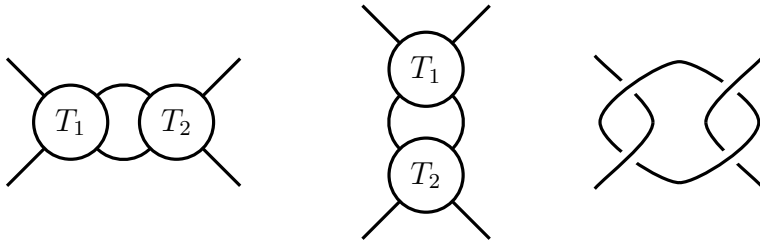


Figure 1.1.3: LEFT The sum (+) of 4 point tangles T and S . MIDDLE The product (*) of 4 point tangles T and S . RIGHT The tangle $[\bar{2}] + [\bar{2}]$ is not rational, since it contains three connected components.

Using these operations and the $[\pm 1]$ tangles illustrated above, we can give an alternative, and much more usable, definition of a rational tangle.

Definition 1.1.5 A tangle is *rational* if it is created from $[0]$ or $[\infty]$ by a finite sequence of additions and multiplications with the tangles $[\pm 1]$. If a rational tangle is presented in this way we say it is in *twist form*.

For instance, the rational tangle constructed in Figure 1.1.1 is in twist form, since it is given by $[-1] + [-1] + ((([\infty] * [-1] * [-1] * [-1]) + [1])$.

We omit the proof of the equivalence of this definition and that of Definition 1.1.4, but refer the interested reader to Note 1 of [KL03b]. Unless otherwise stated, in the sequel we assume that any rational tangle is in twist form.

One can also define operations on 4 point tangles T called *mirror image*, *rotation* and *inversion*. The mirror image of T is the tangle obtained from T by switching all the crossings, and is denoted $-T$. The rotation of T is obtained by rotating T by $\pi/2$ counterclockwise and is denoted T^r . Finally, the inversion of T is defined by $T^{-1} := -T^r$. Examples of the mirror image and inverse of a tangle are below.



Figure 1.1.4: LEFT A tangle and its mirror image. RIGHT A tangle and its inverse.

The reasons why the first two operations are called the mirror image and rotation of a tangle are self-explanatory, but it may be unclear why their composition should be called the inverse. This is because for rational tangles, the tangle fraction respects the inverse of a tangle. That is, $F(T^{-1}) = F(T)^{-1}$. We describe this, and other relations the tangle fraction satisfies in the next section.

We now define a type of isotopy, and use it to show some surprising properties of rational tangles. These in turn allow us to simplify the definition of a rational tangle.

Definition 1.1.6 A *flype* is an isotopy of a tangle applied to a 4 point subangle of the form $[\pm 1] + T$ or $[\pm 1] * T$ as illustrated below in Figure 1.1.5. A flype fixes the endpoints of the subangle to which it is applied.

Flypes are important in the theory of alternating tangles.

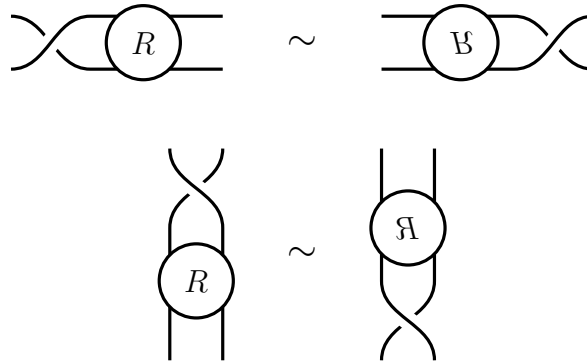


Figure 1.1.5: Flypes are a family of isotopies specific to 4 point tangles.

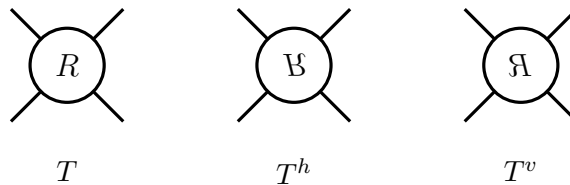
Definition 1.1.7 A tangle diagram is said to be *alternating* if the crossings encountered when following a component of the tangle around the diagram alternate from undercrossings to overcrossings. A tangle is *alternating* if it admits an alternating tangle diagram.

For example, in Figure 1.1.4 above, the two rightmost tangle diagrams are alternating while the first two diagrams are not alternating. It will follow from the main theorem of the chapter, the classification of rational tangles, (Theorem 1.2.6) that rational tangles are alternating.¹

The proof of the classification theorem of rational tangles by the tangle fraction uses some heavy machinery involving flypes. The *Tait conjecture for knots*, proved by W. Menasco and M. Thistlethwaite in 1993 ([MT93]), states that two alternating knots are isotopic iff any two diagrams of the knots on S^2 are related by a finite sequence of flypes.

Using the Tait conjecture for knots, one proves the corresponding statement of the conjecture for rational tangles, thereby characterizing how alternating rational tangles are isotopic. Using this statement, one can then show that isotopic rational tangles have the same tangle fraction simply by checking that the tangle fraction is invariant under flypes. This task is not difficult once Proposition 1.1.9 below has been established.

Definition 1.1.8 The *horizontal flip* of a 4 point tangle T , denoted T^h , is obtained by rotating T by π through a horizontal line in the plane of T . Similarly the *vertical flip* of T , denoted T^v , is obtained via rotation of T by π through a vertical axis in the plane.



Flypes can be described more concretely in terms of these operations. Namely, a flype on a 4 point sub-tangle T is an isotopy of the form

$$[\pm 1] + T \sim T^h + [\pm 1] \quad \text{or} \quad [\pm 1] * T \sim T^v * [\pm 1].$$

Both horizontal and vertical flips are order 2 operations on 4 point tangles. Surprisingly, on rational tangles these operations have order 1.

¹To prove this theorem, one actually first shows that rational tangles are alternating, but for the sake of space we omit this.

Proposition 1.1.9 *If T is rational, then $T \sim T^h \sim T^v$.*

Proof: We prove that $T \sim T^h$; the other statement follows from this result by twisting T by $\pi/2$, locally applying the result, and twisting back. The proof is by induction.

The statement is clearly true for the $[0]$, $[\infty]$ and $[\pm 1]$ tangles. Assume the statement is true for a rational tangle with n crossings. Any rational tangle with $n + 1$ crossings can be expressed as $[\pm 1] + T$, $T + [\pm 1]$, $[\pm 1] * T$ or $T * [\pm 1]$ where T is a rational tangle with n crossings.

The induction hypothesis easily gives

$$([\pm 1] + T)^h \sim [\pm 1] + T^h \sim [\pm 1] + T,$$

and similarly for $T + [\pm 1]$. Of the other two cases, we have

$$([\pm 1] * T)^h \sim T^h * [\pm 1] \sim T * [\pm 1] \sim [\pm 1] * T^v \sim [\pm 1] * T.$$

(in the third isotopy we applied a flype) and similarly $(T * [\pm 1])^h \sim T * [\pm 1]$. \square

Corollary 1.1.10 *Rotation and inversion are operations of order 2 on rational tangles*

Corollary 1.1.11 *For a rational tangle T ,*

$$[\pm 1] + T \sim T + [\pm 1] \quad \text{and} \quad [\pm 1] * T \sim T * [\pm 1].$$

Proof: This is easy. With a flype, we have

$$[\pm 1] + T \sim T^h + [\pm 1] \sim T + [\pm 1].$$

The same argument shows multiplication by $[\pm 1]$ commutes. \square

Note that this means every rational tangle can be constructed from the $[0]$ or $[\infty]$ tangles by a sequence of right additions or bottom multiplications of $[\pm 1]$: working from the outermost to innermost crossings of a tangle in twist form, if a crossing was added to the left or top, simply isotope it to the right or bottom respectively. We give a name to such rational tangles.

Definition 1.1.12 A rational tangle is said to be in *standard form* if it created from $[0]$ or $[\infty]$ by consecutive additions or products of $[\pm 1]$ on the right and bottom respectively. Every rational tangle is isotopic to a tangle in standard form.

(Note that as $[\infty] = ([0] + [1]) * [-1]$, we could actually remove $[\infty]$ in the definition above.)

Using the notation $[n] := \underbrace{[1] + \dots + [1]}_{n \text{ times}}$ illustrated earlier in Figure 1.1.2, we can write a rational tangle in standard form as an expression

$$(\dots ((([a_1] * [\overline{a_2}]) + [a_3]) * [\overline{a_4}]) + \dots * [\overline{a_{n-1}}]) + [a_n]$$

where a_i are integers. We will abbreviate such an expression as $\langle a_1, \dots, a_n \rangle$. Some

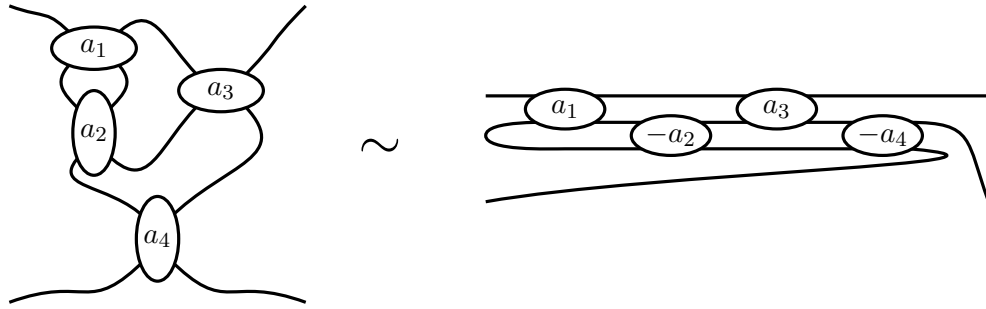
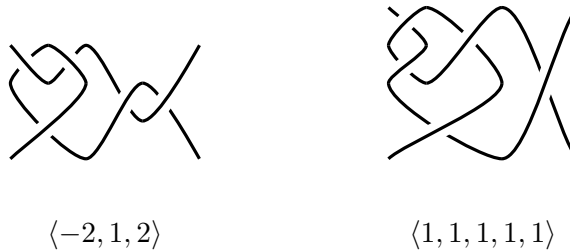


Figure 1.1.6: Although most rational tangles we consider will be in standard form (left), it is sometimes convenient to consider them as (partial closures) of elements of B_3 .

illustrative examples of this notation are included below.



Most rational tangles we draw will be in standard form. We can also consider rational tangles to be a partial closures of elements of B_3 , the three-strand braid group, as illustrated in Figure 1.1.6. We will revisit this viewpoint in Chapter 4 when we look at how the reduced Burau representation of B_3 can be obtained from the Khovanov homology of rational tangles.

From this point on, we will assume all rational tangles are in standard form, unless otherwise stated.

1.2 The tangle fraction

We saw in the previous section that rational tangles are very structured. In particular, each admits a standard form (Definition 1.1.12). Because of their structure, rational tangles admit a nice classification. In this section we define the tangle fraction (Definition 1.2.4), and state the classification of rational tangles that uses it (Theorem 1.2.6). A consequence is that every rational tangle other than $[\infty]$ admits a unique canonical form (Corollary 1.2.9), a result crucial to Theorem 3.3.1, the main result of our thesis.

The tangle fraction has several definitions², but we consider the one presented in this section to be the most intuitive. For the remainder of this chapter, it will often be convenient to denote the inverse of a tangle as a fraction $1/T$ instead of T^{-1} .

Lemma 1.2.1 *If a 4 point tangle T is rational, then*

$$T * [\bar{n}] = \frac{1}{[n] + \frac{1}{T}}, \quad \text{and} \quad [\bar{n}] * T = \frac{1}{\frac{1}{T} + [n]}. \quad (1.2.1)$$

²The interested reader is referred to [KL03a] for alternative descriptions of the tangle fraction.

Proof: Since

$$(T * [\bar{n}])^r = T^r + [-n],$$

we have

$$(T * [\bar{n}])^{-1} = -(T^r + [-n]) = T^{-1} + [n].$$

The results follow. \square

Since every rational tangle is isotopic to a rational tangle in standard form

$$\langle a_1, \dots, a_n \rangle = (\dots ((([a_1] * [\bar{a}_2]) + [a_3]) * [\bar{a}_4]) + \dots * [a_{n-1}]) + [a_n],$$

the lemma allows us to write a rational tangle as ‘continued fraction’ of tangles.

Definition 1.2.2 A rational tangle is a *continued fraction in integer tangles* if it has the form

$$[a_1, a_2, \dots, a_n] := [a_1] + \frac{1}{[a_2] + \frac{1}{[a_3] + \dots + \frac{1}{[a_{n-1}] + \frac{1}{[a_n]}}}}.$$

We stipulate that $a_2, \dots, a_n \in \mathbb{Z} \setminus \{0\}$ and $a_1 \in \mathbb{Z}$. If $a_1 = 0$ in a continued fraction of integer tangles, when we write the expression we omit the $[0]$.

Rational tangles in standard form can be converted to a continued fraction of tangles by multiple applications of the relation $[n] + T \sim T + [n]$ and Lemma 1.2.1. The interconversion can be summarized by

$$\langle a_1, a_2, \dots, a_n \rangle \sim [a_n, a_{n-1}, \dots, a_1].$$

We now list some properties of rational tangles in continued fraction form. The proof of each is not difficult.

Lemma 1.2.3 Let $T = [a_1, \dots, a_n]$ be a rational tangle in continued fraction form. Then

1. $T + [\pm 1] = [a_1 \pm 1, a_2, \dots, a_n]$,
2. $\frac{1}{T} = [0, a_1, a_2, \dots, a_n]$,
3. $-T = [-a_1, -a_2, \dots, -a_n]$.

We now come to the main definition of this section.

Definition 1.2.4 Let $T = [a_1, \dots, a_n]$ be a rational tangle in continued fraction form. Define the *fraction* or *tangle fraction* $F(T)$ of T to be the rational number obtained by replacing the integer tangles in the expression for T with their corresponding integers. That is,

$$F(T) = a_1 + \frac{1}{a_2 + \frac{1}{a_3 + \dots + \frac{1}{a_{n-1} + \frac{1}{a_n}}}}. \quad (1.2.2)$$

If $T = [\infty]$ we define $F([\infty]) = \infty$.

Although the tangle fraction is well-defined for rational tangles in a continued fraction form, it is not clear if this is well-defined for rational tangles up to isotopy. That is, isotopic rational tangles expressed as different continued fractions have the same tangle fractions. This is one of the directions of the main theorem of this chapter (Theorem 1.2.6). Namely, if $S \sim T$, then $F(S) = F(T)$ for any choice of a continued fraction of tangles for S and T .

We now list some properties of the tangle fraction. They all follow easily from Lemma 1.2.3.

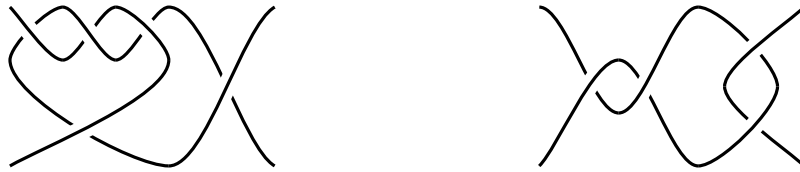
Lemma 1.2.5 Let $T = [a_1, \dots, a_n]$ be as above. Then

1. $F(T + [\pm 1]) = F(T) \pm 1$,
2. $F(\frac{1}{T}) = \frac{1}{F(T)}$,
3. $F(T * [\bar{n}]) = \frac{1}{[n] + \frac{1}{F(T)}}$,
4. $F(-T) = -F(T)$.

We are now in a position to state the main result of this chapter, though omit its proof. (The proof is given in [KL03b]. Though it is technical, it uses no other tools than the ones previously described.)

Theorem 1.2.6 The tangle fraction is well-defined up to isotopy, and two rational tangles are isotopic iff they have the same fraction.

Example 1.2.7 Consider the rational tangles below. The first has standard form $\langle -3, 1, 1 \rangle$ with the second is $2 + [\bar{2}]$, which has continued fraction form $[2, 2]$.



After computing their fractions,

$$F(\langle -3, 1, 1 \rangle) = 1 + \frac{1}{1 + \frac{1}{-3}} = 1 + \frac{3}{2} = 2 + \frac{1}{2} = F([2, 2]),$$

we find the tangles are isotopic. This may not be immediately evident from inspection.

One consequence of the Theorem 1.2.6 is that every rational tangle is alternating. To see this we introduce another definition.

Definition 1.2.8 A continued fraction

$$a_1 + \frac{1}{a_2 + \dots + \frac{1}{a_{n-1} + \frac{1}{a_n}}}$$

is said to be in *canonical form* if n is odd and either $a_1 \geq 0$ and $a_i > 0$, or $a_i \leq 0$ and $a_i < 0$ (for $i \neq 1$). The same definition extends to rational tangles, provided they are in continued fraction form.

Corollary 1.2.9 Every rational tangle other than $[\infty]$ has a unique canonical form.

Proof: Consider an arbitrary rational tangle T . Without loss of generality assume $F(T) > 0$. By Euclid's algorithm we can uniquely write $F(T)$ as a continued fraction

$$a_1 + \frac{1}{a_2 + \dots + \frac{1}{a_{n-1} + \frac{1}{a_n}}}$$

where $a_1 \geq 0$ and $a_i > 0$ for all $1 < i < n$, and $a_n > 1$. If n is even, we replace a_n with $a_n - 1 + \frac{1}{1}$. Now $F(T)$ is in canonical form, and is unique by construction. The claim follows from Theorem 1.2.6 by considering the corresponding continued fraction of tangles. \square

Note that this implies that every rational tangle admits a diagram whose crossings are all of the same type. (That is, the gradients of the overcrossing lines all agree.) This follows by considering the standard form $\langle a_1, \dots, a_n \rangle$ of a tangle in canonical form. If $a_i \geq 0$ or $a_i \leq 0$ for all i then by definition of the standard form of a rational tangle, every crossing has the same configuration. We will use this fact in Chapter 3 to inductively construct the Khovanov homology of a rational tangle.

Corollary 1.2.10 *Every rational tangle is alternating.*

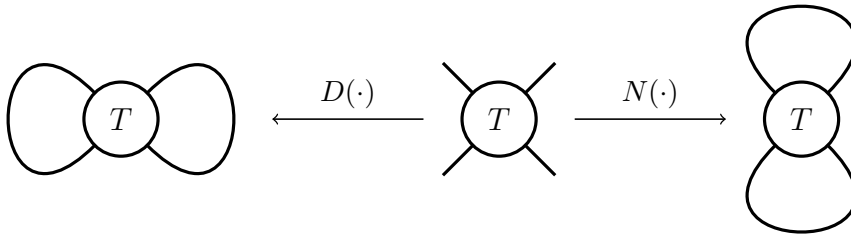
Proof: The claim follows by considering the standard form of a rational tangle in canonical form. When this standard form is viewed as the partial closure of a 3-braid (as in Figure 1.1.6 above), all the crossings in the top row are of one type, whereas the crossings in the bottom row are of the other. It is easy to see that such a diagram is alternating, from which the claim follows. \square

We have now seen the main components and highlights to the theory of rational tangles. Strictly speaking, we've seen all we need for the later chapters, but it'd be a shame to skip some of the nice results regarding rational links that the theory of rational tangles provides. As such, before we begin the next topic, Khovanov homology, we briefly pause to look at links obtained from rational tangles.

1.3 Rational links

Given a rational tangle, one can close the ends in several ways to obtain a *rational link*. Two of these, the *numerator closure* $N(\cdot)$ and *denominator closure* $D(\cdot)$ are illustrated below. The Hopf link, for example, can be expressed as $N([2])$. The links we consider in examples in the sequel will be rational.

Sometimes both types of closure give isotopic links; trivially $N([1])$ and $D([1])$ are both isotopic to the unknot. Sometimes non-isotopic tangles close to give the same link; trivially $N([\overline{n}])$ is isotopic to the unknot for any n . Since $D(T) = N(T^r)$, we will only consider the numerator closure of a rational tangle in the sequel.



Since rational tangles are alternating, rational links are too. Once again, this can easily be seen by examining an alternating diagram of a rational tangle depicted as the partial closure of an element of B_3 as described in the previous section. In such a presentation, it is clear that when the ends are closed the link obtained is alternating.

Given a rational tangle, it may not be immediately clear if its numerator closure will yield a link with one or two components. The distinction is trivial using the tangle fraction. ([KL03a])

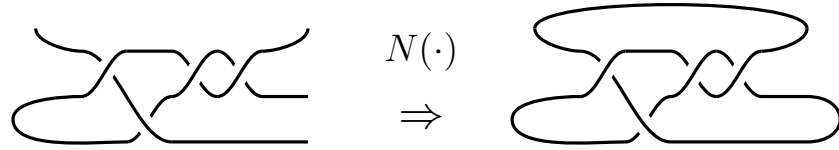


Figure 1.3.1: The figure-8 knot, like any rational link, is alternating.

Proposition 1.3.1 Let $N(p/q)$ denote the rational link obtained by taking the numerator closure of the rational tangle with fraction p/q , where p and q are relatively prime. Then $N(p/q)$ has two connected components iff p is even and q is odd. That is, iff p/q has parity e/o .

Given that the tangle fraction classifies rational tangles, it is perhaps unsurprising that it classifies rational knots too. The following theorem is due to Schubert. ([Sch56])

Theorem 1.3.2 Rational links $N(p/q)$ and $N(p'/q')$ are isotopic iff:

1. $p = p'$, and
2. either $q \equiv q' \pmod p$ or $qq' \equiv 1 \pmod p$.

Schubert originally stated this classification of rational links in terms of 2-bridge links as his work predates Conway’s theory of rational tangles. A combinatorial proof that uses the classification of rational tangles appears in [KL03a]. An oriented version of the theorem also exists and is due to Schubert too; its phrasing and proof can be found in [KL03a] as well.

A consequence of Theorem 1.3.2 is that chiral rational links admit an easy classification.

Definition 1.3.3 A link L is *chiral* if it is isotopic to its mirror image. That is, if $L \sim -L$. A link is *achiral* if it is not chiral.

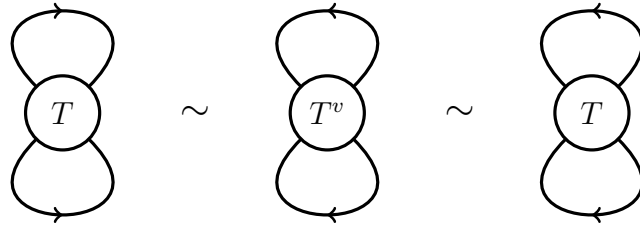
Proposition 1.3.4 Let $L = N(p/q)$ as above. Then L is achiral iff $q^2 \equiv -1 \pmod p$.

Example 1.3.5 It is well-known that the trefoil and figure-8 knot are chiral and achiral respectively, these properties follow trivially from the previous proposition. The knots can be realized as $N([3])$ and $N([2, 2])$, illustrated below. Since $F([3]) = 3/1$ and $1 \not\equiv -1 \pmod 3$, the trefoil is chiral. As $F([2, 2]) = 5/2$, and $4 \equiv -1 \pmod 5$, the figure-8 knot is achiral.



Definition 1.3.6 Given an oriented link K , the *inverse* of K , denoted K^* , is obtained by reversing the orientation of each component. A link is *invertible* if it is isotopic to its inverse, that is, if $K \sim K^*$.

It is an easy consequence of Proposition 1.1.9 that every rational link is invertible. The proof follows by applying a vertical flip to the knot, as illustrated below.



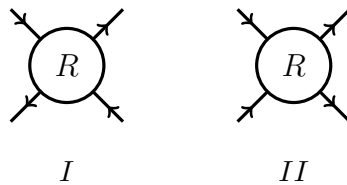
A stronger notion of invertibility can be defined for links with more than one component.

Definition 1.3.7 A link L is said to be *strongly invertible* if any link formed by reversing orientations of any of the components of L is isotopic to L .

Strongly invertible rational links admit a classification using the oriented version of the classification theorem for oriented rational links. ([KL03b])

Proposition 1.3.8 Let L be a two-component oriented link with $L = N(p/q)$ as above, with $|p| > |q|$. Then L is strongly invertible iff $q^2 = 1 + op$ for some odd integer o .

Finally, for notation purposes, we note that oriented rational tangles that have well-defined numerator closures are isotopic to one of two forms, illustrated below. We refer to these as *type I* and *type II* (oriented) rational tangles. We use this notation in Chapter 3.



This concludes our foray into rational links.

Khovanov homology

Khovanov homology is a categorification of the Jones polynomial. It was constructed by Mikhail Khovanov in the late 90s for links, ([Kho99]) and has since been generalized to tangles ([Kho01, Bar04]). Several variants of the theory also exist ([Lee02], [Bar04]).

The purpose of this chapter is to construct Bar-Natan’s dotted Khovanov homology theory of tangles. We will use this version of Khovanov homology to study the Khovanov homology of rational tangles in Chapter 3.

In Section 2.1 we introduce and discuss link invariants. These are maps taking links to algebraic objects that are invariant under isotopy. The Jones polynomial, and Khovanov homology, are both link invariants, though we delay the proof of these claims until Sections 2.2 and 2.6 respectively. This section is based on material covered in more depth in [Kas95, CDM11, PS96].

In Section 2.2 we introduce the Kauffman bracket. This is a tool that can be used to define the Jones polynomial and give a simple proof of its existence. The primary resource for this section was [Kau87].

In Section 2.3 we briefly discuss categorification in general, and motivate Khovanov’s construction that categorifies the Jones polynomial. Categorification is an informal process taking set-theoretic structures to category-theoretic structures. This section was inspired from material in [Kho16].

In Section 2.4 we construct Bar-Natan’s extension of Khovanov homology to tangles, as described in [Bar04]. His exposition is so generally excellent that we hardly deviate from it. As such if the reader has any trouble with our ‘compressed’ version of his material, we refer her to the source.

In Section 2.5 we modify the Khovanov homology theory developed in the previous section to a ‘dotted’ version. In the dotted version complexes are far easier to manipulate, and when restricted to links the theory is equivalent to ordinary Khovanov homology. The dotted theory is described in [Bar06].

Finally, in Section 2.6 we prove the Khovanov bracket is invariant under the Reidemeister moves, following the proof as hinted by Bar-Natan in [Bar06].

2.1 Link invariants

Khovanov homology, and the Jones polynomial it categorifies, are both link invariants. This means they associate algebraic objects to links, and do so in such a way that isotopic links give the same algebraic object. As such they can help distinguish links: if the value of a link invariant on two links differs, by definition the links are not isotopic.

In this section we illustrate the range of link invariants that exist. We begin by looking

at link invariants defined from geometric and topological means, before transitioning to link invariants defined by combinatorial data, such as the Jones polynomial.

Link invariants usually have wider applications than as a tool to classify links however, and it is this point that underpins much of the research, and interest, in the field. The Jones polynomial, for instance, has connections with statistical physics, operators algebras and quantum field theories. Naturally Khovanov homology also has connections with other areas, including geometric representation theory, symplectic geometry and algebraic geometry ([Kho16]).

Despite their general promise to be interesting objects to study, link invariants are often hard to define. The requirement that a link invariant respects isotopy imposes a barrier.

One way to overcome this problem when defining a link invariant is to measure some quantity over all possible configurations of a link, then take the minimum. The *stick number* of a link, for instance, is the minimum number of straight ‘sticks’ needed to realize the link in \mathbb{R}^3 . That is, if we view a knot as an embedding of S^1 into \mathbb{R}^3 but require that the image be a finite union of line segments (instead of the usual requirement that the map be smooth), the stick number of the knot is the minimum number of line segments used over all possible configurations. In this way an aspect of the geometry of the knot is captured – the minimum number of times the knot will ‘turn’ in space. Upper bounds of the stick number are easy to obtain, but like many invariants defined by taking minimums, it is hard to obtain satisfactory lower bounds.

The space around a link is more interesting than the link itself: as topological spaces, links are all essentially the same – a disjoint collection of circles. The same is not true for the surrounding space. By considering a link L in B^3 and taking a tubular neighborhood N of L , we define the *knot complement of L* to be the compact 3-manifold $X_L = B^3 \setminus \text{int}(N)$. (Also note that this can be defined for links embedded in 3-manifolds other than B^3 .) Isotopies of links induce homeomorphisms of the corresponding complements, so we can produce knot invariants by studying knot complements. (In fact, the Gordon-Luecke Theorem tells us that in the case of knots, the knot complement is a *complete invariant* – that is, knots are isotopic iff their knot complements are homeomorphic. The corresponding claim is not true for links, however.)

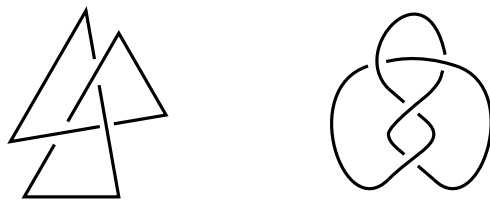


Figure 2.1.1: LEFT The stick number is a basic, if difficult to compute, link invariant. RIGHT The figure-8 knot is hyperbolic, so has hyperbolic volume. This is an invariant specific to hyperbolic links.

Some links have a complement which has a hyperbolic geometry. Tools from this field can then be used to define invariants for these links, such as the *hyperbolic volume*. Methods from algebraic topology can also be applied to complements; the *knot group* $\pi(K)$ of a knot K is the fundamental group of its complement. This invariant is actually quite powerful: $\pi(K) = \mathbb{Z}^n$ iff K is the trivial link with n components, and two prime knots are isotopic iff they have isomorphic knot groups. While algorithms exist for calculating the



Figure 2.1.2: The two possible types of oriented crossing, referred to as negative and positive crossings respectively.

knot group in terms of generators and relations (the Wirtinger presentation), showing two presentations are non-isomorphic is a difficult question in general.

Another class of manifolds which yield information about links are *Seifert surfaces*. These are compact, connected, oriented surfaces embedded in \mathbb{R}^3 with boundary that is a link. A link can have several different Seifert surfaces, and the minimum genus over all Seifert surfaces of a given link is called the *genus* of the knot.

The knot group and genus of a link both involved the construction of an object that resembles the link, from which we extracted information to create the invariant. There is however, another, perhaps simpler, approach to construct a link invariant. We create a diagram that represents the link, and directly use the combinatorial information in the diagram to compute the invariant of the link.

In the last chapter we saw *link (tangle) diagrams*, which are the most common and intuitive of way of representing a link in two dimensions. Despite their simplicity, a variety of link invariants have been constructed from these diagrams. Some are quite simple. The *crossing number* is just the minimum number of crossings in any link diagram of the link. The *bridge number*, meanwhile, is the minimum number of local maxima in any link diagram of the knot.

These may be interesting, but it is often theoretically and computationally convenient to have an invariant which can be calculated given a single link diagram, instead of needing to consider all possible diagrams.

Reidemeister, and independently Alexander and Briggs showed that two link diagrams represent isotopic links iff one can be obtained from the other via planar isotopies and a finite number of Reidemeister moves. (There were illustrated before in Theorem 1.1.3 from the previous chapter.) To check that a link invariant defined via link diagrams is really an invariant, one simply needs to make sure it does not change under planar isotopies and the Reidemeister moves.

Example 2.1.1 The *linking number* is easily proved to be a link invariant using the previous criteria. We define this as follows. Given an oriented link, choose two components L_1, L_2 , and define the linking number of the two of the components as the integer

$$\text{lk}(L_1, L_2) = \frac{1}{2} \sum_S \varepsilon(S),$$

where S runs over all crossings of L_1 and L_2 . The value $\varepsilon(S) \in \{\pm 1\}$ assigned to each crossing depends on the crossing's orientation and is indicated below.

To verify that this is a link invariant, note that the number of crossings, and their orientations, are preserved under planar isotopy. We therefore just need to check invariance of the linking number under the Reidemeister moves. Since we only consider crossings composed of different link components, it is trivially invariant under R1. For R2 invariance, first note that reversing the orientation of all the components of the link does not change

the orientations of crossings.

This means we only need to check two of the possible orientation configurations of the R2 components, illustrated below. Since the local contribution to the linking number from each of these configurations is zero, it follows that the linking number does not change after an application of R2.

To prove invariance under R3, we examine both sides of the move in Figure 2.1.3 below. It is clear that if the orientations of the vertical and diagonal components of these diagrams are consistent across both, the values assigned to the intersections in the left diagram determine the values assigned to the intersections in the right diagram. The sum of the values over the diagrams are the same. We have hence verified all the criteria, proving the linking number is indeed a link invariant.

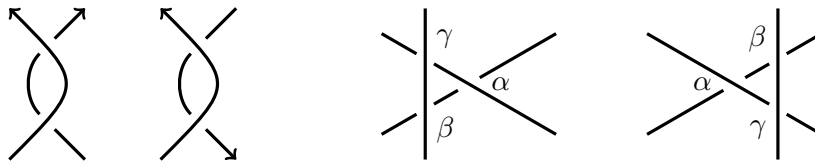


Figure 2.1.3: Showing the linking number is invariant under R2 and R3. The Greek letters indicate crossings with the same orientation.

Although this invariant is rudimentary, it is easy to calculate and can quickly distinguish many simple links. (For instance, the linking number of the 2-component unlink is trivially 0, whilst the Hopf links below take values ± 1 , proving that the Hopf link is not isotopic to the unlink. This seemingly obvious fact is hard to prove directly from the definition of isotopy.

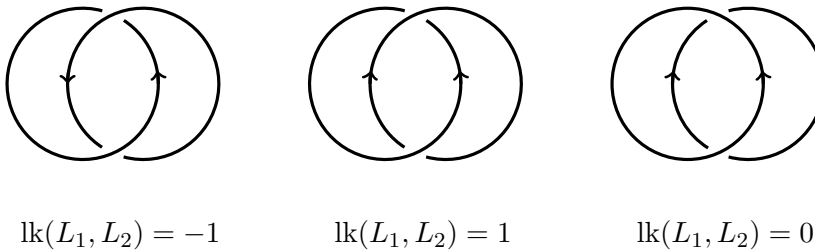


Figure 2.1.4: The linking number can be used to quickly prove the Hopf link is not trivial.

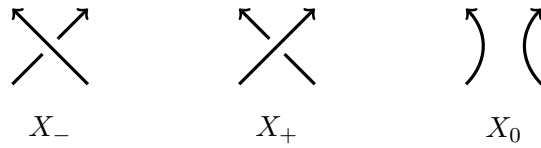
While this, and many of the invariants previously mentioned take values in the integers, one of the most interesting classes of link invariants are *polynomial invariants*. These assign to each link a polynomial in one or more variables, and most of the well-known link invariants are of this type.

Such an example is the *Alexander polynomial*. This was the first polynomial invariant to be discovered, and it has several definitions. One of these is in terms of the Seifert matrix of a Seifert surface whose boundary is the link. In this definition, the Seifert matrix M of a Seifert surface X is defined as $(M)_{ij} = \text{lk}(a_i, a_j^+)$, where $a_i \in H_1(X)$ are distinct generators of the first homology group of X , and a_i^+ represents a copy of a_i lifted slightly off the surface in the positive direction. (Recall that Seifert surfaces are required to be oriented.) One then obtains the Alexander polynomial via the formula $\Delta_L(x) = \det(x^{1/2}M - x^{-1/2}M^T)$.

Example 2.1.2 Let us compute the Alexander polynomial for the first Hopf link illustrated in Figure 2.1.4 above. A Seifert surface for the Hopf link is an annulus with two twists.

Since this Seifert surface is homotopic to a circle, the first homology has one generator x . To compute $\text{lk}(x, x^+)$, since the Seifert surface is an annulus with two twists, we note that the link formed by x and x^+ is isotopic to the boundary of the surface. The Seifert matrix is thus $[-1]$. We then obtain that $\Delta(\text{Hopf}) = -x^{1/2} + x^{1/2}$.

Alexander defined his invariant 1923, but it was only decades later in 1969 that it received its simplest formulation. In his seminal paper [Con70], Conway introduced a link invariant $\nabla_L(t)$ defined using the diagrams X_+, X_-, X_0 below, and showed that, after a change of variables, his link invariant was the Alexander polynomial.



Define a *Conway triple* (L_+, L_-, L_0) to be a triple of oriented links in \mathbb{R}^3 which can be represented by link diagrams that are identical outside of a disk, but which are isotopic inside to the diagrams X_+, X_-, X_0 respectively. Define the *Conway polynomial* of an oriented link L to be a polynomial in $\mathbb{Z}[t]$ taking value 1 on the unknot, and satisfying

$$\nabla(L_+) - \nabla(L_-) = t\nabla(L_0)$$

for all Conway triples (L_+, L_-, L_0) .

The definition of this link invariant is quite different from the others we've encountered so far. For starters, it isn't obvious from the definition why this should be invariant under the Reidemeister moves, or that it's even well-defined.

Unlike the other link invariants defined so far, we are defining the polynomial by describing a relation it satisfies. This is an example of a *skein relation*, and many polynomial link invariants admit descriptions in terms of skein relations.

Example 2.1.3 Let us calculate the Conway polynomial of the first Hopf link in Example 2.1.4 above.

$$\begin{aligned}
 \nabla(\text{Hopf}) &= \nabla(\text{Hopf}_+) - t\nabla(\text{Hopf}_0) \\
 &= \nabla(\text{Hopf}_-) - t\nabla(\text{Hopf}_0) \\
 &= t^{-1}(\nabla(\text{Hopf}_-) - \nabla(\text{Hopf}_+)) - t \\
 &= -t.
 \end{aligned}$$

Though the skein relation and the Seifert matrix seem to have little to do with one another, the Alexander polynomial can be recovered from the Conway polynomial by the simple change of variables $\Delta_L(x) = \nabla_L(x^{1/2} - x^{-1/2})$. Indeed, when we apply the change

of variables to the calculation for the Hopf link above, the result agrees with our calculation via Seifert surfaces.

We now turn towards the *Jones polynomial*, $V_L(t)$. This is arguably the most important polynomial link invariant to date, and was discovered in 1984 by Vaughan Jones [Jon85]. Like the Alexander polynomial, it can be defined in terms of a skein relation:

$$t^{-1}V_{L_+} - tV_{L_-} = (t^{1/2} - t^{-1/2})V_{L_0},$$

and is normalized to take the value of 1 on the unknot. (Here, as before, (L_+, L_-, L_0) is a Conway triple.) The invariant was not discovered by playing around with skein relations though. The original construction involved, among other things, Hecke and von Neumann algebras, as well as the Ocneanu trace. The method was by no means elementary, but we need not concern ourselves with the construction: as we shall see in the next section, Kauffman devised an alternative definition of the Jones polynomial that allows for an easy proof of its existence.

The discovery of the Jones polynomial led to the discovery of the *Homfly polynomial*. This is a polynomial link invariant in two variables, defined by the skein relation

$$xP(L_+) - x^{-1}P(L_-) = yP(L_0)$$

and normalized to 1 on the unknot.

It was discovered by many people simultaneously and independently, and as such has several names. Known also as the *two-variable Jones polynomial* or *Jones-Conway polynomial*, the name Homfly is an acronym of the authors who were the first to publish it in [FYH⁺85].¹

The Homfly polynomial is a generalization of the Alexander and Jones polynomials. These specializations are given by

$$\nabla(L) = P(1, t)$$

and

$$V(L) = P(t, t^{-1/2} - t^{1/2}).$$

As we will see in the next section, the proof of the existence of the Jones polynomial is easy with the Kauffmann bracket. Unfortunately, there is currently no analogous piece of machinery that gives such an easy proof of the existence of the Homfly polynomial, though purely skein theoretic constructions of the polynomial exist.

2.2 The Kauffman bracket

Soon after the discovery of the Jones polynomial, Louis Kauffman gave an alternative description of the link invariant by introducing a gadget known as the *bracket polynomial* [Kau87]. Known also as the *Kauffman bracket*, the tool had many benefits. The original construction of the polynomial was technical and long; Kauffman constructed it in a very elementary manner within the first six pages of his paper. Many proofs of the polynomial's properties became trivial when using the bracket, and many long-held conjectures were

¹It has other names too; *HOMFLY-PT* acknowledges the work of two Polish mathematicians who published later ([PT88]). Dror-Bar Natan suggested ([BN95]) the invariant carry the name *LYMPH-TOFU*. Here the U... stands for unknown discoverers.

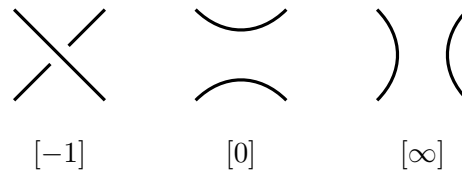
proven using the bracket. Computations of the Jones polynomial before the bracket could only really be done using the Skein relation; the Kauffman bracket by its definition provided an alternative route.

Khovanov homology would not exist without the Kauffman bracket either. As we will soon see, the bracket is fundamental to the construction at the core of the theory. As such it will be of great benefit to discuss Kauffman’s beautiful tool.

In this section we define the Kauffman bracket (Definition 2.2.2), then use it to redefine the Jones polynomial (Theorem 2.2.6). Our exposition follows the layout that Kauffman used in his paper that defined it [Kau87], but we use the conventions appropriate for Khovanov homology.² We construct the Kauffman bracket, show how it can be tweaked into a link invariant, and show this link invariant is the Jones polynomial. In this section, unless otherwise specified, by a link diagram we mean an unoriented link diagram.

The main idea of the Kauffman bracket is that of smoothings.

Define the *0-smoothing* and *1-smoothing* of a crossing in a link diagram to be the link diagram obtained by replacing the crossing with the $[0]$ or $[\infty]$ tangle. When replacing a crossing, we rotate the diagram around until the crossing locally looks like the $[-1]$ tangle, perform the appropriate replacement, then rotate the diagram back.



In a given link diagram, a *state* is an assignment of a 0- or 1-smoothing to every crossing. (So a diagram with n crossings has 2^n states.) The diagram obtained after applying the smoothings of a state S is called the *smoothing associated to the state S* . For brevity we often refer to such a diagram as a *smoothing*. Note that a smoothing of a link diagram is a union of disjoint (perhaps nested) circles. One can of course take smoothings of tangle diagrams, though in this case the smoothings may contain components other than circles. Equation 2.2.2 over the page illustrates the four possible smoothings of the tangle diagram of $[-1] * [1]$.

Let \mathcal{D} be the set of link diagrams up to planar isotopy. Then define a function $\langle \cdot \rangle_g : \mathcal{D} \rightarrow \mathbb{Z}[A, B, d]$ by the relations

1. $\langle \emptyset \rangle_g = 1$,
2. $\langle O \sqcup L \rangle_g = d \langle L \rangle_g$, and
3. $\langle \times \rangle_g = A \langle \rangle_g + B \langle \smile \rangle_g$.

The diagrams in the last line represent a crossing of link diagram, and its 0- and 1-smoothing respectively.

Proposition 2.2.1 *The function $\langle \cdot \rangle_g : \mathcal{D} \rightarrow \mathbb{Z}[A, B, d]$ exists and is unique.*

Proof: We first show uniqueness. Given a link diagram L , by repeatedly applying the third relation to each crossing we expand $\langle L \rangle_g$ as a sum of 2^n terms. Each of these terms is the result of $\langle \cdot \rangle_g$ evaluated on a smoothing of L , multiplied by $A^i B^j$ where i, j are the number of 0- and 1- smoothings in the state which produced the smoothing.

²In particular we set the Kauffman bracket of the unknot to be $(q + q^{-1})$ instead of 1.

Let γ be the number of disjoint loops in a smoothing. By applying the first and second relations to each term in the expansion of $\langle L \rangle_g$, we have

$$\langle L \rangle_g = \sum_S A^{i_S} B^{j_S} d^{\gamma_S}, \quad (2.2.1)$$

where the sum is over all the possible states of L . This shows the defining relations of the function determine the polynomial of any link diagram, proving uniqueness.

To prove existence of the function, we can use Equation 2.2.1 to define $\langle \cdot \rangle_g$, then simply need to verify the equation satisfies the three defining relations. This is not difficult. \square

We have constructed a function that assigns a polynomial to every link diagram in a straightforward combinatorial way, but as it stands $\langle \cdot \rangle_g$ is hardly useful. It is not a link invariant since it is not invariant under any of the Reidemeister moves, but it may be possible to force it to be a link invariant by imposing conditions on A , B and d .

Consider the result of the following calculation.

$$\langle \text{crossing} \rangle = A^2 \langle \text{smoothing 1} \rangle + AB \langle \text{smoothing 2} \rangle + BA \langle \text{two crossings} \rangle + B^2 \langle \text{cup and cap} \rangle \quad (2.2.2)$$

Since $\langle \rangle$ and $\langle \text{crossing} \rangle$ are linearly independent, in order for $\langle \cdot \rangle_g$ to be invariant under R2, we need $A^2 + ABd + B^2 = 0$, and $AB = 1$. These choices define the Kauffman bracket.

Definition 2.2.2 Let the *Kauffman bracket* $\langle \cdot \rangle : \mathcal{D} \rightarrow \mathbb{Z}[q, q^{-1}]$ be the function $\langle \cdot \rangle_g$ above with $A = q$, $B = q^{-1}$ and $d = -(q^2 + q^{-2})$.

Lemma 2.2.3 *The bracket polynomial is a regular isotopic invariant of links.*

Proof: By construction, the bracket polynomial is invariant under R2; that the bracket polynomial is invariant under R3 follows from R2 and is a standard and elementary exercise in knot theory. \square

The Kauffman bracket is unfortunately not invariant under R1, but it is possible to counter this deficiency by combining the bracket with another regular isotopy invariant.

Definition 2.2.4 To an oriented link diagram L , assign ± 1 to each crossing according to the convention in Figure 2.1.2. The sum over all the crossings is known as the *writhe* (or *twist number*) of L , denoted $\omega(L)$. The writhe is regular isotopic.

The idea behind this invariant is similar to that of the linking number in Example 2.1.1 of the previous section. The argument used to show the linking number was a link invariant can be used to show the writhe is regular isotopic.

Proposition 2.2.5 *For an oriented link L , define a Laurent polynomial $V(L)$ in q via the formula*

$$V(L) = (-q)^{-3\omega(L)} \langle L \rangle / (q + q^{-1}), \quad (2.2.3)$$

where the Kauffman bracket of an oriented link is defined to be the Kauffman bracket of the link with orientations forgotten. Then $V(\cdot)$ is a link invariant.

Proof: The result follows from simple computations. Explicitly, one can show that the Kauffman bracket satisfies the following relations.

$$\begin{aligned}\langle \text{diagram 1} \rangle &= -q^{-3} \langle \text{diagram 2} \rangle \\ \langle \text{diagram 3} \rangle &= -q^3 \langle \text{diagram 4} \rangle\end{aligned}$$

The local writhe contributions of the first and second diagrams on the left are -1 and 1 respectively, from which it follows that $V(\cdot)$ is invariant under R1. Since the bracket polynomial and the writhe are regular isotopy invariants, the result follows. \square

Recall that the Jones polynomial V_L is defined by its value on the unknot $V_O = 1$ and the Skein relation

$$t^{-1}V_{L_+} - tV_{L_-} = (t^{1/2} - t^{-1/2})V_{L_0}. \quad (2.2.4)$$

Theorem 2.2.6 *After changing variables by setting $q = t^{-1/4}$, the polynomial link invariant $V(\cdot)$ defined in (2.2.3) above satisfies the Skein relation (2.2.4) and takes the value of 1 on the unknot. That is, $V(\cdot)$ is the Jones polynomial.*

Proof: By definition, the bracket polynomial satisfies

$$\langle \text{diagram 5} \rangle_g = q \langle \text{diagram 6} \rangle_g + q^{-1} \langle \text{diagram 7} \rangle_g,$$

$$\langle \text{diagram 8} \rangle_g = q \langle \text{diagram 9} \rangle_g + q^{-1} \langle \text{diagram 10} \rangle_g.$$

These imply

$$q \langle \text{diagram 5} \rangle_g - q^{-1} \langle \text{diagram 8} \rangle_g = (q^2 - q^{-2}) \langle \text{diagram 6} \rangle_g$$

which in turn imply

$$-q^4 V(L_+) + q^{-4} V(L_-) = (q^2 - q^{-2}) V(L_0)$$

for any Conway triple (L_+, L_-, L_0) . This is exactly the Skein relation (2.2.4) after substituting $q = t^{-1/4}$ and multiplying through by -1 . \square

The Kauffman bracket not only simplifies computations, but is useful theoretically too. As Kauffman wrote after proving this theorem, “Some formal results about the Jones polynomial follow immediately and trivially from [Theorem 2.2.6] and the definition of the bracket polynomial.” Indeed, in the same paper, Kauffman shows that any two simple alternating projections of a given link have the same number of crossings, a conjecture held for more than a century.

We will not pause to look into such deep results, but will look at some basic properties of the Jones polynomial which are easily explained with the bracket polynomial.

Proposition 2.2.7 *Let $L!$ denote the mirror image of a link L . Then $V_{L!}(t) = V_L(t^{-1})$.*

Proof: The result follows from a number of observations. First, note that evaluating the Kauffman bracket on a crossing is the same as evaluating the Kauffman bracket on the mirror image of the crossing then changing variables via $q \mapsto q^{-1}$. Secondly, $-(q^2 + q^{-2}) = -((q^{-1})^2 + (q^{-1})^{-2})$. Finally, the writhe of $L!$ is the negative of the writhe of L . \square

This implies that if the Jones polynomial of a given link is not invariant under the change of variables $t \mapsto t^{-1}$, then it is chiral. For instance, the trefoil has Jones polynomial $-t^4 + t^3 + t$, so is chiral. (Although as we saw in Example 1.3.5, this fact is proved more easily by noting that the trefoil is given by $N([3])$.)

The Kauffman bracket also gives a quick proof of results regarding connected sums and disjoint unions: for two oriented links L_1, L_2 , $V(L_1 \# L_2) = V(L_1) \cdot V(L_2)$, and $V(L_1 \sqcup L_2) = -(q^{-1/2} + q^{1/2})V(L_1) \cdot V(L_2)$.

Before moving on to the next section, let us reflect on what we have seen in the chapter so far. We saw in the previous section that the Jones polynomial is an example of a polynomial link invariant, and can be defined in terms of a skein relation. In this section we saw how the Kauffman bracket gives an alternating description of the Jones polynomial using the idea of smoothings.

Khovanov homology *categorifies* the Jones polynomial. We explain what this means in the next chapter, but crucial to the construction is the idea of smoothings. The Jones polynomial of a link is computed by evaluating the Kauffman bracket on all the smoothings of a link diagram, then summing these up (and then normalizing the result). Similarly in Khovanov's original categorification of the Jones polynomial, the Khovanov complex of link is constructed by assigning a vector space to each smoothing of a link diagram, then assembling the vector spaces together into a complex. We briefly discuss this construction, and categorification more generally, in the following section.

2.3 Categorifying the Jones polynomial

In this section we briefly discuss Khovanov original categorification of the Jones polynomial [Kho99]. We'll first motivate categorification by looking at the Euler characteristic of a surface, and why simplicial homology categorifies this. We'll then describe categorifications of \mathbb{Z} and $\mathbb{Z}[q, q^{-1}]$ before sketching Khovanov's categorification of the Jones polynomial. Much of the content of this section is based on an expository paper by Khovanov, [Kho16].

One of the most elementary connections between low-dimensional topology and algebra is *Euler's polyhedron formula*. This states that $V - E + F = 2$ for all convex polyhedra. The formula does not hold for polyhedra in general, so we can give the quantity $\chi = V - E + F$ a name: the *Euler characteristic*. We can easily extend the definition to simplicial complexes and finite CW-complexes. (For an n -complex, $\chi = \sum_i (-1)^n k_i$, where k_i is the number of i -simplices; for a CW-complex, $\chi = \sum_i (-1)^i k_i$ where k_i is the number of i -cells in the complex.) In either case we can regard the Euler characteristic as a map

$$\chi : \text{nice topological spaces} \longrightarrow \mathbb{Z}.$$

From this viewpoint one can say something more interesting about the Euler characteristic of a space. In particular, it is an invariant of the homotopy type of the space. (Euler's polyhedron formula just expresses the fact that all convex polyhedra are homotopic to a sphere.) In this way, the Euler characteristic can distinguish many objects, such as all closed orientable surfaces. But the fact that the Euler characteristic is an integer limits its usefulness as an homotopy type invariant. There are other alternatives, and as Bar-Natan puts it [Bar04] "homology is way better."

The simplicial homology groups of a space provide far more information about the space than the Euler characteristic, and exist for any topological space, not just the nice ones. We can use this property to generalize the Euler characteristic to all topological spaces via

the formula

$$\chi(M) = \sum_{n \geq 0} (-1)^n \dim H_n(M).$$

It is a result of simplicial homology theory that this definition agrees with the previous definitions of the Euler characteristic defined for nice spaces.

It is nice that the Euler characteristic admits a generalization with homology groups, but the real reason why simplicial homology is important is that it provides another level of connection between topology and algebra that the Euler characteristic couldn't. Homology is a *functor*

$$\text{Top} \xrightarrow{H} \text{GrAb},$$

so (continuous) maps between topological spaces induce maps between the homology groups. Simplicial homology a functor at the heart of algebraic topology, and underpins many deep results of the field.

The Euler characteristic is a useful, though admittedly quaint, map, but *categorifies* to homology. The set of nice spaces is lifted to the category of topological spaces, the set of integers is lifted to graded abelian groups, and the Euler characteristic is lifted to homology.

Categorification in general follows the same idea: a set-theoretic structure is replaced with a category-theoretic structure. Elements, sets, and functions become objects, categories and functors respectively. Usually categorified structures provide additional structures and information that their decategorified counterparts do not, making them a subject of interest in contemporary mathematics.

Khovanov homology is a categorification of the Jones polynomial. Just as the Euler characteristic sent surfaces to integers, which simplicial homology lifted to graded abelian groups, the Jones polynomial sends oriented links to Laurent polynomials, which Khovanov homology lifts to bigraded complexes.

Since we use a generalization of the Khovanov homology of links to tangles in this thesis³ (described in the next sections), we will not examine the original construction in depth. We will briefly sketch the idea behind it, and explain how the complexes of the construction decategorify to give the (unoriented) Jones polynomial.

Before we do this though, we categorify the ring of Laurent polynomials $\mathbb{Z}[q, q^{-1}]$ in one variable. Since the Jones polynomial takes values in this ring, a sensible place to start thinking about how the link invariant categorifies is to consider what objects the values of the Jones polynomial can lift to. We wish to find a category whose objects decategorify to give Laurent polynomials, and which is ideally equipped with structures that descend to addition and multiplication of Laurent polynomials.

Let us first consider the analogous question for the ring of integers. What structure(s) categorify \mathbb{Z} ? The category Vect_k of finite-dimensional vector spaces over a field k almost works. To each vector space, one can take its dimension, an integer. Moreover, Vect_k is equipped with two operations, direct sum and tensor product, that respect dimension and descend to addition and multiplication of integers:

$$\dim(V \oplus W) = \dim(V) \oplus \dim(W), \quad \dim(V \otimes W) = \dim(V) \otimes \dim(W).$$

This said, there is a serious problem. The dimension of a vector space is, by definition non-negative. One can also negate, and hence subtract integers, but there are no corresponding

³More precisely, we use a weaker version of a generalization of Khovanov homology to tangles which is equivalent on links to the original theory.

operations in Vect_k that descend to these. The category Vect_k categorifies the semiring \mathbb{Z}_+ of positive integers, but not \mathbb{Z} itself.

A solution is to expand Vect_k to $\text{Kom}(\text{Vect}_k)$, the category of *complexes* of vector spaces. In Vect_k we decategorified structures by taking dimension, but in $\text{Kom}(\text{Vect}_k)$, the Euler characteristic of a complex decategorifies structures. (That is, we take the alternating sum of the dimensions of the homology groups of the complex. To make sure this is well-defined we can require the complexes to be finite, that is to only have a finite number of non-zero terms.)

Like vector spaces, complexes can be summed and tensored and in either case the Euler characteristic respects both. Importantly, the category $\text{Kom}(\text{Vect}_k)$ comes with a tool that descends to subtraction when we take the Euler characteristic: the *cone* of a map of complexes.

Let $f : V \rightarrow W$ be a map of complexes. Then $\text{Cone}(f)$ is the complex with objects $V^{n-1} \oplus W^n$, with the differential defined by $-d_V + d_W + f$. A property of this construction is that

$$\chi(\text{Cone}(f)) = \chi(W) - \chi(V).$$

In this way the category of finite complexes of finite vector spaces categorifies the integers, though we can state the relationship more precisely.

By considering each Hom set in $\text{Kom}(\text{Vect}_k)$ up to chain homotopies, the category becomes a *triangulated* category \mathcal{K} . This is a strong property we need not define nor go into, suffice to say that we can take the Grothendieck group of it, and it acquires the structure of a ring. The Euler characteristic then induces a ring isomorphism

$$K(\mathcal{K}) \cong \mathbb{Z}.$$

As a side, there is still much work to be done in categorification; it is still unknown how to categorify the rational numbers for instance. (That is, to find a triangulated monoidal category with Grothendieck ring isomorphic to \mathbb{Q} . [Kho16])

Having categorified \mathbb{Z} , we return to the problem of finding a category with Grothendieck ring isomorphic to $\mathbb{Z}[q, q^{-1}]$. It turns out most of the work is done. The solution is to consider graded vector spaces.

Explicitly, let GVect_k be the category of graded vector spaces over some k . Here every object is written as a direct sum of finite vector spaces $V = \bigoplus_{n \in \mathbb{Z}} V_n$ (where only finitely many V_n are non-zero), and morphisms respect the grading. The objects of GVect_k are assigned a *graded dimension* via

$$\text{qdim}(V) = \sum_{n \in \mathbb{Z}} \dim(V_n) \cdot q^n.$$

The objects of GVect_k hence descend to Laurent polynomials, but as with Vect , none of the coefficients of the polynomials will be negative. Just as when we categorified \mathbb{Z} , we consider $\text{Kom}(\text{GVect}_k)$, requiring that differentials respect the gradings. (That is, $\partial : V_n^m \rightarrow V_n^{m+1}$ for all n, m .)

The homology of a complex V is then a bigraded vector space

$$H(V) = \bigoplus_{n, m \in \mathbb{Z}} H_n^m(V),$$

where each $H_n^m(V)$ is defined as the m th homology of the subcomplex

$$\dots \rightarrow V_n^{m-1} \rightarrow V_n^m \rightarrow V_n^{m+1} \rightarrow \dots .$$

When we take the Euler characteristic of a complex we obtain a Laurent polynomial,

$$\chi(V) = \sum_n \chi(V_n) \cdot q^n = \sum_{n,m} (-1)^m \dim(H_n^m(V)) \cdot q^n .$$

Since V is finite dimensional this is equal to

$$\chi(V) = \sum_{n,m} (-1)^m \dim(V_n^m) \cdot q^n$$

(by the Rank-nullity theorem). As before, direct sums, tensor products and cones of morphisms descend to addition, multiplication and subtraction in $\mathbb{Z}[q, q^{-1}]$.

The category of finite complexes of finite-dimensional graded vectors spaces appears to be an appropriate candidate in which to lift the Jones polynomial. A categorification of the Jones polynomial via this route would associate to each link diagram some complex in this category, which when we take the Euler characteristic gives us the Jones polynomial. Just as the Jones polynomial respects the Reidemeister moves, the homology groups of the complexes would need to respect the Reidemeister moves too.

Khovanov's construction [Kho99] that satisfies these conditions utilizes the Kauffman bracket. Once the Kauffman bracket of a link diagram has been expanded into a sum of smoothings, Khovanov lifts the smoothings to graded vector spaces, and assembles them to form a complex.

As mentioned earlier, since we will be using a variant of Khovanov homology of tangles later on, we won't recreate the original construction here. The interested reader is referred to Bar-Natan's excellent exposition of it in [Bar02]. We will instead briefly sketch the construction and motivate how, if given the idea and the time, one might conceivably create it.

We wish to associate to each link diagram a complex in such a way that the Euler characteristic of the complex gives us the Jones polynomial, and the homology groups of the complex are invariant under the Reidemeister moves. Let us not worry about latter issue for the time being, and just focus on the construction of the complex.

In many respects it is unnatural to normalize the Jones polynomial to take the value of 1 on the unknot. It will be of great benefit to instead consider the *unnormalized Jones polynomial* defined by $\hat{V}(L) = V(L) \cdot (q + q^{-1})$. Furthermore, we will replace the third relation of the Kauffman bracket $\langle \nearrow \searrow \rangle = q^{-1} \langle \nearrow \rangle \langle \searrow \rangle + q^{-1} \langle \nwarrow \rangle \langle \swarrow \rangle$ with $\langle \nearrow \searrow \rangle = \langle \nearrow \rangle \langle \searrow \rangle - q \langle \nwarrow \swarrow \rangle$. Replacing the relation means that the unnormalized Jones polynomial is now defined from the Kauffman bracket via $\hat{V}(L) = (-1)^{n_-} q^{n_+ - 2n_-} \langle L \rangle$ where n_+, n_- are the number of positive and negative crossings in L respectively. The Kauffman bracket is no longer regular isotopic with this definition, but this presents no obstacle.

Instead of requiring that the complex $\mathcal{C}(L)$ we will associate to a link diagram L satisfy $\chi(\mathcal{C}(L)) = J(L)$, we will instead require that $\chi(\mathcal{C}(L)) = \hat{J}(L)$.

Let us now try to directly categorify the (unoriented) Jones polynomial. We will assume that in our method for associating a link diagram to a complex, each possible smoothing of the diagram corresponds to some vector space that forms part of the complex. The complex associated to a link diagram is then created by assembling the vector spaces from all the smoothings into a series of vector spaces, then endowing the series with a differential.

Such assumptions about the construction may at first seem too broad to help shape the construction, but this is not true. Consider for instance the crossingless diagram of the unknot. This trivially has one smoothing, namely itself, and as such the chain complex we associate to the diagram will have the form

$$0 \rightarrow V \rightarrow 0.$$

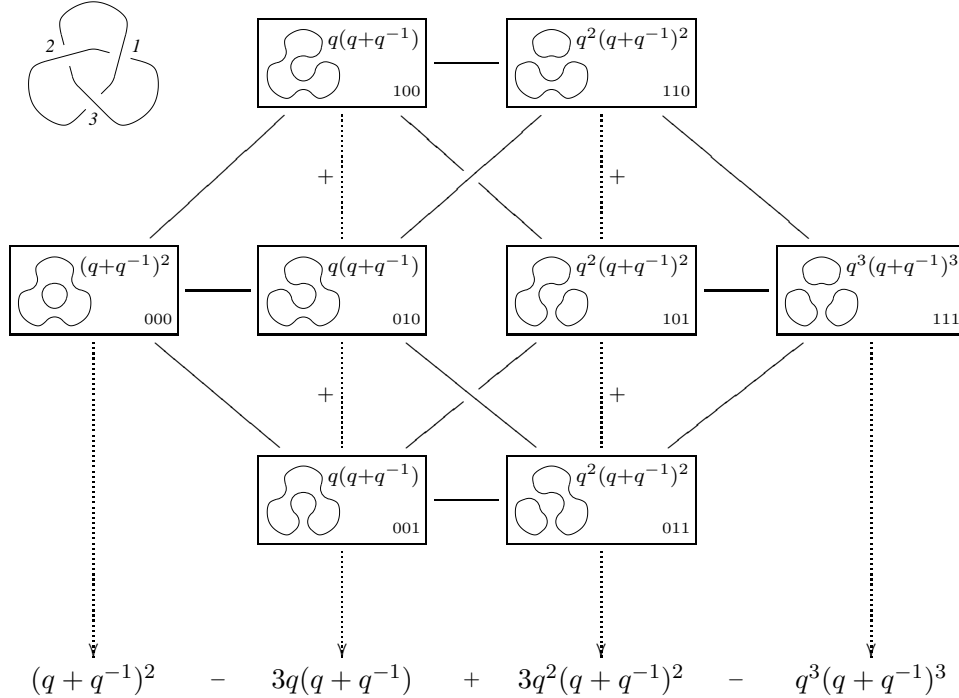
We'll assume V is in homological degree 0. If we want the Euler characteristic to descend to the unoriented Jones polynomial we need $\chi(\mathcal{C}(O)) = \text{qdim}(V) = \hat{V}(O) = q + q^{-1}$. This forces V to have two basis vectors, denoted 1 and X , in degrees -1 and 1 respectively.

The complex associated to a crossingless diagram $O^{\otimes n}$ of n circles will also consist of one non-trivial vector space. In this case however, we need $\chi(\mathcal{C}(O^{\otimes n})) = \hat{V}(O^{\otimes n}) = (q + q^{-1})^n$. The sensible complex to assign to $O^{\otimes n}$ is then

$$0 \rightarrow V^{\otimes n} \rightarrow 0.$$

Since any smoothing of a link diagram is a disjoint union of circles, we've determined the vector spaces the construction will assign to each smoothing. It is not obvious how to assemble the vector spaces corresponding to the smoothings of link diagram into a complex though.

The solution is hinted at by the following illustration computing the unoriented Jones polynomial of the trefoil by Bar-Natan. [Bar02]



Each of the smoothings contributes $(-q)^a(q + q^{-1})^b$ to the overall unoriented Jones polynomial where b is the number of disjoint circles in the smoothing, and a is the number of 1-smoothings in the state associated to the smoothing of a diagram.

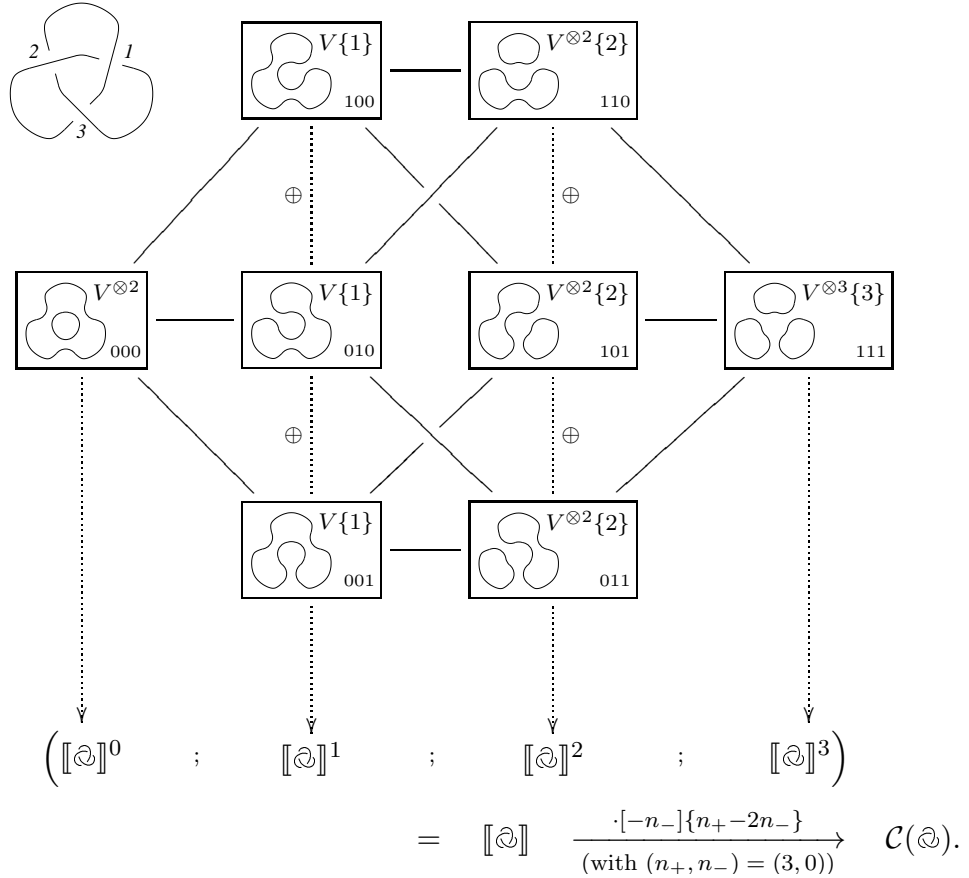
We have already assigned to every smoothing with b disjoint circles a vector space $V^{\otimes b}$ with graded dimension $(q + q^{-1})^b$. By shifting the internal gradings of the vector spaces, we can modify their graded dimension to $(-q)^a(q + q^{-1})^b$.

More precisely, for an arbitrary graded vector space $V = \bigoplus_n V_n$, define a graded vector space $V\{l\}$ by $V\{l\} := V_{n-l}$. Then $\text{qdim } V\{l\} = q^l \text{qdim } V$.

One can also shift the spaces comprising a chain complex. If $\dots \rightarrow C^n \rightarrow C^{n+1} \rightarrow \dots$ is a chain complex, then define a chain complex $C[m]$ by $C[m]^n := C^{n-m}$.

With these notions, if we forget for the moment the issue of differentials, we can associate to each link diagram a complex whose Euler characteristic is the unnormalized Jones polynomial.

We consider all the smoothings of a link diagram L , and assign to each the vector space $V^{\otimes b}\{a\}$, where b is the number of disjoint circles in the smoothing and a is the number of 1-smoothings in the state associated to the smoothing of a diagram. We take the direct sum of all the vector spaces whose gradings have been shifted by the same amount i , and place the vector space in homological degree i . Assuming it is possible to add differentials between these spaces, we obtain a complex C . This process is illustrated below for the trefoil. The figure is also due to Bar-Natan. [Bar02]



By construction, we have that $\chi(C[-n_-]\{n_+ - 2n_-\}) = \hat{V}(L)$. (One can see this by comparing Bar-Natan’s illustrations above.)

We will not discuss the construction any further, but note that it isn’t actually to difficult to determine what differential of the complex should be. (That is, to determine the maps (edges) between the vectors spaces (vertices) in the above diagram.) The interested reader is referred to [Kho16] for further details.

Of course, there is much work in setting setting up this construction rigourously, and proving that the homology of the complexes associated to a link diagram is invariant under

the Reidemeister moves.

In this thesis we examine the Khovanov homology of rational *tangles*, but the construction above doesn't immediately extend to tangles: in the construction, the vector spaces we assigned to the smoothings depended on the number of disjoint loops they contained. It is not obvious how to assign a vector space to a smoothing with boundary.

Khovanov's solution was to instead consider a complex of bimodules ([Kho01]). He constructed a family of rings, then associated to each smoothing a bimodule over these rings. The bimodules were then assembled to form a complex in a way similar to the original construction.

Soon after Khovanov formulated his extension, Bar-Natan created an alternative extension to tangles. Whereas Khovanov's extension was very algebraic, Bar-Natan's version was very topological. Bar-Natan's theory also provided an easier proof of several properties of Khovanov homology, such as its functorality (though we don't discuss this), as well as satisfying a very nice composition property.

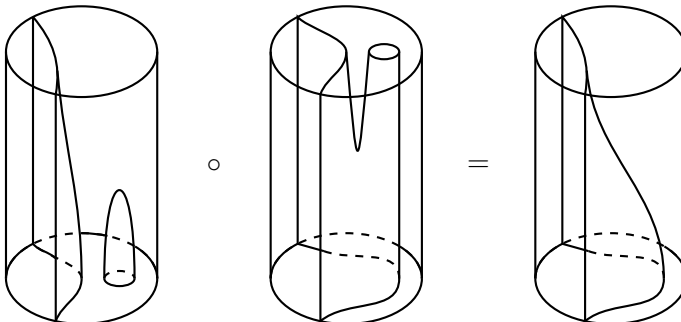
In the next section, we construct Bar-Natan's 'topological' version of Khovanov homology. By the chapter's end, we will have specialized this to the theory we will use in Chapter 3, as well as proving that the Khovanov complex the theory constructs is invariant under the Reidemeister moves.

2.4 Bar-Natan's approach

In an effort to try and keep this thesis as self-contained as possible, we present Bar-Natan's extension to Khovanov homology to tangles. His exposition is so clear and self-contained that we think it would be a mistake from it. As such, we embarrassingly present a 'compressed' version of the exposition from [Bar04] we need. If at any stage the reader is lost by what we write below, we refer her directly to the source.

Definition 2.4.1 The category $Cob^3(\emptyset)$ is defined as follows. Its objects are smoothings (simple curves in the plane) with morphisms that are cobordisms between such smoothings. By a cobordism we mean an oriented two-dimensional surface embedded into $\mathbb{R}^2 \times [0, 1]$ whose boundary lies in $\mathbb{R}^2 \times \{0, 1\}$. More generally, for a finite set of points B in S^1 , define a category $Cob^3(B)$ as follows. Its objects are smoothings now with boundary boundary B . The Hom-sets $Cob^3(B)(\mathcal{O} \rightarrow \mathcal{O}')$ between two smoothings in $Cob^3(B)$ consist of all oriented two-dimensional surfaces embedded into a cylinder with boundary $(\mathcal{O} \times \{0\}) \cup (B \times [0, 1]) \cup (\mathcal{O}' \times \{1\})$. In both categories we consider cobordisms up to boundary preserving isotopies. Composition is defined by placing one cobordism on top of the other and vertically renormalizing the result.

The term Cob^3 will sometimes be used as a generic reference to $Cob^3(\emptyset)$ or $Cob^3(B)$.



We now create a category consisting of vectors and matrices in $\mathcal{C}ob^3$. Recall that a category is *preadditive* if its Hom-sets are Abelian groups and composition of morphisms is bilinear. Note that every category \mathcal{C} , if not already preadditive, can be modified to a preadditive category \mathcal{C}' by defining the Hom-sets $\mathcal{C}'(\mathcal{O} \rightarrow \mathcal{O}')$ to be the free Abelian group generated by $\mathcal{C}(\mathcal{O} \rightarrow \mathcal{O}')$.

Definition 2.4.2 Given a preadditive category \mathcal{C} , define a preadditive category $\text{Mat}(\mathcal{C})$ as follows. The objects of $\text{Mat}(\mathcal{C})$ are formal direct sums (possibly empty) of objects of \mathcal{C} . The Hom-sets $\text{Mat}(\mathcal{C})(\oplus_{i=1}^m \mathcal{O}_i \rightarrow \oplus_{j=1}^n \mathcal{O}'_j)$ consist of $m \times n$ matrices (F_{ij}) of morphisms $F_{ij} : \mathcal{O}_i \rightarrow \mathcal{O}'_j$ in \mathcal{C} . Addition in $\text{Mat}(\mathcal{C})(\oplus_{i=1}^m \mathcal{O}_i \rightarrow \oplus_{j=1}^n \mathcal{O}'_j)$ is just matrix addition while composition of morphisms in $\text{Mat}(\mathcal{C})$ is defined in the obvious way:

$$((F_{ij}) \circ (G_{jk}))_{ik} := \sum_j F_{ij} \circ G_{jk}.$$

We will sometimes represent the objects of $\text{Mat}(\mathcal{C})$ by column vectors and the morphisms of $\text{Mat}(\mathcal{C})$ as (marked) arrows taking one column to another. (Such as in the proof of the invariance of the Khovanov bracket under R2 and R3 in Section 2.6.)

Definition 2.4.3 Given a preadditive category \mathcal{C} , define the category of complexes $\text{Kom}(\mathcal{C})$ to be the category with objects chains of finite length

$$\dots \xrightarrow{\partial_{n-1}} C_n \xrightarrow{\partial_n} C_{n+1} \xrightarrow{\partial_{n+1}} C_{n+2} \xrightarrow{\partial_{n+2}} \dots$$

(only finitely many terms are not the zero object) such that $\partial_n \circ \partial_{n-1} = 0$ for all n .

Define the Hom-sets $\text{Kom}(\mathcal{C})(C \rightarrow D)$ to be the set of all chain maps from C to D . Chain maps $F : C \rightarrow D$ are, as usual, collections of morphisms $(F_i)_{i \in \mathbb{Z}}$ taking $F_i : C_i \rightarrow D_i$ and satisfying $\partial_n F_n = F_{n-1} \partial_n$. Composition in $\text{Kom}(\mathcal{C})$ via $(F \circ G)_r = F_r \circ G_r$.

We now have the appropriate definitions to define the Khovanov complex $[[T]]$ of an oriented tangle diagram T .

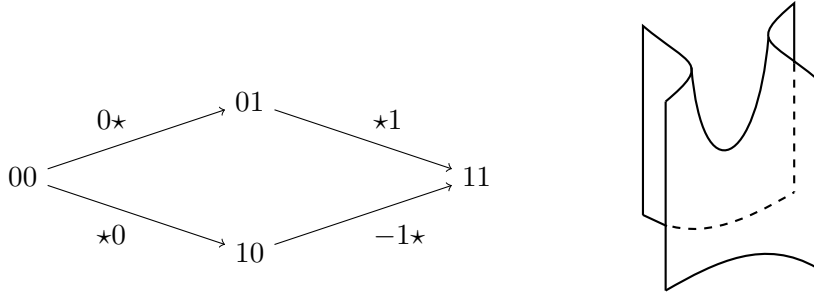
Definition 2.4.4 Let n_+ and n_- be the number of positive and negative crossings in T , and the total number of crossings be n . Number the crossings from 1 to n . Let S be the set of states for T , expressed as a word in $\{0, 1\}$ where the n -th letter denotes the smoothing assigned to the n -th crossing. (That is, S is the set of all words of length n in $\{0, 1\}$.)

Construct a n -dimensional ‘combinatorial’ cube from S as follows. The vertices are the elements of S , and two vertices are connected by an edge iff the vertices differ from each other by one letter. Furthermore orient these edges, representing them as arrows, so that the head of the arrow points towards the larger word (when the words are viewed as integers).

We also attach a word of length n in $\{0, 1, \star\}$ to each arrow. The word is identical in each letter to the words on the head and tail of the arrow, except in the place where they differ, for which the word has letter \star .

To finish constructing the combinatorial cube, assign a positive or negative sign to each arrow depending on the word attached to it: if an arrow is labeled by the word $\xi = \xi_1 \xi_2 \dots \xi_n$, then the arrow has sign $(-1)^{\sum_{i < j} \xi_i}$ where $\xi_j = \star$.

The combinatorial cube corresponding to a diagram with 2 crossings is pictured below.



Now turn the combinatorial cube into a ‘topological’ cube. Replace each vertex V with the smoothing of T associated to the state V . Leave the arrows, but replace the word ξ on each arrow by a cobordism M in $\mathcal{Cob}^3(\partial T)(\xi(0) \rightarrow \xi(1))$ as follows. (Here $\xi(i)$ is the smoothing of T associated to the state obtained from ξ by replacing \star with i .)

Aside from a small disk D containing the smoothings of the crossing corresponding to \star , the smoothings $\xi(0)$ and $\xi(1)$ are identical. Define M to be equal to the identity morphism outside of $D \times [0, 1]$ — that is, equal to $(D^c \cap T) \times [0, 1]$. To complete M , fill in the missing cylindrical slot with a saddle cobordism, illustrated above.

To complete the construction of the topological cube, view the cobordism as an element in the preadditive category $\mathcal{Cob}^3(\partial T)$, making it positive or negative depending on the sign associated to the arrow ξ is on.

We have constructed a topological cube whose vertices are objects of $\mathcal{Cob}^3(\partial T)$ and whose edges are morphisms in $\mathcal{Cob}^3(\partial T)$.

We now view the cube as an element of $\text{Kom}(\text{Mat}(\mathcal{Cob}^3(\partial T)))$. To achieve this, first consider the set of states S , viewed as words in $\{0, 1\}$. Partition S into $n + 1$ sets by the number of 0s in a word. Now turn each set into a vector, arranging the words from smallest to largest (when viewed as integers). Refer to the vector consisting of words with i 0s as the i -th vector.

This series of vectors of words in $\{0, 1\}$ encode a way to arrange the vertices of the topological cube into a series of vectors of smoothings in the obvious way. Once the vertices of the topological cube have been arranged into these vectors, each vector of smoothings can be regarded as an object of $\text{Mat}(\mathcal{Cob}^3(\partial T))$. The set of arrows between the vectors can be regarded as a matrix in $\text{Mat}(\mathcal{Cob}^3(\partial T))$. (If there is no arrow between entries in the vectors, the map is a zero morphism.)

Finally, in order to view the topological cube as a complex in $\text{Mat}(\mathcal{Cob}^3)$, we must assign homological degrees to each vector. Assign to the n -th vector the homological degree $n - n_-$. This complex is the *Khovanov complex of T* , denoted $\llbracket T \rrbracket$. We call $\llbracket \cdot \rrbracket$ the *Khovanov bracket*.

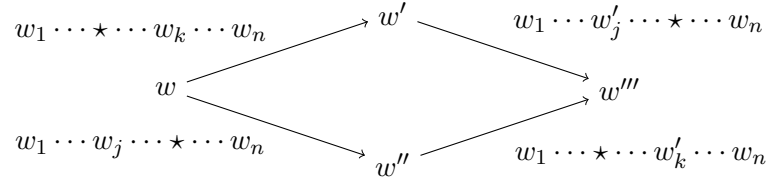
We need to check that the Khovanov bracket is well-defined. That is, that $\llbracket T \rrbracket$ is actually a complex for all T .

Proposition 2.4.5 *For any oriented tangle diagram T , $\llbracket T \rrbracket \in \text{Kom}$.*

Proof: The claim will follow if we can show that every face of the topological cube anticommutes. To see why, note that the entry $(\partial_{n+1} \circ \partial_n)_{ij}$ is equal to the sum of all paths in the cube from $\llbracket T \rrbracket_i^n$ to $\llbracket T \rrbracket_j^{n+2}$. (Where $\llbracket T \rrbracket_i^n$ is the i th entry in the vector $\llbracket T \rrbracket^n$.) These paths are precisely the paths on the face of the topological cube containing $\llbracket T \rrbracket_i^n$ and $\llbracket T \rrbracket_j^{n+2}$. It follows that if every face anticommutes, every entry of $\partial_{n-1} \circ \partial_n$ will be zero.

If we ignore signs on the cobordisms, each face in the topological cube commutes. This is because we are considering cobordisms up to isotopy, and spatially separated saddles in a cobordism can be time-reordered by isotopy.

The anticommutativity of the faces then follows if we can show each face has an odd number of negative cobordisms. Consider a face (without signs) of the combinatorial cube, illustrated below. Here words w and w''' differ in the j -th and k -th letters. Letters that have changed are indicated with a dash.



Recalling the definition of the combinatorial cube, one can see that arrows from $w \rightarrow w'$ and $w'' \rightarrow w'''$ will have the same sign, while the sign of $w' \rightarrow w'''$ and $w \rightarrow w''$ will differ. It follows that each face in the topological cube has an odd number of cobordisms. \square

We now have a way of associating a complex to a diagram of a tangle, but it's currently not a tangle invariant. When considered up to homotopy equivalence in a certain quotient category $\text{Kom}(\text{Mat}(\text{Cob}_{\mathcal{L}}^3))$, however, it is.

Definition 2.4.6 Two morphisms $F, G : C \rightarrow D$ in $\text{Kom}(\mathcal{C})$ are said to be *homotopic*, denoted $F \sim G$, if there exist morphisms $(h_i)_{i \in \mathbb{Z}}$ with $h_i : C_i \rightarrow D_{i-1}$ for which $F_i - G_i = \partial_{i+1}h_i + h_{i-1}\partial_i$.

We note that this notion of homotopy is no different to that in usual homological algebra, except that we are now in a more complicated category than vector spaces or modules. It is not difficult to verify that homotopy is an equivalence relation, and is invariant under left and right composition. We write $\text{Kom}_{/h}(\mathcal{C})$ to denote $\text{Kom}(\mathcal{C})$ modulo homotopies. In order to simplify notation, we will denote $\text{Kom}(\text{Mat}(\text{Cob}_{\mathcal{L}}^3(\partial T)))$ and $\text{Kom}(\text{Mat}(\text{Cob}_{\mathcal{L}}^3(\emptyset)))$ by $\text{Kob}(\partial T)$ and $\text{Kob}(\emptyset)$. We will sometimes refer to both categories collectively as Kob .

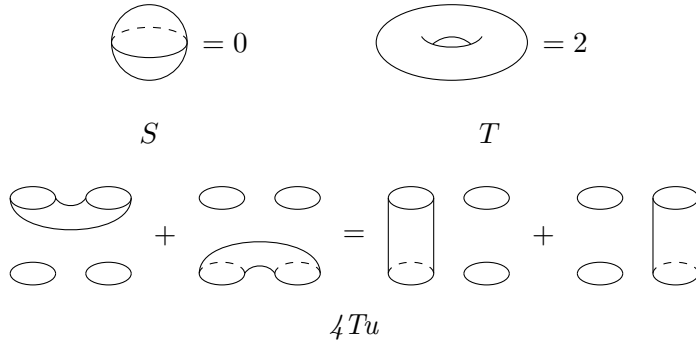
Definition 2.4.7 Two complexes C, D are said to be *homotopy equivalent*, denoted $C \sim D$, if they are isomorphic in $\text{Kom}_{/h}(\mathcal{C})$. That is, if there are chain maps $F : C \rightarrow D$ and $G : D \rightarrow C$ in $\text{Kom}(\mathcal{C})$ for which $G \circ F$ and $F \circ G$ are homotopic to the identity.

It is easy to check that homotopy equivalence is an equivalence relation on complexes. We now define the quotient category for which the Khovanov bracket is a tangle invariant.

Definition 2.4.8 Let $\text{Cob}_{\mathcal{L}}^3$ be the quotient category obtained from Cob^3 by reducing Cob^3 by the local relations S, T and $4Tu$ described below.

- S : Whenever a cobordism contains a component isotopic to a sphere, the cobordism is equal to 0.
- T : Whenever a cobordism contains a component isotopic to a torus, the component may be removed and the remaining cobordism multiplied by a factor of 2.
- $4Tu$: Assume the intersection of a cobordism C with a ball is the union of four disks D_1 through to D_4 . Let C_{ij} denote the result of removing D_i and D_j from C and replacing them by a tube with the same boundary. The $4Tu$ relation states $C_{12} + C_{34} = C_{13} + C_{24}$.

We can summarize the above relations with the following pictures.



We are now in a position to state exactly how the Khovanov bracket is a tangle invariant.

Theorem 2.4.9 *The isomorphism class of $[[T]]$ regarded in $\text{Kob}_{h_j}(\partial T)$ is an invariant of the tangle T . The complex does not depend on the ordering of the crossings chosen in its construction, and is invariant under the Reidemeister moves.*

We will not prove this form of the Khovanov bracket is invariant under the Reidemeister moves. (But will prove the ‘dotted’ version of Bar-Natan’s theory we use is in Section 2.6.) The proof in [Bar04] involves the construction of explicit chain homotopies, and is in many respects the most difficult section of the paper. We now discuss the excellent composition properties the Khovanov bracket enjoys.

Definition 2.4.10 A d -input planar arc diagram D is an ‘output’ disk with:

- d smaller ‘input’ disks removed. The input disks are numbered 1 to d , each with a basepoint $(*)$ on its boundary.
- a collection of disjoint embedded arcs that are closed or begin and end on the boundary of an output or input disk transversely.

The output disk contains a basepoint on its boundary too. We consider planar arc diagrams up to isotopy, and they may be oriented or unoriented.

An example of a planar arc diagram can be found in Example 2.4.17. In the sequel, we will often drop the basepoints from planar arc diagrams.

Definition 2.4.11 A collection of sets $\mathcal{P}(k)$ along with operations defined for each (oriented) unoriented planar arc diagram is an (*oriented*) planar algebra if the radial planar arc diagrams act as identities and the following associativity condition holds: if D_i is the result of placing D' into the i -th hole of D (providing the diagrams are compatible), then as operations $D_i = D \circ (I \times \cdots \times D' \times \cdots I)$.

The lack of restrictions on the operations defined for each planar arc diagram makes the definition quite general, though we usually consider sets comprised of topological objects.

Example 2.4.12 Let $\mathcal{T}^0(k)$ denote the collection of all unoriented tangle diagrams in a based disk (a disk with a basepoint on its boundary) with k ends on the boundary, considered up to planar isotopies as usual. Let $\mathcal{T}(k)$ denote the quotient of $\mathcal{T}^0(k)$ by the three Reidemeister moves.

Then $(\mathcal{T}^0(k))_k$ and $(\mathcal{T}(k))_k$ are planar algebras. Let D be a d -input planar arc diagram D with k_i arcs ending on the i -th input disk and k arcs on output disk. Then define an operator

$$D : \mathcal{T}^0(k_1) \times \cdots \times \mathcal{T}^0(k_d) \longrightarrow \mathcal{T}^0(k)$$

by placing the d input tangles into the holes of D . The operators are similarly defined for $(\mathcal{T}(k))_k$. It is clear that the radial planar arc diagrams act as the identity operators. The associativity condition is easily seen to hold too.

Example 2.4.13 The collection $\text{Obj}(\text{Cob}_{/l}^3)$ and the Hom-sets $\text{Mor}(\text{Cob}_{/l}^3)$ are both planar algebras. The first is just a sub planar algebra of $\mathcal{T}(k)$. For the second, we need to specify how a planar arc diagram can act as an operator on cobordisms. The solution is not difficult – $D \times [0, 1]$ is a vertical cylinder with d vertical cylindrical holes connected by vertical curtains. One simply places cobordisms in the holes, which defines an operation from $D : (\text{Mor}(\text{Cob}_{/l}^3))^d \rightarrow \text{Mor}(\text{Cob}_{/l}^3)$.

Both the previous examples may seem, for lack of a better word, obvious: clearly one can fill up the holes of a planar arc diagram with tangles to obtain more tangles.

There are situations where the operator a planar arc diagram should correspond to is not obvious. For instance, say we decided to put tangle complexes in the holes of a planar arc diagram. That is, put elements of Kob into planar arc diagrams. Can the planar arc diagrams act as operators on these complexes?

The answer is yes, and the operation is essentially the notion of a tensor product of complexes, with planar arc diagram gluing together the pieces. Let us formalize this. Consider $\text{Kob}(B_k)$ and $\text{Kob}_{/h}(B_k)$ where B_k is some placement of k points on a based circle.

Given a d -input planar arc digram D with k_i arcs ending on the i -th input disk and k arcs ending on the outer boundary, D acts as an operator as follows.

Given complexes $(\Omega_i, d_i) \in \text{Kob}(k_i)$, define $D(\Omega_1 \dots, \Omega_d) = (\Omega, d)$ by

$$\Omega^r := \bigoplus_{r=r_1+\dots+r_d} D(\Omega_1^{r_1}, \dots, \Omega_d^{r_d}), \quad (2.4.1)$$

$$d_{|D(\Omega_1^{r_1}, \dots, \Omega_d^{r_d})} := \sum_{i=1}^d (-1)^{\sum_{j<1} r_j} D(I_{\Omega_1^{r_1}}, \dots, d_i, \dots, I_{\Omega_d^{r_d}}). \quad (2.4.2)$$

The basic properties of tensor products transfer over to tensor products in this context; in particular a morphism $\Psi_i : \Omega_{ia} \rightarrow \Omega_{ib}$ induces a morphism $D(I, \dots, \Psi_i, \dots, I) : D(\Omega_1, \dots, \Omega_{ia}, \dots, \Omega_d) \rightarrow D(\Omega_1, \dots, \Omega_{ib}, \dots, \Omega_d)$. Homotopies at the level of tensor factors induce homotopies at the levels of tensor products.

These facts essentially constitute the proof of the following proposition.

Proposition 2.4.14 *The collection $(\text{Kob}(B_k))$ is a planar algebra. Furthermore, the operations D on $(\text{Kob}(B_k))$ send homotopy equivalent complexes to homotopy equivalent complexes, meaning $\text{Kob}_{/h}(B_k)$ also has a natural structure of a planar algebra.*

The upshot of all this is that the Khovanov bracket respects the tensoring operations associated to a planar arc diagram. We need another definition to state this precisely.

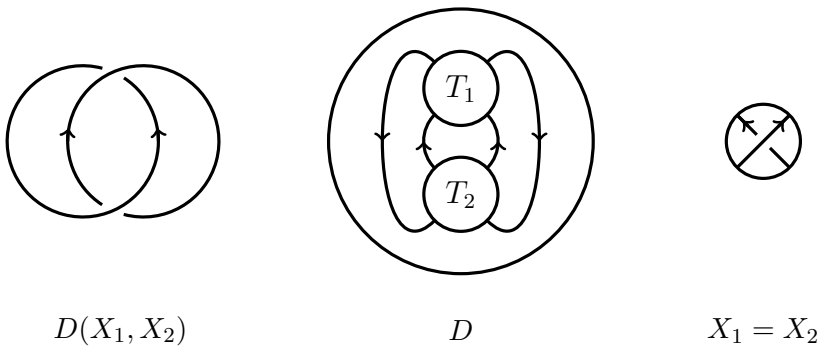
Definition 2.4.15 A morphism Φ of planar algebras from $(\mathcal{P}(k)) \rightarrow (\mathcal{Q}(k))$ is a collection of maps $\Phi : \mathcal{P}(k) \rightarrow \mathcal{Q}(k)$ satisfying $\Phi \circ D = D \circ (\Phi \times \dots \times \Phi)$ for every D .

Theorem 2.4.16 *The Khovanov bracket $[[\cdot]]$ is an oriented planar algebra morphism $[[\cdot]] : (\mathcal{T}(s)) \rightarrow (\text{Kob}_{/h}(B_s))$.*

One proves this by showing that the theorem holds when all inputs to a planar arc diagram are restricted to single crossings; the result in general follows from this and the associativity of the planar algebras involved.

We will use Theorem 2.4.16 extensively in the sequel. Before we develop the theory further we pause to go through an example utilizing these concepts.

Example 2.4.17 Let us calculate the the Khovanov complex of the Hopf link below. We can view the link as the result of inserting the tangle diagrams below into the planar arc diagram illustrated.



We can then use the property that $[[\cdot]]$ is a morphism of planar algebras:

$$[[\text{Hopf}]] = [[D(X_1, X_2)]] = D([[X_1]], [[X_2]]).$$

From the definition of $[[\cdot]]$ we have

$$[[X_1]] = [[X_2]] = \underbrace{)}_{(1)} \underbrace{(}_{(2)} \xrightarrow{\text{H}} \underbrace{)}_{(2)} \underbrace{(}_{(1)}.$$

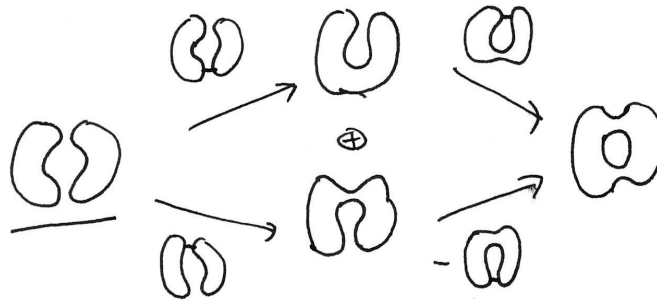
Here, and in the sequel, we've underlined the object of the complex that is in homological degree zero. The symbol H is a shorthand to denote the saddle map; in depictions of saddle cobordisms in the sequel we will use the same notation.

Using equations (2.4.1) and (2.4.2), we construct $[[\text{Hopf}]]$.

$$\begin{array}{ccccc}
 & & D(1, \text{H}) & \rightarrow & D(\rangle \langle, \underline{\text{H}}) & \xrightarrow{D(\text{H}, 1)} & & & D(\underline{\text{H}}, \underline{\text{H}}) \\
 & & & & & & & & & \\
 D(\rangle \langle, \rangle \langle) & & & & & \oplus & & & & \\
 & & & & & & & & & \\
 & & D(\text{H}, 1) & \rightarrow & D(\underline{\text{H}}, \rangle \langle) & \xrightarrow{-D(1, \text{H})} & & & \\
 & & & & & & & & & \\
 \underline{[[\text{Hopf}]]}^0 & \longrightarrow & \underline{[[\text{Hopf}]]}^1 & \longrightarrow & \underline{[[\text{Hopf}]]}^2 & & & & &
 \end{array}$$

When we calculate the objects and morphisms of this complex by placing the appropriate

smoothings and cobordisms into D , we obtain



The original Khovanov homology theory was bigraded. We now equip the theory so far with a bigrading too.

Definition 2.4.18 A *graded category* is a preadditive category \mathcal{C} with the following two properties:

1. The Hom-sets of \mathcal{C} form a graded abelian group, composition respects the gradings ($\deg f \circ g = \deg f + \deg g$), and all identity maps have degree 0.
2. There is a \mathbb{Z} -action $(m, \mathcal{O}) \mapsto \mathcal{O}\{m\}$, called “grading shift by m ” on the objects of \mathcal{C} . As plain abelian groups, morphisms are unchanged by the action, $\text{Mor}(\mathcal{O}_1\{m_1\}, \mathcal{O}_2\{m_2\}) = \text{Mor}(\mathcal{O}_1, \mathcal{O}_2)$, but gradings do: if $f \in \text{Mor}(\mathcal{O}_1, \mathcal{O}_2)$ and $\deg f = d$, then as an element of $\text{Mor}(\mathcal{O}_1\{m_1\}, \mathcal{O}_2\{m_2\})$ we have $\deg f = d + m_2 - m_1$.

If a preadditive category \mathcal{C} satisfies only the first property above, it can be extended to a category \mathcal{C}' that has the second property too: let the objects of \mathcal{C}' be copies of the original objects but with integers attached. (That is, $\mathcal{O}\{m\}$ for all $\mathcal{O} \in \mathcal{C}$ and $m \in \mathbb{Z}$.) It is clear how to define a \mathbb{Z} -action on \mathcal{C}' , how to define the Hom-sets $\text{Mor } \mathcal{C}'$, and how to grade $\text{Mor } \mathcal{C}'$.

If we extend a preadditive category \mathcal{C} to a graded category we will still refer to the graded version as \mathcal{C} . When writing a complex in a graded category, we will often denote the gradings of its objects in brackets. (Such as in the proof of the invariance of the Khovanov bracket under R1 in Section 2.6.)

We note that if \mathcal{C} is graded category then $\text{Mat}(\mathcal{C})$ can be considered as a graded category: a matrix is homogeneous in degree d iff all its entries are of degree d . Similarly complexes in $\text{Kom}(\mathcal{C})$ (or $\text{Kom}(\text{Mat}(\mathcal{C}))$) are graded categories.

We now define a grading on the Hom-sets of Cob^3 , and as a result Kob becomes a graded category.

Proposition 2.4.19 For a cobordism $C \in \text{Mor}(\text{Cob}^3(B))$ with $|B|$ vertical boundary components, define $\deg C := \chi(C) - \frac{1}{2}|B|$, where χ is the Euler characteristic. Then $\text{Cob}^3(B)$, and $\text{Cob}_{\text{fl}}^3(B)$ are graded categories.

Proof: It is not hard to verify that the degree is additive under composition in $\text{Cob}^3(B)$, and under horizontal composition using the planar algebra structure of $\text{Cob}^3(B)$. It is easy to verify that the S , T and $4Tu$ relations are degree-homogeneous, from which it follows that $\text{Cob}_{\text{fl}}^3(\mathcal{C})$ is a graded category. \square

We now refine the definition of the Khovanov bracket, and the invariance theorem, to accommodate gradings.

Definition 2.4.20 In the definition of the Khovanov bracket, if T has n_+ positive crossings and n_- negative crossings, $\llbracket T \rrbracket$ has the form

$$\bullet \rightarrow \llbracket T \rrbracket^{-n_-} \longrightarrow \dots \longrightarrow \llbracket T \rrbracket^{n_+} \rightarrow \bullet$$

where \bullet is the zero object. Now add gradings to the objects of $\llbracket T \rrbracket$ by endowing $\llbracket T \rrbracket^r$ with grading $\llbracket T \rrbracket^r \{r + n_+ - n_-\}$, so that the complex is now

$$\bullet \rightarrow \llbracket T \rrbracket^{-n_-} \{n_+ - 2n_-\} \longrightarrow \dots \longrightarrow \llbracket T \rrbracket^{n_+} \{2n_+ - n_-\} \rightarrow \bullet.$$

In the sequel the Khovanov bracket, unless otherwise stated, will be assumed to have graded objects as just described.

This allows us to recast the results as follows.

Theorem 2.4.21 *With the Khovanov bracket graded as per Definition 2.4.20, the following properties hold.*

1. *All differentials in $\llbracket T \rrbracket$ are of degree zero.*
2. *Up to degree-0 homotopy equivalence, $\llbracket T \rrbracket$ is an invariant of the tangle T . That is, if T_1 and T_2 differ by some Reidemeister moves, then there is a degree-0 homotopy equivalence $F : \llbracket T_1 \rrbracket \rightarrow \llbracket T_2 \rrbracket$.*
3. *The Khovanov bracket descends to a planar algebra morphism $(\mathcal{T}(s)) \rightarrow (\text{Kob}(s))$ and all the planar algebra operations are of degree 0.*

Proof: We omit the proof, though it is not difficult. It essentially amount to checking that the constructions created up to this point (in particular the homotopy equivalences use to prove the invariance of the bracket). \square

We have seen how to extend Khovanov's categorification of the Jones polynomial to the case of tangles, and do in such a way that allows us to work with a topological complex instead of an algebraic one. One of the benefits of working in this setting is the excellent composition properties of the Khovanov bracket. But we haven't addressed the issue of whether the bracket is a useful invariant. That is, how good is it at distinguishing tangles?

If we wished to answer this question we would need to be able to determine when two complexes in Kob are not homotopy equivalent. Showing this directly is very difficult, so we instead construct a functor to take the topological complex into an algebraic one. In the process much information about the complex is lost, but at least in the algebraic world it is easier to determine if two complexes are not homotopy equivalent – one takes homology, and if the homology groups differ, the complexes are not homotopy equivalent.

Formally, consider a functor $\mathcal{F} : \text{Cob}_{\mathcal{I}}^3 \rightarrow \mathcal{A}$ where \mathcal{A} is some abelian category. It extends easily to a functor $\mathcal{F} : \text{Mat}(\text{Cob}_{\mathcal{I}}^3) \rightarrow \mathcal{A}$, and hence to a functor $\mathcal{F} : \text{Kob} \rightarrow \text{Kom}(\mathcal{A})$. Just as $\llbracket T \rrbracket$ is an invariant of T up to homotopy equivalence in Kob , so too is $\mathcal{F}\llbracket T \rrbracket$ an invariant up to homotopy equivalence in \mathcal{A} . Hence the isomorphism class of the homology groups $H^*(\mathcal{F}\llbracket T \rrbracket)$ is an invariant of T . Of course, if \mathcal{A} is graded and \mathcal{F} is degree respecting, then $H^*(\mathcal{F}\llbracket T \rrbracket)$ is a graded invariant of T .

We will now construct such a functor for $\text{Cob}_{\bullet}^3(\emptyset)$. The objects of the category $\text{Cob}_{\bullet}^3(\emptyset)$ are just disjoint unions of circles (\circ), while the morphisms are generated by the the cap, cup, pair of pants and upside-down pair of pants. (This is a well-know result about $(1+1)$ -dimensional TQFTs, refer to any standard text for a proof of the claim.) For brevity

we will denote the pair of pants and upside-down pair of pants cobordisms by \bigcirc and $\bigcirc\bigcirc$ respectively. As such a functor $\mathcal{F} : \mathcal{Cob}_1^3(\emptyset) \rightarrow \mathcal{A}$ doesn’t need much data.

Definition 2.4.22 Let V be the free abelian group generated by $\mathbf{1}$ and X . We make V into a graded abelian group by assigning $\deg \mathbf{1} = -1$ and $\deg X = 1$.

Now define a TQFT $\mathcal{F} : \mathcal{Cob}^3 \rightarrow \mathbb{Z}\text{Mod}$ by $\mathcal{F}(\bigcirc) = V$, $\mathcal{F}(\text{cup}) = \varepsilon : \mathbb{Z} \rightarrow V$, $\mathcal{F}(\text{cap}) = \eta : V \rightarrow \mathbb{Z}$, $\mathcal{F}(\bigcirc\bigcirc) \rightarrow m : V \otimes V \rightarrow V$, and $\mathcal{F}(\bigcirc) = \Delta : V \rightarrow V \otimes V$. These maps are defined by

$$\begin{aligned} \mathcal{F}(\text{cap}) &= \varepsilon : \mathbf{1} \mapsto \mathbf{1}, \\ \mathcal{F}(\text{cup}) &= \eta : \mathbf{1} \mapsto 0, \quad X \mapsto 1 \\ \mathcal{F}(\bigcirc\bigcirc) &= m : \begin{cases} \mathbf{1} \otimes X \mapsto X, & \mathbf{1} \otimes \mathbf{1} \mapsto \mathbf{1}, \\ X \otimes \mathbf{1} \mapsto X, & X \otimes X \mapsto 0, \end{cases} \\ \mathcal{F}(\bigcirc) &= \Delta : \begin{cases} \mathbf{1} \mapsto \mathbf{1} \otimes X + X \otimes \mathbf{1}, \\ X \mapsto X \otimes X. \end{cases} \end{aligned}$$

Proposition 2.4.23 *The functor \mathcal{F} defined above is well-defined and degree respecting. It descends to a functor $\mathcal{F} : \mathcal{Cob}_1^3(\emptyset) \rightarrow \mathbb{Z}\text{Mod}$.*

In Khovanov’s original construction for links [Kho99], he essentially constructed the topological cube, though didn’t view it as an element in Kob . Instead he immediately turned the vertices and cobordisms into modules and maps and obtained a complex. The functor used to do this was precisely the one above; as such for links we have that $H^*(\mathcal{F}[[L]]) \cong Kh(L)$, where $Kh(L)$ is Khovanov’s original categorification of the Jones polynomial.

This concludes the section. We have seen Bar-Natan’s extension of Khovanov’s original homology theory to the case of tangles. We saw that one of the benefits of this topological perspective is the composition properties of the Khovanov bracket – it is a morphism of planar algebras. We also saw that in the case of links, one can recover the homology groups of Khovanov’s original construction by applying a certain TQFT to the construction.

We did not sketch the proof of that the Khovanov bracket is actually a link invariant. One of the reasons we avoided this is because Kob is a difficult category to work with, and as such the proof is not elementary. As will we see in the next section, by tweaking Kob to a different category Kob_\bullet , a tool for simplifying complexes is introduced that makes life significantly easier. Almost all of the theory developed so far carries over, so moving to Kob_\bullet presents no problem. As a bonus, in Kob_\bullet the proof of the invariance of the Khovanov bracket is much nicer, as we will see in Section 2.6.

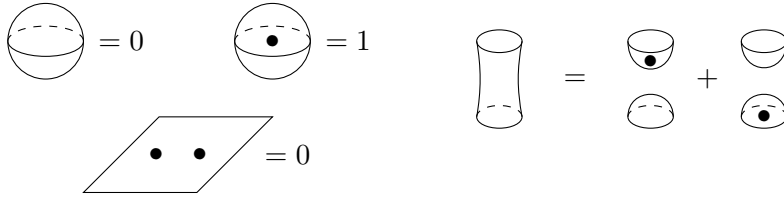
2.5 Bar-Natan’s dotted theory

We now construct a ‘dotted’ version of the theory presented in the previous section. We change the category Kob in which the complexes lie to a ‘dotted’ version Kob_\bullet , but it is otherwise business as usual. The reason we move to the dotted setting is that it allows us to consider new homotopy equivalences. (Our main result, Theorem 3.3.1, is built on two such isomorphisms.) In the case of links however, the theory is equivalent to standard Khovanov homology. After first constructing Kob_\bullet , we show the equivalence of the restricted theory

by constructing a TQFT (Proposition 2.5.2). We then introduce an isomorphism involving cobordisms specific to Kob_\bullet (Lemma 2.5.3), then close the section with a more general tool for simplifying complexes (Lemma 2.5.4).

We extend Cob^3 to a category of dotted cobordisms Cob_\bullet^3 . This has the same objects as Cob^3 , but morphisms are now allowed to have dots (of degree -2) on their surface. Dotted cobordisms are considered to be isotopic if their underlying cobordisms are isotopic and contain the same number of dots on each connected component. As with Cob^3 , morphisms in Cob_\bullet^3 are considered up to boundary-preserving isotopy.

We then quotient out Cob_\bullet^3 by the following local relations to form $\text{Cob}_{\bullet/l}^3$.



We call the last relation *neck cutting*. Note that the S , T and $4Tu$ relations of $\text{Cob}_{\bullet/l}^3$ hold in Cob_\bullet^3 too: by definition S holds. When neck cutting is applied to a torus (viewed as a cobordism), it splits into a sum of dotted spheres; the sum then simplifies into a sum of two empty diagrams from which relation T follows. Similarly one applies neck cutting to either side of the $4Tu$ relation; both sides simplify to the same four-term sum of dotted disks.

Just as we denoted $\text{Kom}(\text{Mat}(\text{Cob}_{\bullet/l}^3))$ by Kob , we will denote $\text{Kom}(\text{Mat}(\text{Cob}_{\bullet/l}^3))$ by Kob_\bullet .

Since the S , T and $4Tu$ relations hold in $\text{Cob}_{\bullet/l}^3$, the proof that $\llbracket T \rrbracket$ is an isotopy invariant of T up to degree-0 homotopy equivalences in $\text{Kob}(\partial T)$ extends to $\text{Kob}_\bullet(\partial T)$. But as we mentioned previously, verifying the invariance of $\llbracket T \rrbracket$ under the Reidemeister moves in $\text{Kob}(\partial T)$ is hard. Not so in $\text{Kob}_\bullet(\partial T)$, as we will see in the next section. The reduction in complexity of the proof is due to an isomorphism that uses dotted cobordisms. The isomorphism is also central to our work in the next chapter.

But we must first create a TQFT for this dotted setting. The presence of dots in the theory mean TQFTs well-defined in $\text{Cob}_{\bullet/l}^3$ don't immediately extend to Cob_\bullet^3 . This said, the functor in Definition 2.4.22 which gives ordinary Khovanov homology does extend to a functor from $\text{Cob}_{\bullet/l}^3$ to the category $\mathbb{Z}\text{Mod}$ of graded \mathbb{Z} -modules. Instead of describing this functor directly, we will create the functor as a specialization of the following functor.

Definition 2.5.1 Let B be a finite set of points in S^1 and let \mathcal{O} be an object of $\text{Cob}_{\bullet/l}^3(B)$. Define a *tautological functor* $\mathcal{F}_{\mathcal{O}} : \text{Cob}_{\bullet/l}^3(B) \rightarrow \mathbb{Z}\text{Mod}$ on objects by $\mathcal{F}_{\mathcal{O}}(\mathcal{O}') := \text{Mor}(\mathcal{O}, \mathcal{O}')$ and on morphisms by composition on the left. That is, send the morphism $F : \mathcal{O}' \rightarrow \mathcal{O}''$ to the map $\mathcal{F}_{\mathcal{O}}(F) : \text{Mor}(\mathcal{O}, \mathcal{O}') \rightarrow \text{Mor}(\mathcal{O}, \mathcal{O}'')$ which takes $G \in \text{Mor}(\mathcal{O}, \mathcal{O}')$ to $F \circ G \in \text{Mor}(\mathcal{O}, \mathcal{O}'')$.

Various specializations of this tautological functor lead to different variants of Khovanov homology. Lee's variant [Lee02], for example, is obtained by setting

$$\mathcal{F}(\mathcal{O}') := \mathbb{Z}/2\mathbb{Z} \otimes_{\mathbb{Z}} \text{Mor}(\emptyset, \mathcal{O}')/G$$

where G is the relation setting the genus three surface to a numerical factor of 8.

Proposition 2.5.2 Define tautological functors for objects in $\text{Cob}_{\bullet/l}^3(B)$ as above. Then the functor $\mathcal{F}_{\emptyset} : \text{Cob}_{\bullet/l}^3(\emptyset) \rightarrow \mathbb{Z}\text{Mod}$ restricted to the subcategory $\text{Cob}_{\bullet/l}^3(\emptyset)$ is the functor

exhibited before in Definition 2.4.22. That is, for a link L , $H^*(\mathcal{F}_\emptyset[[L]]) \cong Kh(L)$, the original Khovanov homology of L .

Proof: First consider an arbitrary element of $\text{Mor}(\emptyset, \mathcal{O}')$ for some object $\mathcal{O}' \in \text{Cob}_{\bullet, \ell}^3(\emptyset)$. The element can be reduced, by neck cutting, to a sum of terms in which every connected component touches at most one boundary curve. Further neck cutting can be applied so that no connected component has positive genus. Simplifying each term of the sum using the other local relations whenever possible produces a sum of cobordisms in which every connected component has exactly one boundary curve. By our simplifications these connected components are either disks or dotted disks. Hence if \mathcal{O}' contains k curves, $\mathcal{F}_\emptyset(\mathcal{O}') = U^{\otimes k}$ where U is $\mathbb{Z}\{\circ, \odot\}$, the free \mathbb{Z} -module generated by a disk and a dotted disk.

Now identify U and V of Definition 2.4.22 via $\circ = \mathbf{1}$ and $\odot = X$. To check \mathcal{F}_\emptyset is the functor claimed, we must verify it takes the cup, cap, pair of pants and upside down pair of pants to the appropriate maps.

We check the map agrees on both types of pants; the other verifications are trivial.

Since the pair of pants $\circ\circ$ takes two circles to a circle, the map $\mathcal{F}_\emptyset(\circ\circ) : \text{Mor}(\emptyset, \circ\circ) \rightarrow \text{Mor}(\emptyset, \circ)$ is defined by where it sends the generators of $U^{\otimes 2}$. As these are just pairs of (possibly dotted) disks, the cobordism obtained after composition with $\circ\circ$ is isotopic to a (possibly dotted) disk. Explicitly,

$$\circ\circ \mapsto \circ, \quad \circ\odot \mapsto \odot, \quad \odot\circ \mapsto \odot, \quad \odot\odot \mapsto \emptyset.$$

With the above identifications it follows that $\mathcal{F}_\emptyset(\circ\circ) = m$.

For the upside down pair of pants, the map $\mathcal{F}_\emptyset(\triangleleft) : \text{Mor}(\emptyset, \circ) \rightarrow \text{Mor}(\emptyset, \circ\circ)$ sends the disks \circ and \odot to a tube and a dotted tube respectively. After neck cutting these simplify so that the map sends

$$\circ \mapsto \circ\odot + \odot\circ, \quad \odot \mapsto \odot\odot.$$

This is precisely Δ . It follows that \mathcal{F}_\emptyset is the functor claimed.

Like \mathcal{F} , the tautological functor extends to a functor $\mathcal{F}_\emptyset : \text{Kob}_\bullet(\emptyset) \rightarrow \text{Kom}(\mathbb{Z}\text{Mod})$. Since the construction of $[[L]]$ in $\text{Kob}_\bullet(\emptyset)$ is the same as that in $\text{Kob}(\emptyset)$ (and does not involve the creation of dotted cobordisms), $H^*(\mathcal{F}_\emptyset[[L]]) \cong H^*(\mathcal{F}[[L]])$. Since $H^*(\mathcal{F}[[L]]) \cong Kh(L)$, the proposition follows. \square

The benefit of working in with this ‘dotted’ theory is that we can now consider homotopy equivalences involving dotted cobordisms, allowing us to simplify $[[T]]$ in ways not previously possible. In the case of links, with one such isomorphism it is possible to simplify $[[L]]$ so that all of the objects of the complex are direct sums of empty diagrams, the matrices between them taking only integer entries. The isomorphism is described in Lemma 2.5.3 below.

Although this ‘delooping’ process actually increases the number of diagrams in the complex, in practice many of the maps between the diagrams become isomorphisms. One can then apply a categorical version of Gaussian elimination to discard pairs of subobjects related via an isomorphism. Both tools together dramatically simplify complexes.

Perhaps unsurprisingly, these tools can be implemented on a computer. When combined with the composition properties of the Khovanov bracket, a method for rapidly computing the Khovanov complex associated to a tangle is achieved. Indeed, as Bar-Natan found in [Bar06], an implementation of the tools, once optimized, was able to compute the Khovanov

homology of the $(8, 7)$ torus knot $T_{8,7}$ in a matter of minutes. (Note that this knot has 48 crossings – if the complex was computed using the original definition of Khovanov homology, the complex would contain $2.8 \cdot 10^{14}$ objects and $3.8 \cdot 10^{15}$ morphisms. Obviously computing the homology of such a complex is not feasible.)

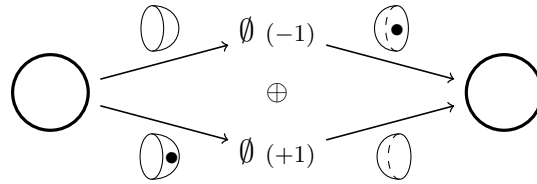
These tools are useful theoretically too – they are bread and butter for our results in the last chapter. The proofs of many results in the dotted setting can be simplified with these tools, such as the invariance of the Khovanov bracket under the Reidemeister moves.

In the undotted setting one proves this via the construction of explicit chain homotopies. The proof still holds in the dotted setting, but one can now instead simplify the complexes associated to either side of a Reidemeister move. As a result the proof is significantly easier. We do this in the next section.

Without further ado, let us see these tools which are used constantly throughout the remainder of the thesis.

Lemma 2.5.3 *If an object S in $\text{Cob}_{\bullet, l}^3$ contains a closed loop l , it is isomorphic in $\text{Mat}(\text{Cob}_{\bullet, l}^3)$ to the direct sum of two copies $S'\{-1\}$ and $S'\{+1\}$ of S in which l is removed, one with a degree shift of -1 and the other with a degree shift of $+1$. Symbolically, $\bigcirc \cong \emptyset\{-1\} \oplus \emptyset\{+1\}$.*

Proof: The isomorphisms are as follows.



The composition taking \bigcirc to \bigcirc follows from neck cutting. The other composition is a matrix whose entries are spheres with various numbers of dots; the other local relations show this matrix is the identity. \square

Lemma 2.5.4 *If $\phi : b_1 \rightarrow b_2$ is an isomorphism in some additive category \mathcal{C} , then the four term complex in $\text{Mat}(\mathcal{C})$*

$$\dots \longrightarrow [C] \xrightarrow{\begin{pmatrix} \alpha \\ \beta \end{pmatrix}} \begin{bmatrix} b_1 \\ D \end{bmatrix} \xrightarrow{\begin{pmatrix} \phi & \delta \\ \gamma & \varepsilon \end{pmatrix}} \begin{bmatrix} b_2 \\ E \end{bmatrix} \xrightarrow{\begin{pmatrix} \mu & \nu \end{pmatrix}} [F] \longrightarrow \dots$$

is isomorphic to the complex

$$\dots \longrightarrow [C] \xrightarrow{\begin{pmatrix} 0 \\ \beta \end{pmatrix}} \begin{bmatrix} b_1 \\ D \end{bmatrix} \xrightarrow{\begin{pmatrix} \phi & 0 \\ 0 & \varepsilon - \gamma\phi^{-1}\delta \end{pmatrix}} \begin{bmatrix} b_2 \\ E \end{bmatrix} \xrightarrow{\begin{pmatrix} 0 & \nu \end{pmatrix}} [F] \longrightarrow \dots$$

Both are homotopy equivalent to the complex

$$\cdots \longrightarrow [C] \xrightarrow{\begin{pmatrix} \beta \end{pmatrix}} [D] \xrightarrow{\begin{pmatrix} \varepsilon - \gamma\phi^{-1}\delta \end{pmatrix}} [E] \xrightarrow{\begin{pmatrix} \nu \end{pmatrix}} [F] \longrightarrow \cdots .$$

Here C, D, E and F are arbitrary columns of objects in \mathcal{C} and all Greek letters (other than ϕ) represent arbitrary matrices of morphisms in \mathcal{C} (having the appropriate dimensions, domains and ranges); all matrices appearing in these complexes are block-matrices with blocks as specified. The claim still holds if b_1 and b_2 are direct sums of objects, provided the matrix ϕ is invertible.

Proof: The 2×2 (block) matrices in the first two complexes above differ by invertible row and column operations – that is, by a change of basis. When the corresponding operations are performed on $\begin{pmatrix} \mu & \nu \end{pmatrix}$ and $\begin{pmatrix} \alpha \\ \beta \end{pmatrix}$ these change to $\begin{pmatrix} \mu - \nu\gamma\phi^{-1} & \nu \end{pmatrix}$ and $\begin{pmatrix} \alpha - \phi^{-1}\delta\beta \\ \beta \end{pmatrix}$ respectively. Since the differentials square to 0 we have $\mu\phi - \nu\gamma = 0 = \phi\alpha - \delta\beta$, from which the isomorphism follows.

Note that the second complex segment is the direct sum of the third complex segment and

$$\cdots \longrightarrow 0 \longrightarrow [b_1] \xrightarrow{\begin{pmatrix} \phi \end{pmatrix}} [b_2] \longrightarrow 0 \longrightarrow \cdots .$$

Since ϕ is an isomorphism this complex is contractible. (That is, homotopy equivalent to the zero complex.) It follows that the second (and hence the first) complex segment is homotopy equivalent to the third complex segment. \square

At first glance the tools may seem humble, but in reality they provide a way to radically simplify complexes that are otherwise inaccessible. Examples of delooping and Gaussian elimination in action may be found in the next section (and subsequent chapter).

2.6 Invariance of the Khovanov bracket under the Reidemeister moves

We now prove the invariance of the Khovanov bracket in Kob_\bullet under the Reidemeister moves. There are three separate arguments we need to make, but our approach in each case is the same. We compute the Khovanov complexes associated to both sides of a Reidemeister move, then simplify them using the tools exhibited in the previous section. Since delooping and Gaussian elimination are both homotopy equivalences, if two complexes simplify down to the same complex, the complexes themselves are homotopy equivalent.

This is in contrast to the corresponding proofs in Kob , available in [Bar04], where explicit homotopy equivalences are constructed to prove R1 and R2, while R3 is proved using the map in R2 and various cone constructions.

The length of the arguments presented increases with the number of crossings in the diagrams; as such we work through the Reidemeister moves in order.

Proof of R1 invariance: The Khovanov complex of the ‘twisted’ side of R1 as as

follows.

$$\left[\text{loop} \right] = \bullet \longrightarrow \underset{(-2)}{\text{cup}} \xrightarrow{\text{saddle}} \underset{(-1)}{\text{cap}} \longrightarrow \bullet$$

We deloop the last term to obtain the following isomorphic complex.

$$\bullet \longrightarrow \underset{(-2)}{\text{cup}} \xrightarrow{\begin{pmatrix} 1 \\ \text{saddle} \end{pmatrix}} \begin{matrix} \text{cup} & (-2) \\ \oplus & \\ \text{cup} & (0) \end{matrix} \longrightarrow \bullet$$

Note that when we composed the saddle cobordism with the various cups of the delooping isomorphism, the shape of the cobordism we obtain resembles an arm of a cactus. As such we can isotope this arm back into the main ‘curtain’ of the cobordism, obtaining the cobordisms shown.

The identity cobordism is an isomorphism, so we can further simplify the complex with Gaussian elimination. To eliminate any ambiguity about how Lemma 2.5.4 may be applied, let us write the complex in the form given in the lemma.

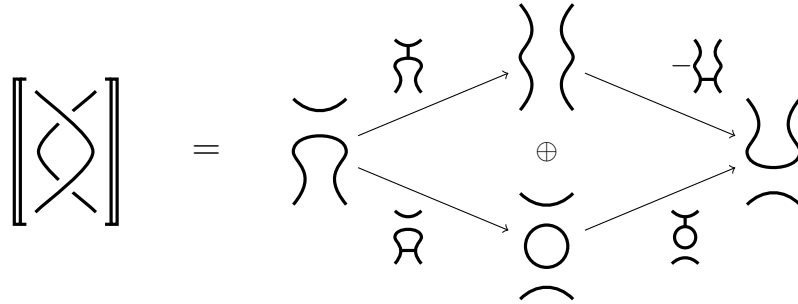
$$\bullet \xrightarrow{\begin{pmatrix} 0 \\ 0 \end{pmatrix}} \begin{matrix} \text{cup} & (-2) \\ \oplus & \\ \bullet & \end{matrix} \xrightarrow{\begin{pmatrix} 1 & 0 \\ \text{saddle} & 0 \end{pmatrix}} \begin{matrix} \text{cup} & (-2) \\ \oplus & \\ \text{cup} & (0) \end{matrix} \xrightarrow{\begin{pmatrix} 0 & 0 \end{pmatrix}} \bullet$$

When the lemma is applied, we obtain

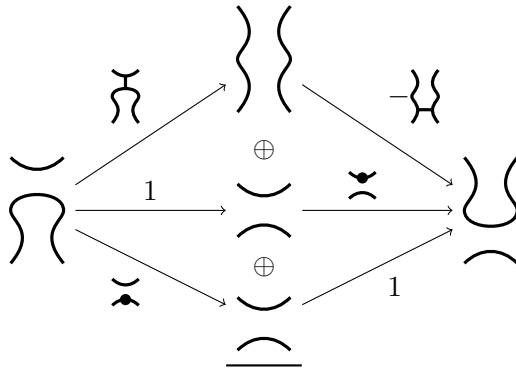
$$\bullet \longrightarrow \underset{(0)}{\text{cup}} \longrightarrow \bullet$$

This is precisely the Khovanov complex of the crossingless tangle corresponding to the other side of R1. □

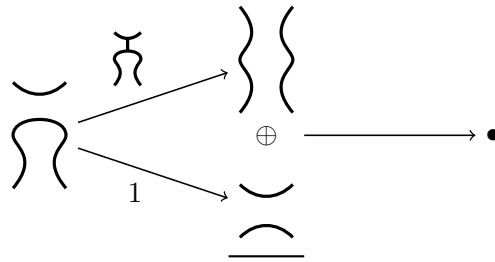
Proof of R2 invariance: The Khovanov complex of the R2 diagram with crossings is as follows.



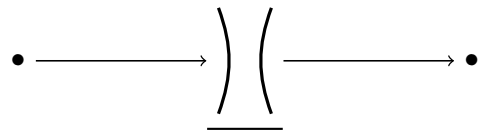
To avoid clutter we've dropped the internal gradings and haven't included the zero objects on the ends. Delooping the only term we can gives us the following complex.



One can instantly see from the isomorphisms here that all but one of the terms will cancel. Applying Gaussian elimination to the isomorphism on the right of the diagram gives



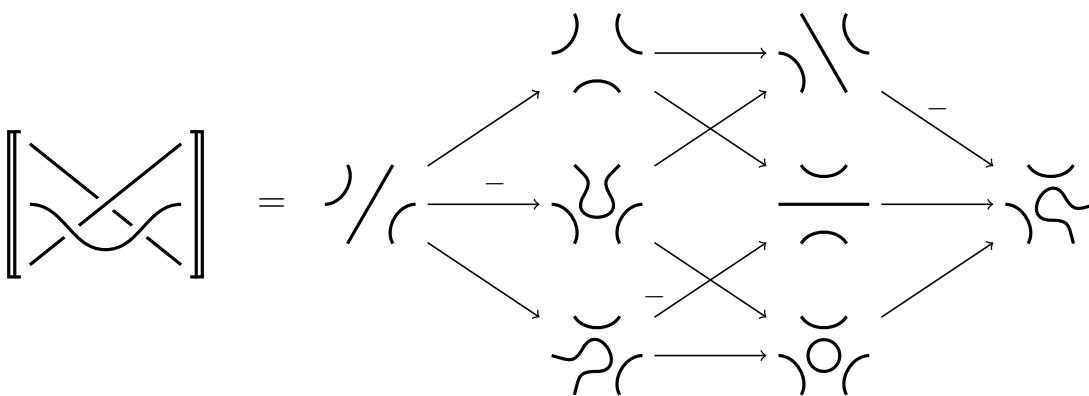
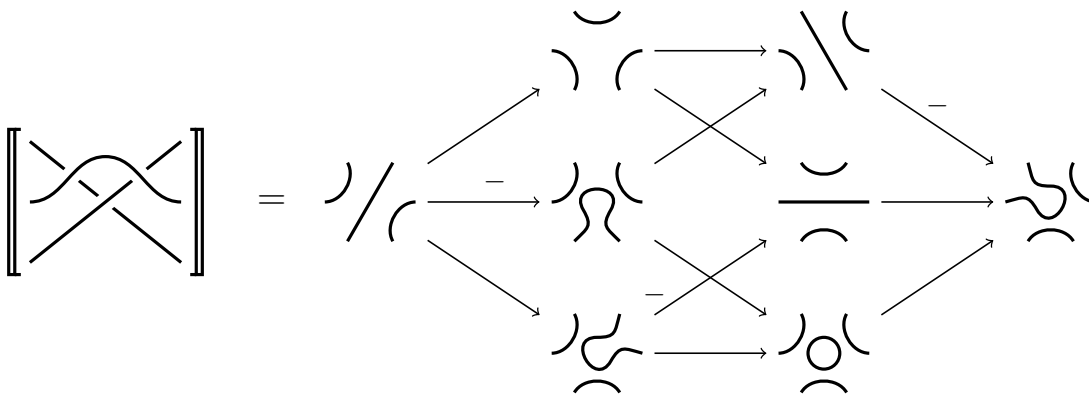
By eliminating the remaining isomorphism we obtain



the complex associated to the 'uncrossed' R2 diagram. □

Proof of R3 invariance: Both sides of the R3 relation contain three crossings and as such the Khovanov complexes are larger than those previously exhibited. The proof is not too bad though.

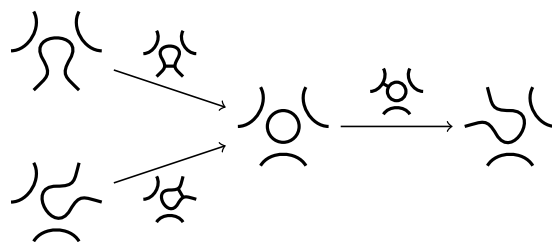
The unreduced Khovanov complexes of both sides of R3 are below.



For clarity we've dropped the cobordisms between the terms; each is a saddle. The minus signs indicate saddles with a negative coefficient. We've also dropped the quantum gradings and homological height information – this depends on the orientation of the components but does not change the argument. We've taken the liberty to isotope several of the objects.

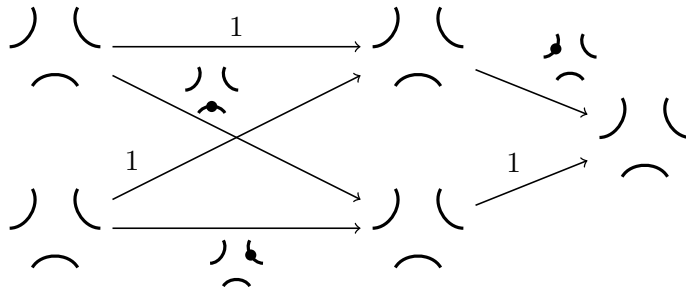
Notice the similarity in the arrangement and type of the subobjects in the complexes.

Let us first simplify the top complex. There is only one indecomposable object in the complex with a loop. The maps going into and out of this object are

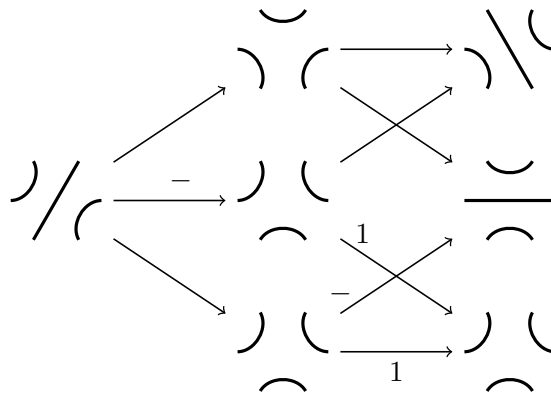


Upon delooping, three isomorphisms are introduced into the complex. The previous part

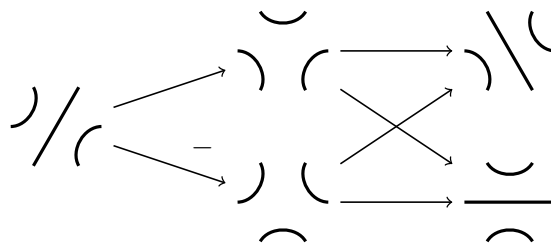
of the complex becomes



Eliminating the right-most isomorphism reduces the complex to

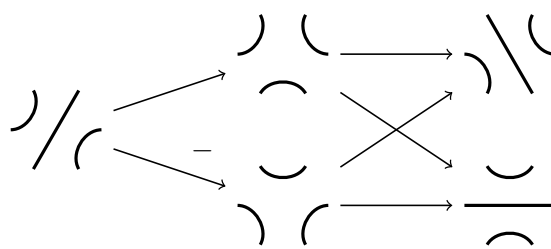


(Here the 1 s indicate identity cobordisms; as before the other maps are saddles.) After eliminating the bottom isomorphism the complex simplifies to



Note that the zero map between the middle diagrams in the second and third columns of the complex has changed to a saddle.

We now examine the Khovanov complex associated to the other side of R3. In exactly the same way as the previous case, this simplifies to



The only difference between this and the other simplified diagram is the location of the negative sign. The following lemma shows the two are the same. \square

Lemma 2.6.1 *Let (C_\bullet, d_\bullet) be a chain complex, and let (C_\bullet, d'_\bullet) denote a chain complex obtained from (C_\bullet, d_\bullet) by negating one of the differential maps. Then $(C_\bullet, d_\bullet) \cong (C_\bullet, d'_\bullet)$.*

Proof: This is trivial, consider the following chain map.

$$\begin{array}{ccccccccccc}
 \cdots & \longrightarrow & C_{n+1} & \xrightarrow{d_{n+1}} & C_n & \xrightarrow{d_n} & C_{n-1} & \xrightarrow{d_{n-1}} & C_{n-2} & \xrightarrow{d_{n-2}} & C_{n-3} & \longrightarrow & \cdots \\
 & & \downarrow 1 & & \downarrow 1 & & \downarrow -1 & & \downarrow -1 & & \downarrow -1 & & \\
 \cdots & \longrightarrow & C'_{n+1} & \xrightarrow{d_{n+1}} & C'_n & \xrightarrow{-d_n} & C'_{n-1} & \xrightarrow{d_{n-1}} & C'_{n-2} & \xrightarrow{d_{n-2}} & C'_{n-3} & \longrightarrow & \cdots
 \end{array}$$

\square

The Khovanov homology of rational tangles

In this chapter we prove that the Khovanov complexes of rational tangles have the structure of zig-zags. Theorem 3.3.1, together with Proposition 4.2.1, essentially provides a complete description of the Khovanov homology of rational tangles. The theorem has practical and theoretical applications. It provides a way to rapidly compute the Khovanov complex of rational tangle (and hence rational knots). The theorem provides an alternative proof of a result for alternating links by Lee [Lee02] in the case of rational knots.

Although in general the Khovanov complex itself is not an invariant, our main Theorem describes how the Khovanov complex of a rational tangle has a particularly simple, and canonical, representative. We describe this representative very explicitly, and suprisingly, the underlying object can be described via the Burau representation of B_3 . The full implications of this observation remain unclear. We will discuss this aspect in the next Chapter.

In Section 3.1 we first use the tools developed in Section 2.5 to determine the Khovanov complex of a integer tangle (Proposition 3.1.1). The proof is by induction, and we find that the complexes $[[n]]$ all share a similar structure. We then introduce a notation with which one can easily describe and visualize the complexes. We illustrate the notation and the result of the section by computing $Kh(7_1)$ (Example 3.1.3).

In Section 3.2 we describe the ‘square isomorphism’ (Proposition 3.2.1). We describe how it can simplify previously inscrutable complexes into the aforementioned canonical form.

Finally, in Section 3.3 we use these results to obtain Theorem 3.3.1. We illustrate the theorem by easily computing $Kh(8_2)$ by hand in Example 3.3.3.

In Chapter 1 we saw that every rational positive (negative) tangle is isotopic to a standard form $\langle a_1, a_2, \dots, a_n \rangle$ where all a_i are non-negative (non-positive) (Definition 1.1.12). In such a form the rational tangle can be constructed from a finite sequence of additions and products with $[+1]$ (*respectively* $[-1]$). This means that the Khovanov complex of a rational tangle can be constructed inductively from $[[\pm 1]]$ by a sequence of intermediate complexes, each one obtained from the next by adding a crossing then immediately simplifying the resulting complex. Theorem 3.3.1 describes precisely how to obtain $[[T + [1]]]$ or $[[T * [1]]]$ from $[[T]]$ by breaking apart the ‘morphism string’ (Section 3.3) of $[[T]]$ into several subwords, applying certain rules to the subwords, and concatenating the result.

For the rest of the thesis, we’ll work with positive tangles. The results for the case of negative tangles are completely analogous. We will also use the notation $[[a_1, a_2, \dots, a_n]]$ throughout the chapter to denote the Khovanov complex of the rational tangle $\langle a_1, \dots, a_n \rangle$.

For those hard-pressed for time, the chapter can be summarized in a triptych of diagrams: Figure 3.1.1, Figure 3.2.5 and Figure 3.3.1. If you understand these, you've understood this chapter.

3.1 The Khovanov complex of integer tangles

In this section we compute the Khovanov complex $[[n]]$ of the integer tangle $[n]$. We do this inductively, using only the aforementioned tools of delooping and Gaussian elimination. The process is summarized in the illustration over the page.

Integer tangles are the building blocks of rational tangles, and understanding their Khovanov homology will allow us to understand the Khovanov homology of rational tangles in general. In particular, the simplification of the Khovanov complexes of integer tangles, described in Proposition 3.1.1 below, is one of the main ingredients in Theorem 3.3.1, the main result of this chapter.

In this section, and in later parts, we will often use Lemma 2.6.1 to simplify results.

Proposition 3.1.1 *Let $n > 0$ and $[n]$ have orientation type II. Then $[[n]]$ is homotopy equivalent to*

$$\begin{array}{ccccccc}) & (\xrightarrow{\quad} \cdots & \xrightarrow{\text{)}(-)\text{)} & (\xrightarrow{\text{)}(+)\text{)} & (\xrightarrow{\text{)}(-)\text{)} & (\xrightarrow{\text{)}\text{)} & \begin{array}{c} \cup \\ \cap \end{array} \\ (-3n+1) & & (-n-5) & (-n-3) & (-n-1) & & (-n) \end{array}$$

Proof: The case $n = 1$ follows directly from the definition of Khovanov homology. The case $n = 2$ is similar to the proof of the invariance of the Khovanov bracket under R2. Namely, we write $[2] = [1] + [1]$ and construct the planar arc diagram D corresponding to tangle addition. Since the Khovanov bracket is a planar algebra morphism, $[[2]] = [[D([1], [1])] = D([[1]], [[1]])$. The complex $D([[1]], [[1]])$ is constructed in Figure 3.1.2 below. We can simplify the complex. Delooping the object in the NW corner gives us

$$\begin{array}{ccc} (-5) &) & \begin{array}{c} \xrightarrow{\text{)}\text{)} \\ \xrightarrow{\text{)}(-)\text{)} \\ \xrightarrow{1} \\ \xrightarrow{-1} \end{array} \\ & & \begin{array}{c} \text{)}\text{)} \\ \text{)}\text{)} \\ \text{)}\text{)} \end{array} \\ (-3) &) & \end{array}$$

After Gaussian elimination, this simplifies to

$$\begin{array}{ccc}) & (\xrightarrow{\text{)}(-)\text{)} & (\xrightarrow{\text{)}\text{)} & \begin{array}{c} \cup \\ \cap \end{array} \\ (-5) & & (-3) & (-2) \end{array}$$

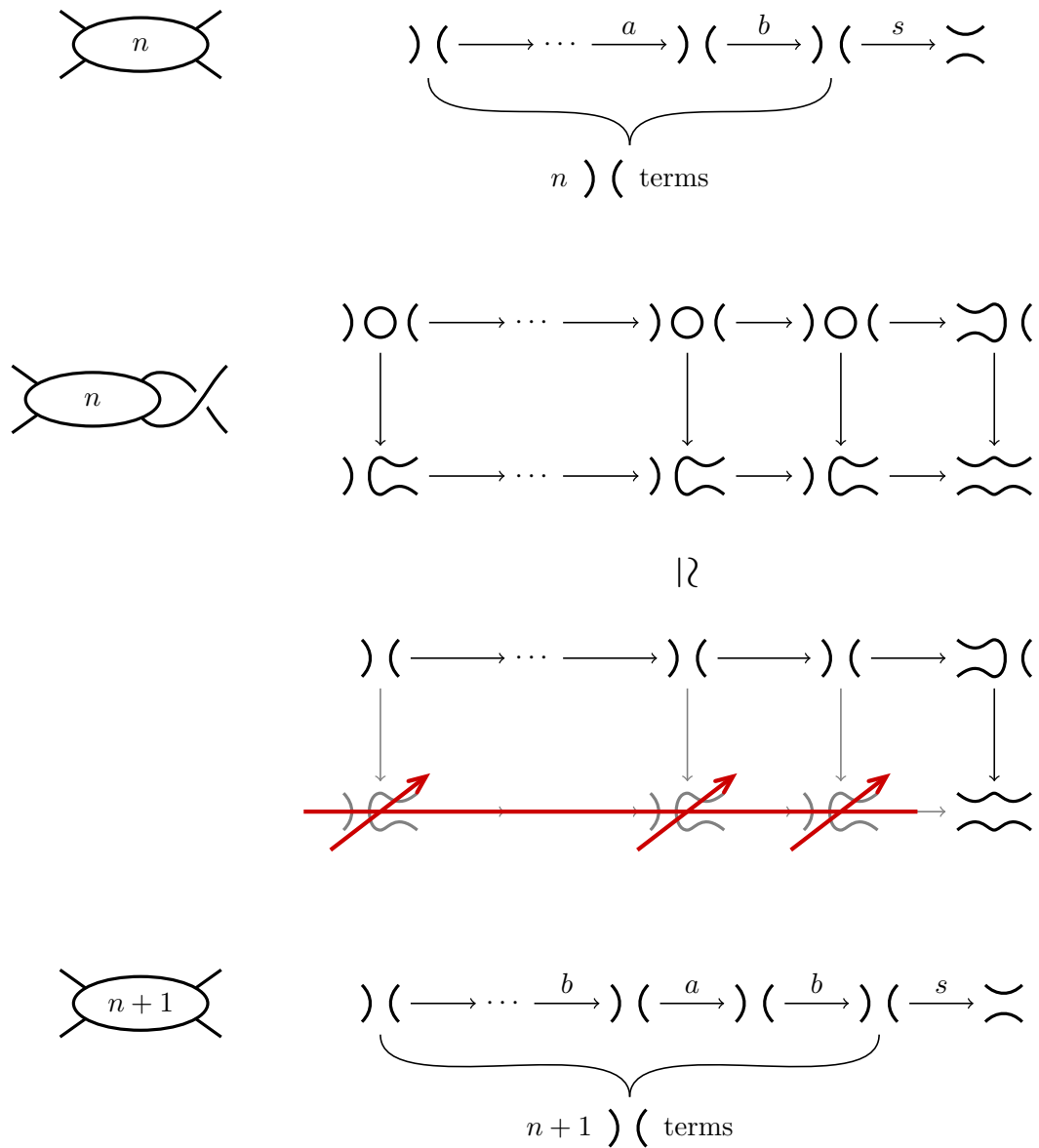


Figure 3.1.1: When an integer tangle is extended by another crossing, the complex picks up another term. This small change in the size of the complex is due to the cancellation of nearly an entire row.

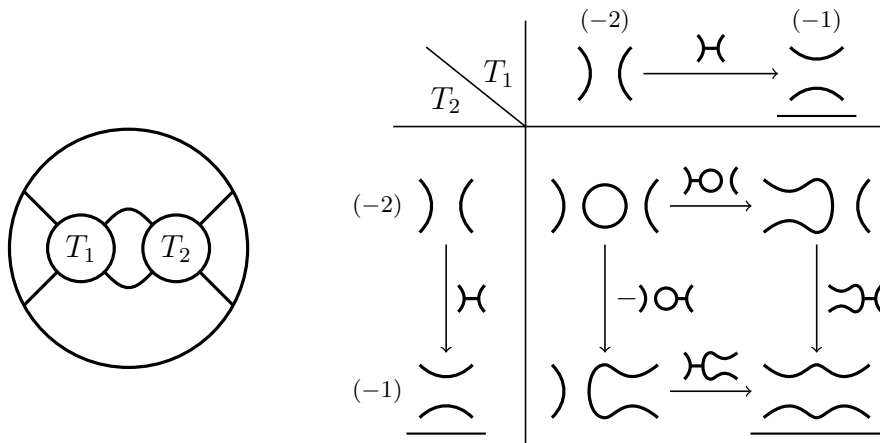


Figure 3.1.2: LEFT The integer tangle [2] is the result of placing the [1] tangle in both holes of the planar arc diagram illustrated. RIGHT Calculating $[[2]]$ from $[[1]]$ and the planar arc diagram to the left.

which is isomorphic to

$$\begin{array}{ccc}
) (\xrightarrow{\text{H}(-)}) (\xrightarrow{\text{H}} \underline{\underline{)}} \\
 (-5) & (-3) & (-2)
 \end{array}$$

Now assume the claim is true for some $n \geq 2$. By using the same ‘addition’ planar arc diagram in Figure 3.1.2 above with $T_1 = [n]$ and $T_2 = [1]$, we have $[[n + 1]] = D([[n]], [[1]])$. This complex is as follows.

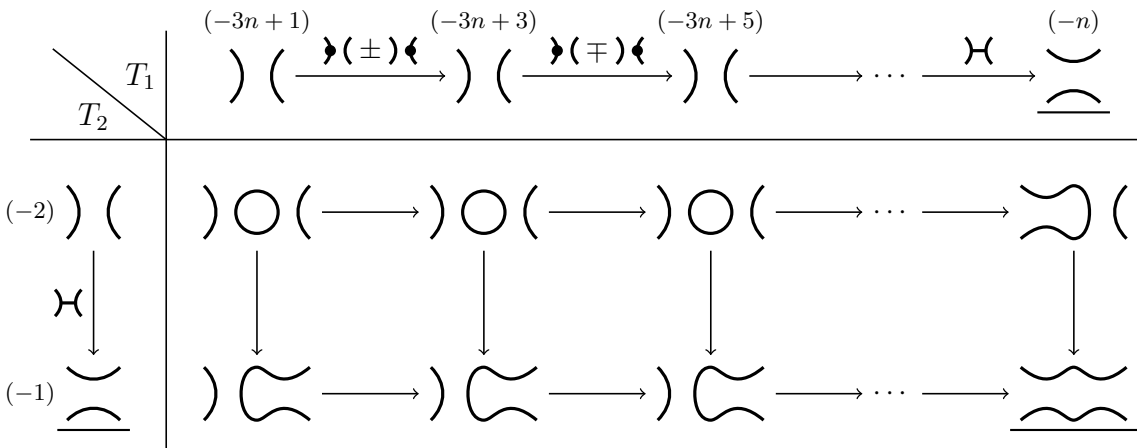
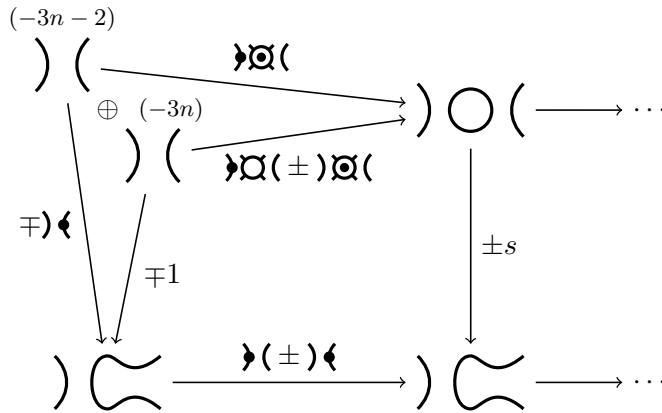


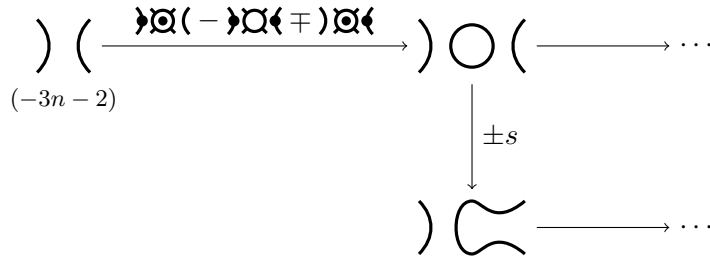
Figure 3.1.3: The complex $[[n + 1]]$ can be computed from $[[n]]$ and $[[1]]$ using the same method in Figure 3.1.2. For readability the morphisms of the complex have been omitted.

We simplify the NW corner of the complex first by delooping, and then Gaussian elimination. The complex obtained after delooping is as follows. (To avoid clutter, in

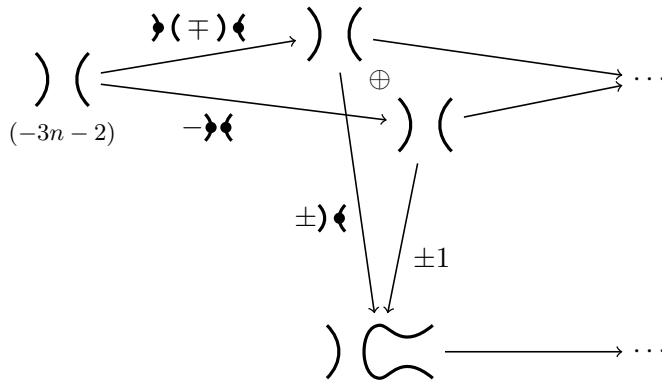
these complexes, and in the sequel, we often denote a saddle morphism by s .)



We then apply Gaussian elimination and obtain the following complex.



Note that the grading on the subobject in the NW corner has decreased by 1 as a result of the simplification. The morphism out of this subobject may appear complicated, but simplifies when the next term is delooped.



A further application of Gaussian elimination clearly removes two more subobjects from this complex.

So far, the complex in Figure 3.1.3 has simplified as follows. Of the four west-most subobjects, the two northern subobjects have been delooped, their quantum grading decreasing by 1, and the two southern subobjects have been eliminated. After each northern subobject was delooped, an isomorphism was introduced, which allowed us to eliminate the subobject directly south of it.

We continue to move left to right through the complex using this method – delooping each successive tangle in the north row and eliminating the object south of it. In general,

when part of the complex has the form

$$\begin{array}{ccccccc}
 \cdots & \longrightarrow & \bigcirc & \left(\xrightarrow{\mathfrak{D}(\pm)\mathfrak{D}(\pm)} \right) & \bigcirc & \left(\longrightarrow \cdots \right. \\
 & & \downarrow \mathfrak{D}(\mp)\mathfrak{D}(\pm) & & \downarrow \mathfrak{D}(\pm)\mathfrak{D}(\pm) & & \\
 \cdots & \longrightarrow & \bigcirc & \xrightarrow{\mathfrak{D}(\pm)\mathfrak{D}(\pm)} & \bigcirc & \longrightarrow \cdots &
 \end{array}$$

it simplifies to

$$\begin{array}{ccccccc}
 \cdots & \longrightarrow & \bigcirc & \left(\xrightarrow{\mathfrak{D}(\mp)\mathfrak{D}(\pm)} \right) & \bigcirc & \left(\longrightarrow \cdots \right. \\
 & & \downarrow \mathfrak{D}(\mp)\mathfrak{D}(\pm) & & \downarrow \mathfrak{D}(\pm)\mathfrak{D}(\pm) & & \\
 \cdots & \longrightarrow & \bigcirc & \xrightarrow{\mathfrak{D}(\pm)\mathfrak{D}(\pm)} & \bigcirc & \longrightarrow \cdots &
 \end{array}$$

That is, we eliminate the southern objects, deloop the northern objects, and ‘conjugate’ the maps between the northern objects. By this, we mean the maps $D(\mathfrak{D}(\pm)\mathfrak{D}(\pm), 1)$ between the northern objects simplify to $\mathfrak{D}(\mp)\mathfrak{D}(\pm)$.

After working down the chain complex, eventually only two subobjects on the southern row remain. These subobjects, together with those directly north of it, form a square consisting only of saddle maps. This square is the complex associated to $\llbracket 2 \rrbracket$, consisting only of saddle maps while the tail consists of the terms of the complex we have delooped. The square is simplified in exactly the same way as we did previously for the $[2]$ tangle, from which the proposition follows. \square

By essentially the same proof, we have the corresponding result for negative integer tangles.

Proposition 3.1.2 *Let $n < 0$ and $[n]$ have orientation type II. Then $\llbracket n \rrbracket$ is homotopy equivalent to*

$$\begin{array}{ccccccc}
 \bigcirc & \xrightarrow{\mathfrak{D}(\mp)\mathfrak{D}(\pm)} & \bigcirc & \left(\xrightarrow{\mathfrak{D}(-)\mathfrak{D}(-)} \right) & \left(\xrightarrow{\mathfrak{D}(+)\mathfrak{D}(+)} \right) & \cdots & \longrightarrow & \bigcirc \\
 (n) & & (n+1) & (n+3) & & & & (3n-1)
 \end{array}$$

As we have just seen, the Khovanov complex of an integer tangle can be dramatically simplified: eventually all the objects of the complex are indecomposable, and there are at most three types of non-zero morphisms between these.

Rational tangles in general do not have complexes as elementary as this. However, it is true that any non-zero map between two indecomposable subobjects in the complex of a rational tangle is (up to sign) one of the six morphisms below.

$$\begin{aligned}
 a &= \text{⤵} (+) \text{⤴} & c &= \text{⤵} + \text{⤴} \\
 b &= \text{⤵} (-) \text{⤴} & d &= \text{⤵} - \text{⤴} \\
 s &= \text{⤵}, \text{⤴}
 \end{aligned}$$

This fact is a consequence of Theorem 3.3.1, and we will often use these abbreviations in the sequel to minimize clutter when depicting complexes.

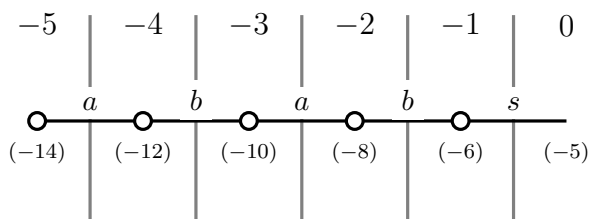
We will also not worry about the signs of morphisms between indecomposable subobjects in general; as one will see, for all of the applications of Theorem 3.3.1 in Chapter 4 such information is irrelevant.

The fact that there are only a small number of map types mean the complexes themselves can be represented in a more efficient way.

To each Khovanov complex of a rational tangle we can construct a *dot diagram*. These contain all the information of the complex but in an easier-to-read form. This notation is useful to visualize the Khovanov complex associated to a rational tangle, and simplifies calculations. By using it we can illustrate how the complex associated to a rational tangle changes when crossings are added to the tangle, as we do in Figure 3.3.1. The chain complexes in this figure contain hundreds of subobjects – it would be impractical to write these out as a sequence of objects and morphisms in the traditional way.

To construct a dot-diagram for a given complex, begin by drawing a number of vertical lines; the spaces between them represent particular homological heights. Denote each $[\infty]$ and $[0]$ subobject in the complex by a circle or dot respectively in the appropriate homological height. If there is a non-zero morphism between two indecomposable objects in the complex, connect the corresponding objects by a line in the dot diagram.

Additional data can be added to the diagram to describe the homological heights, gradings, and morphisms. A dot diagram of $[[5]]$ with such information is illustrated below.



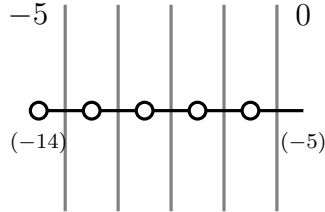
Here the integers at the top denote the various homological degrees, the integers in the brackets represent the gradings of the subobjects, and the letters represent the morphisms using the abbreviations above.

All we've done so far is repeat the information contained in the complex corresponding to $[5]$, but much of this is redundant. By removing all but the essential information we can draw a simpler dot diagram.

- If we assume crossing a vertical line from left to right represents a positive change by 1 in homological degree, we only require one integer at the top of a dot-diagram to calibrate the other homological degrees.
- The morphisms a, b, c, d take objects with grading n to $n + 2$, and saddles s take objects with grading n to $n + 1$. As these are the only morphisms present in the complex of a rational tangle (proved later), provided the dot diagram is connected (in the graph-theoretical sense), the grading of one subobject determines the others.

- Not all morphisms need to be described. Since $d^2 = 0$, the identity of many morphisms can be determined from others.

The last point is best illustrated with an example. Let us redraw the dot diagram of $[[5]]$ above.

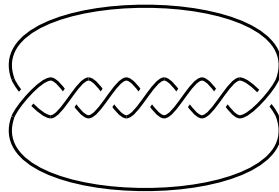


We included more than one homological height and grading for readability, but the point here is that the morphisms don't need to be labeled, since their identity can be determined.

Explicitly, the morphism between homological heights -1 and 0 can only be a saddle, for of the six possible non-zero morphisms between subobjects previously exhibited, no other type of morphism between a $[\infty]$ tangle and a $[0]$ tangle exists. The morphism between homological heights -2 and -1 must then be b : a map between $[0]$ tangles is either a or b but cannot be the former since we require $d^2 = 0$. There are two choices for the morphism between heights -3 and -2 . As $b \circ a = 0 \neq b \circ b$, it follows that the morphism must be a . The other morphisms can be determined from similar logic.

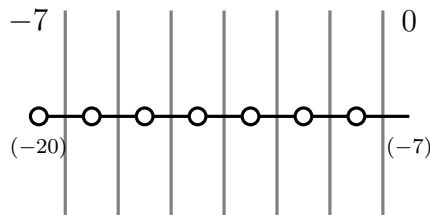
We now conclude the section with a calculation.

Example 3.1.3 Let's compute $Kh(7_1)$, the Khovanov homology of the 7_1 knot pictured below.



The knot 7_1 is the numerator closure of the tangle $[7]$. An orientation of 7_1 induces an orientation on the tangle, making it of type II.

As per Proposition 3.1.1, the Khovanov complex of this tangle is the following.

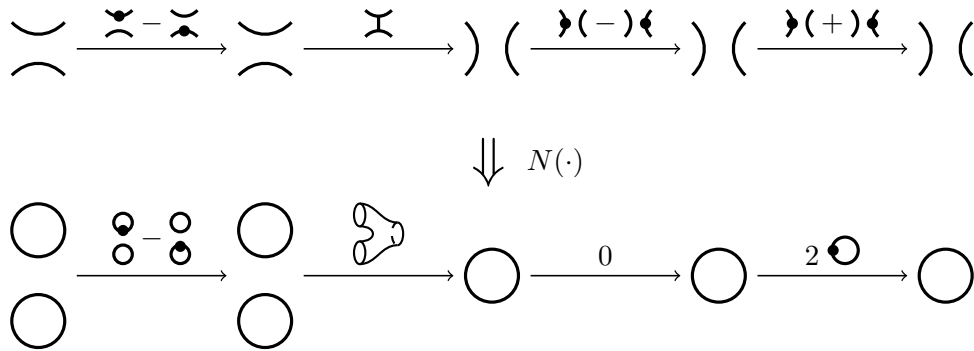


We can recover $[[7_1]]$ by placing $[[7]]$ in the 'figure-8' planar arc diagram illustrated below in Figure 3.1.4. When we do this $[\infty]$ subobjects become circles while $[0]$ subobjects become pairs of circles. Similarly morphisms change, as illustrated below.

Note that b morphisms become zero morphisms: recall that b consists of the formal difference of two morphisms, each of which consists of two sheets, one sheet of which

contains a dot. When either of these is placed in the figure-8 tangle, the ends of the sheets are joined, resulting in a cylinder with a dot. Although the location of the dots on the cylinders are different, in $Cob_{\bullet/l}^3$ the two morphisms are considered identical, so their difference is zero.

Since placing a tangle in the figure-8 planar arc diagram is the same as taking its numerator closure, we'll abuse notation and denote by $N(C)$ the result of putting a complex C in this planar arc diagram.



We can represent complexes $N(\llbracket T \rrbracket)$ by a dot diagram too; in an abuse of notation we'll use the same symbols as before, except now circles represent circles and dots represent two circles. The resulting dot diagram for $\llbracket 7_1 \rrbracket$ is in Figure 3.1.4 below. (We obtained this by simply removing any edge from the dot diagram of $\llbracket 7 \rrbracket$ that was a b map.)

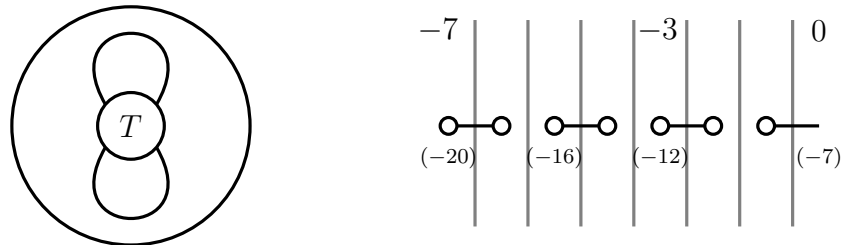
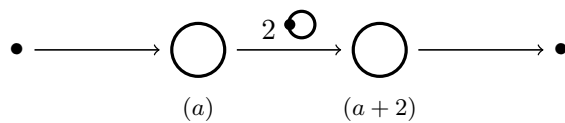


Figure 3.1.4: When numerator closure $N(\llbracket T \rrbracket)$ of the Khovanov complex $\llbracket T \rrbracket$ of a rational tangle T is taken, (placed in the figure-8 planar arc diagram illustrated) the complex splits into a direct sum of several types of components.

The complex $\llbracket 7_1 \rrbracket$ thus simplifies into a direct sum of four components, three of which are the same (ignoring homological and grading shifts).

Let us calculate the homology of the complex corresponding to the $\circ \text{---} \circ$ component of the dot-diagram. That is, the homology of the following complex.



(As before, the numbers in the brackets are the quantum gradings; the dots at the beginning and end represent the zero object in $\text{Mat}(Cob_{\bullet/l}^3(4))$. We can deloop both ends

to simplify it even further. The complex obtained is

$$\bullet \longrightarrow \begin{bmatrix} \emptyset (a-1) \\ \emptyset (a+1) \end{bmatrix} \xrightarrow{\begin{pmatrix} 0 & 2 \\ 0 & 0 \end{pmatrix}} \begin{bmatrix} \emptyset (a+1) \\ \emptyset (a+3) \end{bmatrix} \longrightarrow \bullet.$$

Before we take homology, we need to apply a TQFT. Under the tautological functor defined in Proposition 2.5.2, the complex becomes

$$0 \rightarrow \mathbb{Z} \oplus \mathbb{Z} \xrightarrow{\begin{pmatrix} 0 & 2 \\ 0 & 0 \end{pmatrix}} \mathbb{Z} \oplus \mathbb{Z} \rightarrow 0.$$

The homology groups of this complex are trivial to compute. We obtain

$$Kh^n(\bigcirc \text{---} \bigcirc) = \mathbb{Z}_{(a-1)}, \quad Kh^{n+1}(\bigcirc \text{---} \bigcirc) = \mathbb{Z}_{(a+3)} \oplus \mathbb{Z}/2\mathbb{Z}_{(a+1)}.$$

(The subscripts here indicate the quantum grading of the group.) To complete the calculation of $Kh(7_1)$, we only need to calculate the homology of the last component in the dot diagram. But there is no need to deloop this and do further matrix calculations. Rather, note that the complex corresponding to this is just the Khovanov complex of a diagram of the unknot with one crossing.

$$\bullet \longrightarrow \bigcirc \xrightarrow{\text{crossing}} \begin{matrix} \bigcirc \\ \bigcirc \end{matrix} \longrightarrow \bullet = \llbracket \bigcirc \rrbracket$$

By keeping track of grading and homological shifts, we obtain the following homotopy equivalence.

$$\begin{matrix} n & n+1 \\ \bigcirc & \text{---} \\ (a) & \end{matrix} \quad \simeq \quad \begin{matrix} n & n+1 \\ \text{---} & \bigcirc \\ & (a+2) \end{matrix}$$

This trick greatly simplified the calculation of the Khovanov homology of this component of the dot diagram, since the Khovanov homology of the unknot is trivial to calculate.

Assembling this information together and substituting the relevant grading and homo-

logical height information, we obtain

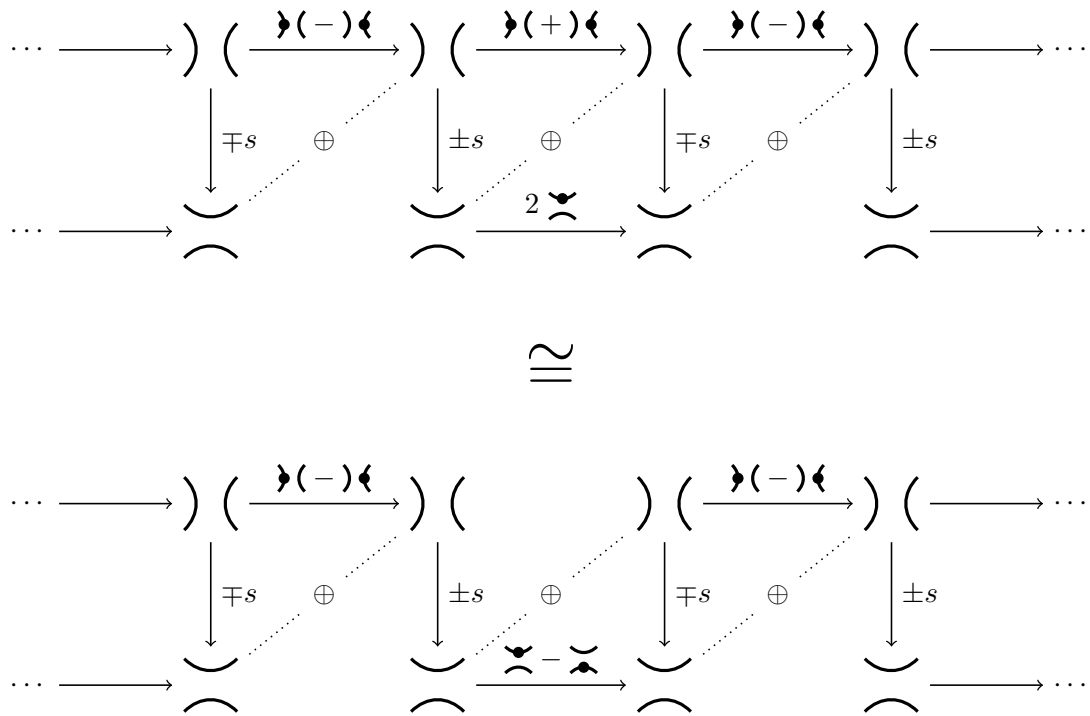
$$Kh^n(7_1) = \begin{cases} \mathbb{Z}_{(-21)} & \text{if } n = -7 \\ \mathbb{Z}/2_{(-19)} \oplus \mathbb{Z}_{(-17)} & \text{if } n = -6 \\ \mathbb{Z}_{(-17)} & \text{if } n = -5 \\ \mathbb{Z}/2_{(-15)} \oplus \mathbb{Z}_{(-13)} & \text{if } n = -4 \\ \mathbb{Z}_{(-13)} & \text{if } n = -3 \\ \mathbb{Z}/2_{(-11)} \oplus \mathbb{Z}_{(-9)} & \text{if } n = -2 \\ \mathbb{Z}_{(-7)} \oplus \mathbb{Z}_{(-5)} & \text{if } n = 0 \\ \{0\} & \text{otherwise.} \end{cases}$$

(This agrees with the values published in the literature, such at those available at The Knot Atlas.¹)

3.2 A new isomorphism

We now come to an important isomorphism. If there is any idea to take from this chapter, this is it, since the entire chapter is based on it.

These words do not do the isomorphism justice, so let us say something stronger. If there is any piece of machinery to take away from this thesis, this is it, since the entire thesis is based on it.



We've presented these complexes using the same format that we used in the previous section for readability. Namely, the objects of the complexes consist of the diagonal direct

¹Available at http://katlas.math.toronto.edu/wiki/Main_Page

sums of subobjects in the diagram, and the non-zero maps between these are indicated. As with the previous section we will drop the direct sum symbols that indicate which subobjects are in the same homological height; this information can be inferred from the arrows in the diagram.

Proposition 3.2.1 *The above complexes are isomorphic in $\text{Kom}(\text{Mat}(\text{Cob}_{\bullet,\mu}^3(4)))$.*

We will see the proof of this shortly, but let us first motivate why this ‘square isomorphism’ is glorious for our purposes.

From the previous section we know that the complexes of integer tangles $\llbracket n \rrbracket$ are essentially all the same: a chain of a and b maps followed by a saddle at the end or beginning. The complex $\llbracket 5 \rrbracket$ for instance, modulo homological shifts and grading information, is

$$\left) \left(\xrightarrow{a} \right) \left(\xrightarrow{b} \right) \left(\xrightarrow{a} \right) \left(\xrightarrow{b} \right) \left(\xrightarrow{s} \begin{array}{c} \cup \\ \cap \end{array} \right).$$

If we add additional crossings to $\llbracket 5 \rrbracket$, how do the corresponding Khovanov complexes change? If we add $\llbracket 5 \rrbracket$ and $\llbracket 1 \rrbracket$ we obtain $\llbracket 6 \rrbracket$, which we know the Khovanov complex of. But what if we were to add a crossing to the bottom of the $\llbracket 5 \rrbracket$ tangle?

Example 3.2.2 Let us calculate $\llbracket 5, 1 \rrbracket$ without worrying about the quantum gradings or the precise homological degrees (but we will keep track of the relative homological degrees). With $\llbracket 5 \rrbracket$ as T_1 and $\llbracket 1 \rrbracket$ as T_2 in the planar arc diagram corresponding to the product of two tangles (illustrated in Figure 3.2.2 below), we obtain the following complex.

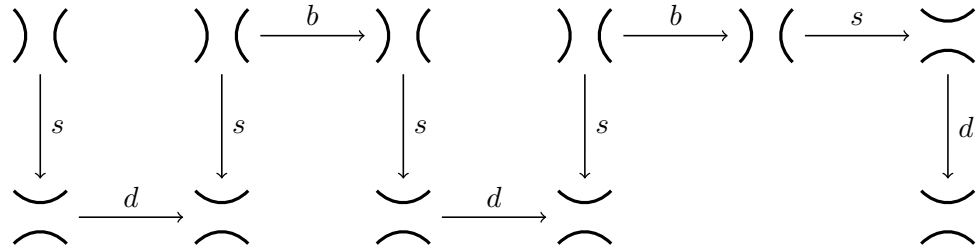
$$\begin{array}{ccccccc} \left) \left(\xrightarrow{a} \right) \left(\xrightarrow{b} \right) \left(\xrightarrow{a} \right) \left(\xrightarrow{b} \right) \left(\xrightarrow{s} \begin{array}{c} \cup \\ \cap \end{array} \right) & & & & & & \\ \downarrow -s & & \downarrow s & & \downarrow -s & & \downarrow s \\ \begin{array}{c} \cup \\ \cap \end{array} & \xrightarrow{2 \begin{array}{c} \cup \\ \cap \end{array}} & \begin{array}{c} \cup \\ \cap \end{array} & & \begin{array}{c} \cup \\ \cap \end{array} & \xrightarrow{2 \begin{array}{c} \cup \\ \cap \end{array}} & \begin{array}{c} \cup \\ \cap \end{array} \\ \downarrow -s & & \downarrow s & & \downarrow -s & & \downarrow s \\ \begin{array}{c} \cup \\ \cap \end{array} & \xrightarrow{s} & \begin{array}{c} \cup \\ \cap \end{array} & & \begin{array}{c} \cup \\ \cap \end{array} & \xrightarrow{s} & \begin{array}{c} \cup \\ \cap \end{array} \end{array}$$

Note the zero maps in the complex. These are the maps $D(b, I) : D([\infty], [0]) \rightarrow D([\infty], [0])$. Although the cobordism b consists of the difference of two pairs of vertical sheets with dots on different sheets, in the cobordism $D(b, I)$ the sheets are glued together. So $D(b, I)$ consists of the difference of two pairs of vertical sheets, both of which contain a dot on the same component, hence is zero.

The right-most anti-commutating square of the complex, consisting only of saddles, simplifies in exactly the same way as in the calculation of $\llbracket 2 \rrbracket$ in the proof of Proposition 3.1.1. But the rest of the complex has now become complicated – at least to the extent that if we were to try adding another crossing, further calculations by hand would be messy and unreasonable. For instance, assume we added another crossing to the bottom of $\langle 5, 1 \rangle$ to obtain $\langle 5, 2 \rangle$. By treating $\langle 5, 1 \rangle$ as T_1 and $\llbracket 1 \rrbracket$ as T_2 , if we were to construct $\llbracket 5, 2 \rrbracket$ using the same ‘product’ planar arc diagram as before, the nodes and maps of the complex we would draw out would now consist of vectors and matrices.

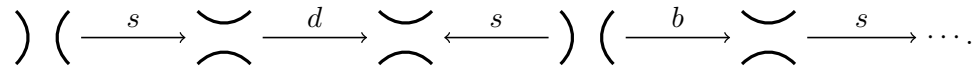
Using the square isomorphism illustrated before bypasses this problem. With it, the structure of $\llbracket T \rrbracket$ for a rational tangle T admits a far nicer description.

If we allow ourselves to use the square isomorphism, the complex $[[5, 1]]$ simplifies as follows.



(We also went a step further and removed the minus signs on the saddle morphisms.)

We have essentially made the complex 1-dimensional, a string of indecomposable subobjects connected via arrows. We can write it as



If we assume a complex has a presentation in this form – a string of objects and morphisms but with arrows going forwards and backwards – can we determine which objects lie in the same homological height? The answer is trivially yes, since the arrows in the unreduced, Khovanov complex cube take objects in homological height n to objects in homological height $n+1$. Delooping and Gaussian elimination rearrange and eliminate objects, but don't shift homological heights. Neither does our square isomorphism, so after simplification, every arrow still spans one homological height.

In practice, recovering the complex by hand from such a ‘string presentation’ is easy – simply construct the corresponding dot diagram, as illustrated below. (However in this situation, and in the sequel, we slope the lines to make sure the diagram doesn't become cluttered. So when we construct a dot diagram, while reading left to right along the string we construct circles and dots while gradually moving north up the diagram. A left arrow encountered in the string presentation corresponds to moving left in the dot diagram; a right arrows encountered indicates going right.) Such a dot diagram for $[[5, 1]]$ is illustrated below.

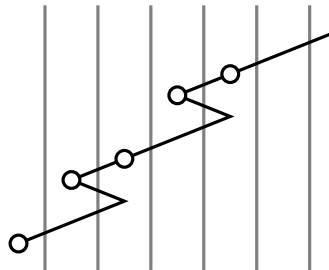


Figure 3.2.1: A dot diagram of $[[5, 1]]$. As with all rational tangles, it can easily be constructed from the string presentation of $[[5, 1]]$.

Notice that in the final dot diagram, we didn't label the morphisms. There was no need to, since all could be determined: each of the five ‘straight’ segments in the dot diagram contain a saddle, which determine the rest of the morphisms along the segment. (As we will soon see, there is no need to label the morphisms in the case of a general rational

tangle too.) This concludes the calculation.

The reason why these string presentations of a complex are useful is that, for computations, we can treat them as we would a normal complex. An example will clarify what we mean.

Example 3.2.3 We can compute $[[0, 2, 2, 1]]$ from $[[0, 2, 2]]$ and $[[1]]$ by placing the complexes in the planar arc diagram corresponding to the product of two tangles, illustrated below. The tangles $\langle 0, 2, 2 \rangle$ and $\langle 0, 2, 2, 1 \rangle$ are depicted in Figure 3.2.4.

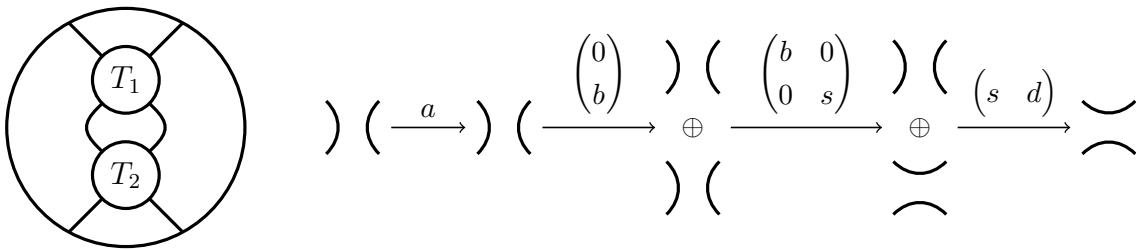
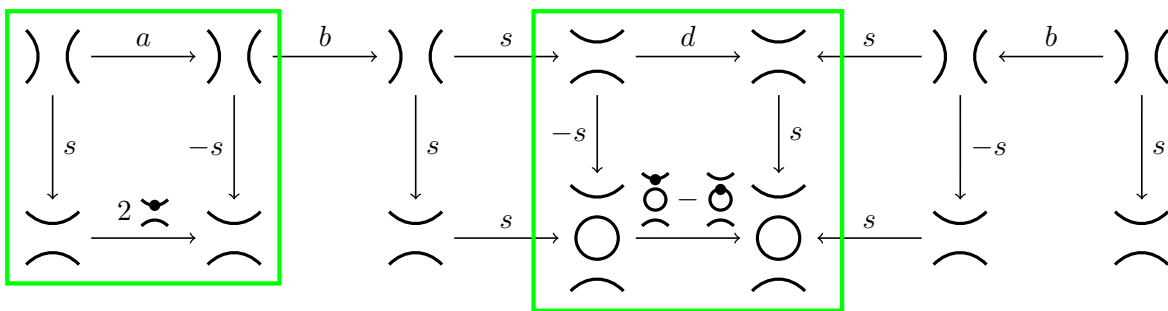


Figure 3.2.2: LEFT The ‘product’ planar arc diagram. RIGHT The complex $[[0, 2, 2]]$ presented in the usual way. The dot diagram for the complex is in Figure 3.2.4 below.

Computing $D([[0, 2, 2]], [[1]])$ is annoying if we write $[[0, 2, 2]]$ in the traditional way (as in Figure 3.2.2 above), since this introduces vectors and matrices into the complex. Obviously this poses no theoretical barrier, but it will be easier for illustrative purposes if we can depict the complexes in the simplest way possible. By treating the string presentation of $[[0, 2, 2]]$ as we would a normal complex, we construct $D([[0, 2, 2]], [[1]])$ below.



One might at first be concerned by the presence of the backwards arrows and question whether we can still treat this as we would a normal complex. We can, since the diagram is simply an unwound form of the bulky complex that we would have otherwise obtained by using the traditional presentation of the complex.

As such, we can deloop and apply Gaussian elimination to our complex as we did in the previous section. (Though we need to be slightly more careful since subobjects may now have more than one arrow entering or leaving them.)

Both of the highlighted areas of the complex simplify. The left area simplifies after applying the square isomorphism, while the right area simplifies in the same way as when we worked with integer tangles in the last section. The result is Figure 3.2.3 below.

We began with a complex corresponding to a rational tangle in string form, and after adding a crossing to the tangle, the complex simplified down until it had a string form too.

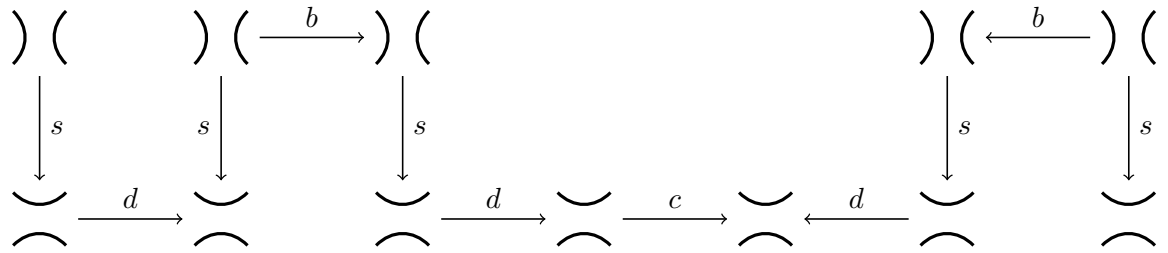


Figure 3.2.3: The simplified $[[0, 2, 2, 1]]$ complex, after an application of the square isomorphism and two delooping / Gaussian elimination steps.

The overall change in the complex is illustrated in Figure 3.2.4. We refer to complexes with a such a string form as *zig-zag complexes*.

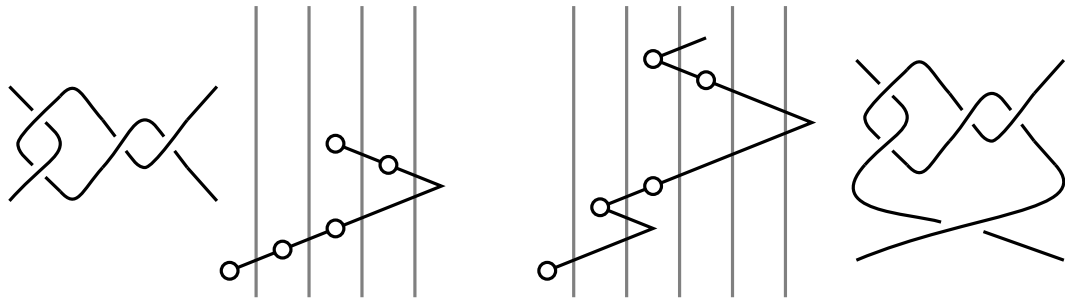


Figure 3.2.4: The tangles $\langle 0, 2, 2 \rangle$, $\langle 0, 2, 2, 1 \rangle$, and their Khovanov complexes. Notice that when a twist was added to the bottom of $\langle 0, 2, 2 \rangle$, the number of $[0]$ tangles in the complex increased by the number of $[\infty]$ tangles.

We will see in the next section that the previous example is representative for rational tangles as a whole: that is, the Khovanov complex associated to a rational tangle is a zig-zag complex. Before we do this though, let us prove the square isomorphism is actually an isomorphism.

Proof of Proposition 3.2.1: The isomorphism and its inverse are in Figure 3.2.5 below. (The other terms in the complex are taken to each other via identity maps.) We need to check three things.

1. The bottom layer is actually a chain complex.
2. The collection of maps constitutes a chain map.
3. The chain maps are inverses of one another.

The first is easy – we just need to check that all the squares in the bottom layer anticommute. Only one of the squares is different from the top layer, so we need only check that $d \circ (\pm s) = -(\mp s) \circ 0 = 0$. This is true since the saddle in $d \circ \pm s$ connects both sheets in each of the cobordisms constituting d ; the components then cancel.

The second point amounts to showing that the diagram in Figure 3.2.6 commutes.

(The other direction is similar.) This is easy and left as an exercise to the reader. (Hint: apply neck-cutting.)

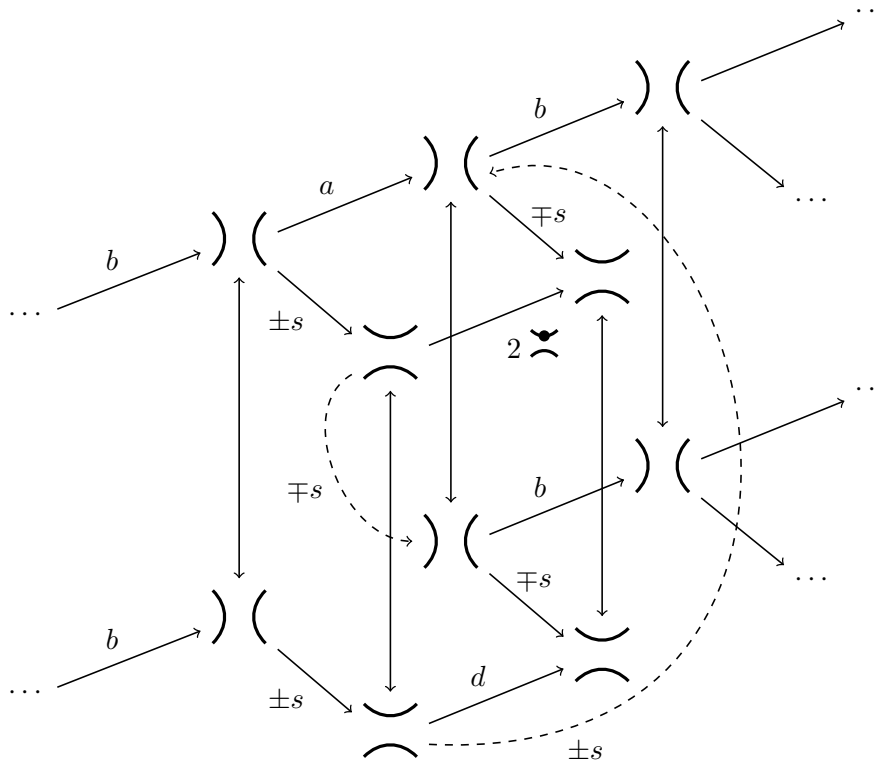


Figure 3.2.5: The square isomorphism, in all its glory. Unmarked vertical maps are identity maps. The identity of the other unmarked maps is irrelevant.

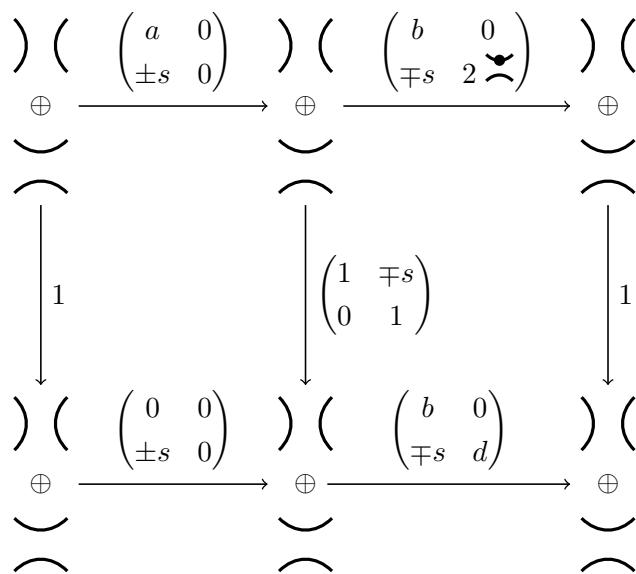


Figure 3.2.6: One direction of the square isomorphism, in a more traditional form.

The third point is easy as we merely need to check that

$$\begin{pmatrix} 1 & \mp s \\ 0 & 1 \end{pmatrix}^{-1} = \begin{pmatrix} 1 & \pm s \\ 0 & 1 \end{pmatrix}.$$

3.3 The Khovanov complex of rational tangles

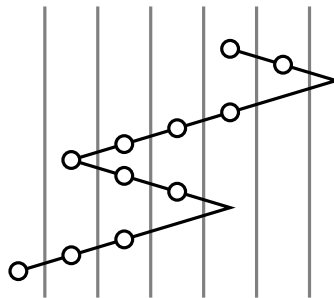
We claimed in the last section that $\llbracket T \rrbracket$ has the structure of a zig-zag complex for every rational tangle T . We now present a constructive proof. To avoid repeating ourselves, we will work with positive rational tangles ($F(T) > 0$) in this section; though all of what we say in this section can be analogously stated for negative rational tangles.

Recall from Chapter I one that positive tangle $F(T) > 0$ can be constructed from $[1]$ by a finite sequence of tangle additions and products with $[1]$. When a rational tangle is positive, and positive crossings are added to T , the resulting Khovanov complex changes in a predictable way. This is essentially the content of Theorem 3.3.1. The proof follows by breaking up the complexes into several components, and applying the results earlier in the chapter to these.

The description of how the complexes change that the theorem provides can almost be summarized by the pictures in Figure 3.3.1 over the page. If you can understand how the differences in the underlying tangles manifest in the pictures, then you've essentially understood the Khovanov homology of rational tangles.

For the purposes of this section we'll write a complex as a word in the letters $\{a, a', b, b', c, c', d, d', s, r\}$. This is just the sequence of maps of a complex in string form, reading left to right. A dash denotes a backwards arrow, and we have adopted the convention $r = s'$. We will call this the *morphism string* of the complex.

For example, the complex given by



has morphism string

$$absdrb'a'babsdrb'.$$

Morphism strings are not particularly readable, in that the structure of the complex is not as apparent as when it is represented as a dot diagram. As such we'll replace any instance of s with a negative-sloping diagonal line, and an r with a positive sloping diagonal line. With these conventions the morphism string above becomes

$$ab \begin{array}{c} \diagdown \\ d \\ \diagup \end{array} b'a'bab \begin{array}{c} \diagdown \\ d \\ \diagup \end{array} b'.$$

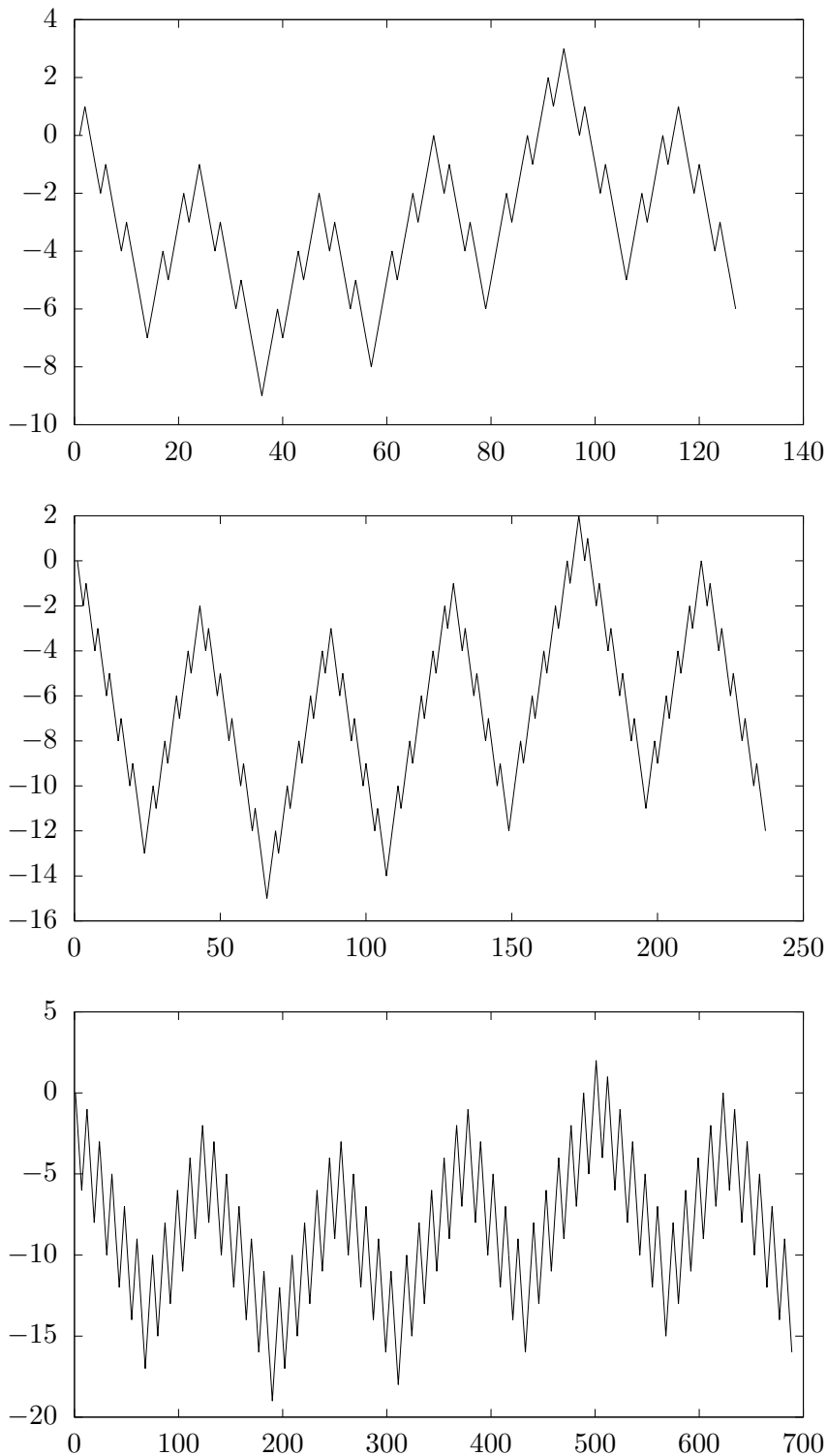


Figure 3.3.1: TOP TO BOTTOM Dot-diagrams for the complexes $[[2, 1, 3, 5, 1]]$, $[[2, 1, 3, 10, 1]]$, $[[2, 1, 3, 10, 5]]$. Observe how the similarities and differences in the structure of the rational tangles manifest in the complexes. For readability we have removed the circles, displayed the diagrams so that the homological height is on the y -axis, and set the complexes to begin in homological height 0. The x -axis denotes the position of the subobjects in the string form of the complex.

Writing the morphisms strings in this way is useful to illustrate how the complexes change when crossings are added to the underlying tangle, as well as a way to rapidly compute the Khovanov complex of a rational tangle by hand.

Theorem 3.3.1 *Let T be a positive rational tangle, that is $F(T) > 0$. (The case $F(T) < 0$ is similar to what we present below.) Then the morphism string associated to the Khovanov bracket $\llbracket T \rrbracket$ of T is a word w in $\{a, b, c, d, r, s\}$, possibly with dashes on the letters $\{a, b, c, d\}$ satisfying the following condition. After removing the dashes from w , if $\tilde{w} = l_1 l_2 l_3$ is any subword of w consisting of three adjacent letters:*

- if $l_2 = a$, then $\tilde{w} = bab$,
- if $l_2 = b$, then $l_1 \in \{a, r\}$, $l_3 \in \{a, s\}$,
- if $l_2 = c$, then $\tilde{w} = dcd$,
- if $l_2 = d$, then $l_1 \in \{c, s\}$, $l_3 \in \{c, r\}$,
- if $l_2 = r$, then $\tilde{w} = drb$,
- if $l_2 = s$, then $\tilde{w} = bsd$.

Furthermore, the morphism string of $\llbracket T + [1] \rrbracket$ or $\llbracket T * [1] \rrbracket$, can be obtained from the morphism string of $\llbracket T \rrbracket$ by the following rules.

To obtain $\llbracket T + [1] \rrbracket$ from $\llbracket T \rrbracket$, split $\llbracket T \rrbracket$ into a list of subwords w_1, \dots, w_n (so that their concatenation $w_1 \cdots w_n$ is the morphism string) such that $w_i \in \{c, c', d, d', r\Box, r\Box s, \Box s\}$ where \Box is a string in $\{a, a', b, b'\}$. The morphism string of $\llbracket T + [1] \rrbracket$ is given by the concatenation $f(w_1) \cdots f(w_n)$ where f is the following collection of rules.

- If \Box is the string obtained from \square by replacing each letter $a/a'/b/b'$ with $b/b'/a/a'$ respectively, then
 - $f(r\Box) = rb'\Box$,
 - $f(r\Box s) = rb'\Box bs$,
 - $f(\Box s) = \Box bs$.
- If $w_i = d, d'$,
 - $f(w_i) = sw_i \quad (i = 1)$,
 - $f(w_i) = w_i \quad (1 < i < n)$,
 - $f(w_i) = w_i r \quad (i = n)$.
- If $w_i = c, c'$, $f(c) = rbs$, $f(c') = rb's$.

To obtain $\llbracket T * [1] \rrbracket$ from $\llbracket T \rrbracket$, split $\llbracket T \rrbracket$ into a list of subwords w_1, \dots, w_n (so that their concatenation $w_1 \cdots w_n$ is the morphism string) such that $w_i \in \{a, a', b, b', s\Box, s\Box r, \Box r\}$ where \Box is a string in $\{c, c', d, d'\}$. The morphism string of $\llbracket T * [1] \rrbracket$ is given by the concatenation $g(w_1) \cdots g(w_n)$ where g is the following collection of rules.

- If \Box is the string obtained from \square by replacing each letter $c/c'/d/d'$ with $d/d'/c/c'$ respectively, then
 - $g(s\Box) = sd\Box$,
 - $g(s\Box r) = sd\Box d'r$,
 - $g(\Box r) = \Box d'r$.
- If $w_i = b, b'$,
 - $g(w_i) = rw_i \quad (i = 1)$,

- $g(w_i) = w_i \quad (1 < i < n),$
- $g(w_i) = w_i s \quad (i = n).$
- If $w_i = a, a', g(a) = sdr, g(a') = sd'r.$

Before embarking on the proof, we look at a few examples.

Example 3.3.2 Let us check that these rules agree with the calculation in Example 3.2.3. Examining Figure 3.2.4, we see that the morphism strings of $\llbracket 0, 2, 2 \rrbracket$ and $\llbracket 0, 2, 2, 1 \rrbracket$ are $absdrb'$ and $sdrbsdcd'rb's$ respectively.

Since $\langle 0, 2, 2, 1 \rangle$ is equal to $\langle 0, 2, 2 \rangle * [1]$, we can compute the morphism string of $\llbracket 0, 2, 2, 1 \rrbracket$ from the morphism string of $\llbracket 0, 2, 2 \rrbracket$. Following the description in Theorem 3.3.1, we break up $\llbracket 0, 2, 2 \rrbracket$ into subwords:

$$absdrb' = a + b + sdr + b'.$$

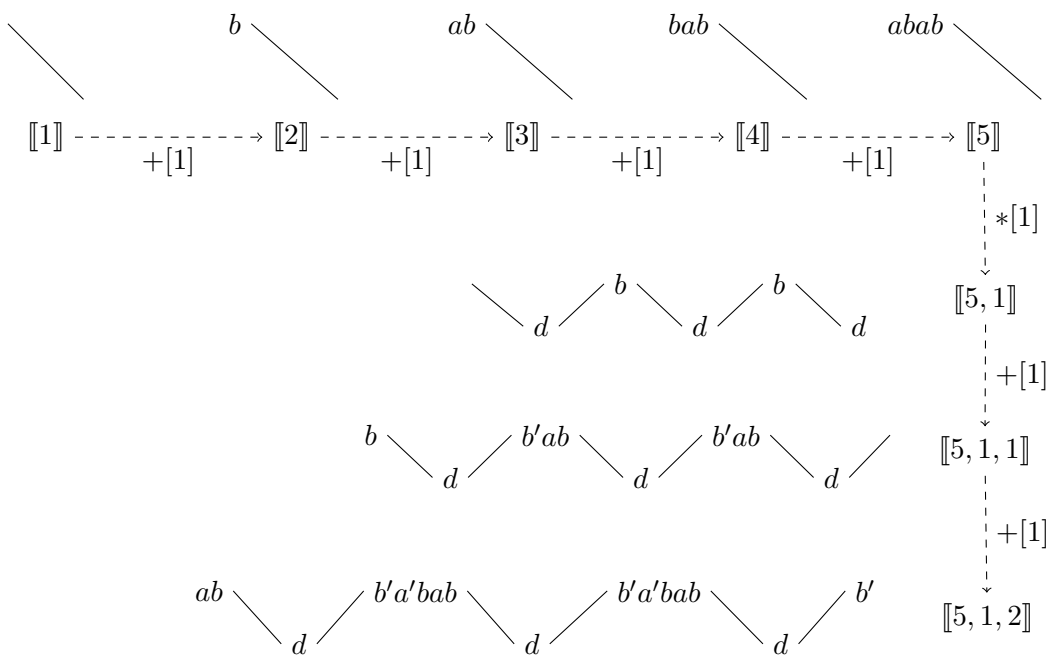
Applying the rules we have $g(a) = sdr, g(b) = b, g(sdr) = sdcd'r$ and $g(b') = b's$. Concatenating these, we have

$$g(a)g(b)g(sdr)g(b') = sdrbsdcd'rb's.$$

Example 3.3.3 Let us compute $Kh(8_2)$ by hand. This will further illustrate how the Khovanov bracket of a rational tangle changes when additional crossings are added to the underlying tangle.

The knot 8_2 is rational, obtained via numerator closure from $\langle 5, 1, 2 \rangle$. Let us compute the structure of the chain complex first; gradings and homological heights will be calculated at the end.

The morphism string corresponding to $\llbracket 1 \rrbracket$ is just s . By applying the rules above and using the notation mentioned earlier, we build the morphism string of $\llbracket 5, 1, 2 \rrbracket$ from s as follows.



All that's left to do is to take the numerator closure of this complex and determine the

homological and grading information. The former is easier to do if we construct the dot diagram of the complex. This and its closure are drawn below in Figure 3.3.2.

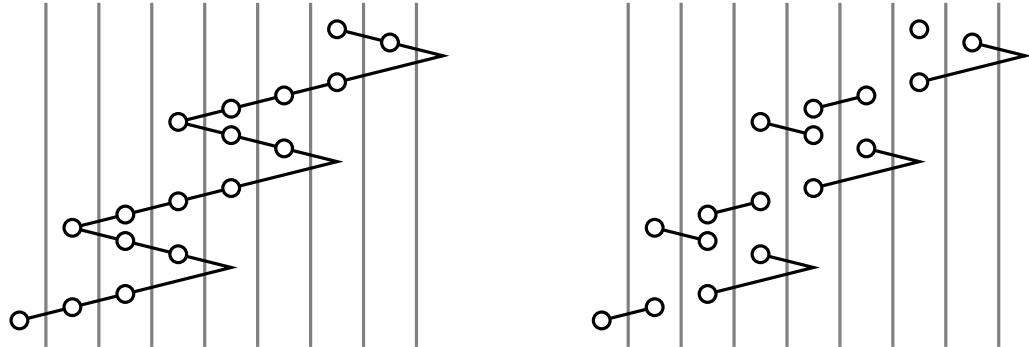
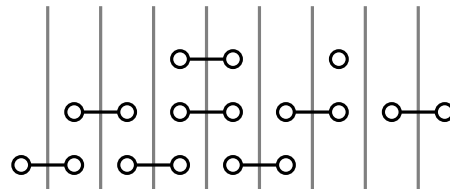


Figure 3.3.2: The dot diagram of the $[[5, 1, 2]]$ and $N([[5, 1, 2]])$. This example is illustrative of the Khovanov homology of rational knots in general.

By a similar argument as that in Example 3.1.3, the wedge-shaped complexes in the dot diagram with four subobjects are homotopy equivalent to the $\circ - \circ$ components.

Therefore $[[8_2]]$ splits into a direct sum of nine complexes which span the homological heights as illustrated below. We have already computed the homology of these complexes in Example 3.1.3, so are nearly finished. We simply need to calibrate the homological heights and gradings.

It is a simple exercise to verify that the internal grading and homological height of one of the subobjects of the complex determines the same information for the rest of the subobjects. As such we only need to compute this grading information for one subobject to have determined the grading information of $[[5, 1, 2]]$.



Further on we will see that this grading information about the subobjects can simply be determined by multiplying certain 2×2 matrices together, but for now we will use the calculation so far.

An orientation of 8_2 orients the underlying tangle. To calibrate both the homological and quantum grading information of $[[5, 1, 2]]$, we keep track of the grading information associated to the subobject at the beginning of each intermediate complex in the construction of $[[5, 1, 2]]$. Determining how the grading information of these subobjects change when crossings are added to the underlying tangle can be done by examining: the morphism leaving the subobject; the orientation of the crossing being added; whether the crossing is being added to the to the right or bottom of the tangle. The relative change for positively oriented crossings is listed in the table below.

The corresponding values for negatively-oriented crossings differ from their positively-oriented counterparts by $-3/-1$. After applying this process to our construction of the morphism string of $[[5, 1, 2]]$ above, we find that the first subobject in string of $[[5, 1, 2]]$ has grading/homological height $-16/-6$.

For all intents and purposes we're done, though it's common to write the result as the

Map	+ [1]	* [1]
a, a'	0/0	1/0
b, b'	0/0	2/1
c, c'	2/1	-1/0
d, d'	1/0	-2 / 1
s	0/0	-3/-1
r	2/1	-1/0

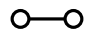
Table 3.1: The relative shifts in internal grading (i) and homological height (h) of the subobject is presented as i/h . These values are for positively oriented crossings.

Khovanov polynomial instead of the actual Khovanov homology. One is more succinct than the other and they essentially contain the same information.

The Khovanov polynomial of a link as a two-variable Laurent polynomial in $\mathbb{Z}[q^{\pm 1}, t^{\pm 1}]$ defined by

$$\sum_j \text{qdim}(Kh^j(L)) \cdot t^j. \tag{3.3.1}$$

It is common to denote the Khovanov polynomial in the form of a table. The positive integer in i -th j -th square of the table corresponds to the coefficient of $t^j q^i$ in the polynomial.

Filling the table in using the information obtained above is a trivial matter;  components in the dot diagram correspond to knights moves while the \bigcirc corresponds to the exceptional pair.

$i \setminus j$	-6	-5	-4	-3	-2	-1	0	1	2
1									1
-1									
-3							2	1	
-5						1	1		
-7					2	1			
-9				1	1				
-11			1	2					
-13		1	1						
-15		1							
-17	1								

Table 3.2: The Khovanov homology of $Kh(8_2)$.

We now return to the main result of this section.

Proof of Theorem 3.3.1: The first claim of the theorem regarding the structure of $[[T]]$ for rational T follows from induction from the rules of the theorem. Namely, since every rational tangle is given by a finite sequence of additions and products of [1], one simply shows that the rules preserve the property of the first claim.

The proof of the rules essentially follows from thinking about the complexes associated to the morphism strings of the subwords in the rules, and how these change when the

underlying tangle changes. Proposition 3.1.1 and the isomorphism in Proposition 3.2.1 are sufficient to describe these changes.

As a sanity-check we wrote a computer program in Python that calculates $\llbracket T \rrbracket$ for positive rational tangles T based on our rules. We then extended the program to calculate $Kh(R)$ for rational R . We checked the results for the first 25 rational knots; they are all correct.²

The proof of the rules describing how the morphism string of $\llbracket T + [1] \rrbracket$ is obtain from $\llbracket T \rrbracket$ is analogous to the proof of the rules for the $\llbracket T * [1] \rrbracket$ case; as such we prove the latter. If the reader is not already familiar with Example 3.2.3 we suggest she look at it now; it is easy to use this as a visual guide to explain the rules.

Let us first explain the general structure of $\llbracket T * [1] \rrbracket$. If the morphism string of $\llbracket T \rrbracket$ contains n letters, can view $\llbracket T * [1] \rrbracket$ as a $2 \times (n + 1)$ complex just as we did in the previous section. That is, as a complex consisting of two rows, each with $n + 1$ tangles, and various left, right, and down arrows between adjacent tangle in the complex. The arrows create squares, and each of these anticommute. We now simplify the complex.

By dropping arrows that are zero morphisms, one can view the complex $\llbracket T * [1] \rrbracket$ as a series of chains of anticommuting squares ‘connected’ by b maps. (For instance, in the aforementioned example, the complex consists of two such chains of squares; one chain consists of one square, the other consists of three squares.) Each of these chains of squares will simplify so that each subobject they contain will have precisely two non-zero maps coming in or out of it.

By virtue of the morphism string structure of $\llbracket T \rrbracket$, there are two types of these chains of squares: single-square chains containing an a or a' map and chains which contain tangles with loops. The first type of square chains simplify by the square isomorphism of Proposition 3.2.1, the other type simplify via the proof of Proposition 3.1.1.

One then sees that the square chains containing an a or a' simplify to have morphism string sdr or $sd'r$ respectively, the third rule regarding $\llbracket T * [1] \rrbracket$. The other type of square chains simplify to give the first rules of $\llbracket T * [1] \rrbracket$. (Note that the first and last rule of this group of three rules describe the cancellation if the square forms the beginning or end of of the $2 \times (n + 1)$ complex resectively.)

The only rule left to describe is that regarding the b maps; since these ‘connect’ the square of chains that simplify, they do not chain, save if they are at the end or beginning of the complex. \square

In the next section we briefly look at some consequences of the Theorem, it particular the unexpected result that the quantum grading and homological degree information about the subobjects in the tangle can be described by matrix actions.

²The code is available at <https://tqft.net/research/BenjaminThompson>

Theoretical implications of Theorem 3.3.1

In this chapter we discuss some of the implications of Theorem 3.3.1.

4.1 Rational knots

Since rational knots are obtained from rational tangles by numerator closure, by describing the Khovanov homology of rational tangle we have *a priori* described the Khovanov homology of rational tangles.

The Khovanov homology of rational tangles is not very interesting. Within a few years of its definition, Bar-Natan wrote a computer program able to calculate the Khovanov homology groups of links. (He later extended the program to calculate the Khovanov complexes of tangles using his dotted theory ([Bar06]). Based on the calculations, Bar-Natan, Khovanov and S. Garoufalidis formulated two several conjectures; the ones formulated in [Bar02] are repeated here for convenience.

Conjecture 4.1.1 For any prime knot L there exists an even integer $s = s(L)$ and a polynomial $Kh'(L) \in \mathbb{Z}[q^{\pm 1}, t^{\pm 1}]$ with non-negative coefficients so that

$$Kh_{\mathbb{Q}}(L) = q^{s-1} \left(1 + q^2 + (1 + tq^4)Kh'(L) \right).$$

Conjecture 4.1.2 For prime alternating L the integer $s(L)$ is equal to the signature of L and the polynomial $Kh'(L)$ is a polynomial in tq^2 .

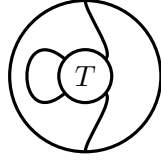
The second conjecture essentially states that the Khovanov polynomial of a prime alternating knot is supported on two diagonals (when presented as a table as in Example 3.3.3) and consists only of knight moves and one exceptional pair.

Lee later proved the second conjecture for any non-split alternating link ([Lee02]). (An alternating link is non-split iff an alternating diagram of the link is connected.) Rational knots hence satisfy this property too, since they are alternating as per Chapter 1.

Theorem 3.3.1 provides an alternative proof of the second conjecture restricted to rational knots. The proof is not difficult, and is essentially just formalizing the idea illustrated in Figure 3.3.2. (Though one does need to prove that ends of the Khovanov complexes produce precisely one exceptional pair. This claim can be proved by induction via Theorem 3.3.1 as it describes how the ends of the complexes are modified when additional crossings are added to the tangle.)

One can generalize this to say something slightly stronger for a certain class of tangles.

Definition 4.1.3 A $(1,1)$ -rational tangle is a tangle that can be created by inserting a rational tangle into the planar arc diagram below.



Corollary 4.1.4 The Khovanov complex $\llbracket T \rrbracket$ of a $(1,1)$ -rational tangle T splits into a direct sum consisting of one copy of the complex

$$\bullet \longrightarrow \big) \longrightarrow \bullet$$

and several copies of

$$\bullet \longrightarrow \big) \xrightarrow{2 \uparrow} \big) \longrightarrow \bullet \cdot$$

Proof: The proof follows from an easy extension of Theorem 3.3.1. □

4.2 The Burau representation from the Khovanov complexes of rational tangles

In this section we consider rational tangles as partial closures of the three-strand braid group B_3 , as illustrated in Figure 1.3.1. For a positive rational tangle $\langle a_1, a_2, \dots, a_n \rangle$ with n odd, we view this as the partial closure of $\sigma_1^{a_1} \sigma_2^{-a_2} \sigma_1^{a_3} \dots \sigma_1^{a_n}$. Adding (positive) crossings to the right of a rational tangle corresponds to multiplying the braid by σ_1 , multiplying a tangle with $[1]$ on the bottom corresponds to multiplying the braid by σ_2^{-1} .

From Chapter 1, every positive rational tangle has a unique canonical form, from which it follows that every rational tangle has a unique presentation $\sigma_1^{a_1} \sigma_2^{-a_2} \sigma_1^{a_3} \dots \sigma_1^{a_n}$ where $a_i > 0$ for $i < n$ and $a_n \geq 0$.

Let $\theta : \mathbb{Q} \rightarrow \mathcal{T}$ be the function taking a rational number to its rational tangle via the correspondence in Theorem 1.2.6. Let $\phi : \mathbb{Q} \rightarrow B_3$ be the function taking a rational number r to $\theta(r)$, presented as an element of B_3 as just described.

Let $\text{BN}(4)$ be the subcategory of $\text{Mat}(\text{Cob}_{\bullet, \mu}^3)$ generated by the $[0]$ and $[\infty]$ tangles. (So in particular, $\llbracket T \rrbracket \in \text{Kom}(\text{BN}(4))$ for all rational tangles T .)

Let $\Psi : \text{Obj}(\text{Kom}(\text{BN}(4))) \rightarrow \mathbb{Z}[q^{\pm 1}, t^{\pm 1}] \langle \succ, \rangle \langle \rangle$ be the function that forgets all the maps of a complex but remembers the bigradings of its subobjects. We present an element $p_0 \succ + p_\infty \rangle \langle \in \mathbb{Z}[q^{\pm 1}, t^{\pm 1}] \langle \succ, \rangle \langle \rangle$ as (p_0, p_∞) .

For example,

$$\Psi(\bullet \rightarrow q \succ \langle \rightarrow q^2 \succ \rightarrow q^4 \succ \rightarrow \bullet) = (q^2 t + q^4 t^2, q).$$

Note that this map is not a homotopy invariant. (For example, $\Psi(\bullet \rightarrow \succ \xrightarrow{\phi} \rangle \langle \rightarrow \bullet) = (0, 1 + t)$, even though this complex is contractible when ϕ is an isomorphism.)

Proposition 4.2.1 Let $r \in \mathbb{Q}_+$, and fix an orientation of $\phi(r)$. Then $\phi(r)$ determines the orientations of additional crossings added to it in what follows.

Let $[\phi(r)]$ be completely reduced. Then $\Psi([\phi(r)\sigma_1])$ is given by $\Psi([\phi(r)])R_{\pm 1}$ and $\Psi([\phi(r)\sigma_2^{-1}])$ is given by $\Psi([\phi(r)])B_{\pm 1}$ where

$$R_+ = q \begin{pmatrix} qt & 1 \\ 0 & q^{-1} \end{pmatrix}, \quad R_- = q^{-2}t^{-1} \begin{pmatrix} qt & 1 \\ 0 & q^{-1} \end{pmatrix},$$

$$B_+ = q^2 \begin{pmatrix} qt & 0 \\ t & q^{-1} \end{pmatrix}, \quad B_- = q^{-1}t^{-1} \begin{pmatrix} qt & 0 \\ t & q^{-1} \end{pmatrix},$$

and the signs correspond to the orientation of the crossing being added.

Proof: We sketch the proof. It follows from the proof of Theorem 3.3.1. Essentially one breaks the complex $[\phi(r)]$ into several segments, (as suggested by the theorem) and showing the Proposition holds on each locally; when these are combined the relation holds for the entire complex too. \square

Proposition 4.2.2 *The pairs of matrices R_+ and B_-^{-1} , and R_- and B_+^{-1} satisfy the braid relation. After a change of basis these give the (reduced) Burau representation of B_3 .*

Proof: The first claim follows from easy computations. Explicitly, one finds that

$$R_+B_-^{-1}R_+ = B_-^{-1}R_+B_- = \begin{pmatrix} 0 & q^3t \\ -q^3t^2 & 0 \end{pmatrix}$$

and similarly for the other pair. With

$$p = \begin{pmatrix} q & 0 \\ 0 & 1 \end{pmatrix},$$

when we change basis we obtain

$$\sigma'_1 = p^{-1}R_+p = \begin{pmatrix} q^2t & 1 \\ 0 & 1 \end{pmatrix}, \quad \sigma'_2 = p^{-1}B_-^{-1}p = \begin{pmatrix} 1 & 0 \\ -q^2t & q^2t \end{pmatrix}.$$

This is exactly the (reduced) Burau representation of B_3 after the change of variables $t \mapsto -q^2t$. \square

We are still very much trying to understand the implications of this observation. This concludes the thesis.

Bibliography

- [Bar02] D. Bar-Natan. On Khovanov’s categorification of the Jones polynomial. *ArXiv Mathematics e-prints*, January 2002.
- [Bar04] D. Bar-Natan. Khovanov’s homology for tangles and cobordisms. *ArXiv Mathematics e-prints*, October 2004.
- [Bar06] D. Bar-Natan. Fast Khovanov Homology Computations. *ArXiv Mathematics e-prints*, June 2006.
- [BN95] Dror Bar-Natan. On the vassiliev knot invariants. *Topology*, 34:423–475, 1995. Available from: <http://www.webcitation.org/6hmwzwh0C>.
- [CDM11] S. Chmutov, S. Duzhin, and J. Mostovoy. Introduction to Vassiliev Knot Invariants. *ArXiv e-prints*, March 2011.
- [Con70] J.H. Conway. *An enumeration of knots and links, and some of their algebraic properties*. Pergamon, New York, 1970.
- [FYH⁺85] P. Freyd, D. Yetter, J. Hoste, W. B. R. Lickorish, K. Millett, and A. Ocneanu. A new polynomial invariant of knots and links. *Bulletin*, 12(2):239–246, 1985. Available from: <http://www.webcitation.org/6hmrVH40y>.
- [Jon85] V. Jones. A polynomial invariant for knots via von neumann algebras. *Bull. Amer. Math. Soc.*, 12:103–111, 1985.
- [Kas95] Christian Kassel. *Quantum Groups*. Springer-Verlag, New York, first edition, 1995.
- [Kau87] Louis H. Kauffman. State models and the jones polynomial. *Topology*, 26(3):395 – 407, 1987.
- [Kho99] M. Khovanov. A categorification of the Jones polynomial. *ArXiv Mathematics e-prints*, August 1999.
- [Kho01] M. Khovanov. A functor-valued invariant of tangles. *ArXiv Mathematics e-prints*, March 2001.
- [Kho16] M. Khovanov. Linearization and categorification. *ArXiv e-prints*, March 2016.
- [KL03a] L. H. Kauffman and S. Lambropoulou. From tangle fractions to DNA. *ArXiv Mathematics e-prints*, November 2003.
- [KL03b] L. H. Kauffman and S. Lambropoulou. On the classification of rational tangles. *ArXiv Mathematics e-prints*, November 2003.
- [Lee02] E. S. Lee. An endomorphism of the Khovanov invariant. *ArXiv Mathematics e-prints*, October 2002.

- [MT93] W. Menasco and M. Thistlethwaith. The classification of alternating links. *Annals of Mathematics*, 138:113–171, 1993.
- [PS96] V.V. Prasolov and A. B. Sossinsky. *Knots, Links, Braids and 3-Manifolds*. AMS, New York, 1996.
- [PT88] J. Przytycki and P. Traczyk. Invariants of links of the conway type. *Kobe J. Math*, 4:115–139, 1988.
- [Rei48] K. Reidemeister. *Knot Theory*. Chelsea Publishing, 1948.
- [Sch56] H. Schubert. Knoten mit zwei BrÄijcken. *Math. Zeitschriften*, 65:133–170, 1956.